



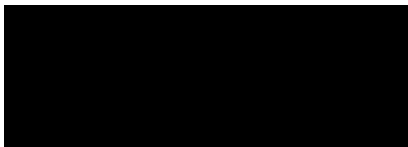
**Università degli Studi Mediterranea di Reggio Calabria
Dipartimento di Agraria**

**Corso di Dottorato di ricerca
Scienze Agrarie Alimentari e Forestali XXXIII ciclo**

**Characterization of Italian onion populations, analysis of plant
responses to onion yellow dwarf virus (OYDV) infection and
plant-potyvirus interactions**

**SSD AGR/12 – Patologia Vegetale
SSD AGR/07 – Genetica Agraria**

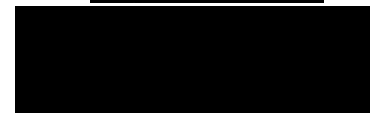
Tesi di dottorato di:



Dot. Giuseppe Micari

Tutor:

Prof. Francesco Sunseri



Coordinatore del corso:

Prof. Marco Poiana

ANNO ACCADEMICO 2017/2020

Contents

Abstract.....	6
Riassunto.....	8
General Introduction	10
1. <i>Allium</i> genus.....	10
1.1 General characteristics	10
1.2 Phylogenies and classification	12
<i>1.2.1 Evolutionary lineages and subgenera of <i>Allium</i> genus</i>	<i>14</i>
<i>1.2.2 The <i>Cepa</i> section.....</i>	<i>16</i>
<i>1.2.3 The <i>Cepa</i> alliance</i>	<i>18</i>
2. <i>Allium cepa</i> L.	19
2.1 Historical information	19
2.2 Botanical traits and agronomic techniques.....	21
2.3 Economic and nutritional importance	24
3. Onion diseases	27
3.1 General description of plant viruses.....	27
3.2 Main viruses of Onion	30
4. Molecular analyses on plant responses to OYVD	35
4.1 EIFs gene family expression.....	35
4.2 Differential gene expression (DEG) analysis after bulbs OYVD infection	38
5. Molecular plant-virus interactions	41
5.1 Replication and cell-to-cell movement of potyviruses are connected processes	41
5.2 Components of the vesicle trafficking machinery are implicated in the replication and movement of plant viruses.....	43
Organization and Aims of research.....	45

Chapter 1. Genetic characterization and analysis of onion populations’ response to OYVD	48
1. Materials and Methods	48
1.1 Plant material	48
1.2 Greenhouse experimental trials and OYDV inoculation	49
1.3 Control of the inoculation success	52
1.4 Assessment of symptoms intensity	53
1.5 Effects on plant growth	55
1.6 Effects of OYDV on bulb long-term storage and water losses	56
1.7 Statistical analysis	57
1.8 DNA extraction, PCR and fragment analysis (SSR)	58
2. Results and Discussion	60
2.1 Resistance/susceptibility of onion populations to OYDV and effects on plant growth	60
2.2 Effects of OYDV on bulb long-term storage and water losses	66
2.3 Cluster analysis of onion populations by SSR	71
Chapter 2. Molecular analyses of plant responses after OYD infection	75
1. Materials and Methods	75
1.1 Gene expression analysis of the Eukaryotic translation Initiation Factors (EIF)	75
<i>1.1.1 Plant material</i>	75
<i>1.1.2 Primers design and housekeeping gene detection</i>	75
<i>1.1.3 RNA extraction and reverse transcription</i>	76
1.2 RNAseq analysis on virus-free and OYVD-infected onion bulbs	78
<i>1.2.1 Plant material</i>	78
<i>1.2.2 OYDV infection evaluation using DAS-ELISA and Real Time RT-PCR</i>	79
<i>1.2.3 RNA isolation and sequencing</i>	80
<i>1.2.4 De novo transcriptome assembly and annotation</i>	80

1.2.5 Differential gene expression analysis and co-network analysis	81
2 Results and discussion	83
2.1 Gene expression analysis of the Eukaryotic translation Initiation Factors (EIF)	83
2.1.1 Differential expression of EIF gene family in OYVD infected onion	83
2.2 RNAseq analysis on virus-free and OYVD-infected onion bulbs	88
2.2.1 De novo assembly and annotation of onion bulb transcriptome.....	88
2.2.2 Transcript abundance estimation and differentially expressed genes (DEGs)	89
2.2.3 OYDV infection alters the onion bulb dormancy	91
2.2.4 Transcription factors differentially expressed during dormancy.....	98
2.2.5 Gene co-expression network analysis	103
2.2.6 Conclusion	105
Chapter 3 Study on molecular plant-pathogen interactions: host factors involved in the cell-cell movement of potyviruses?	106
1. Material and methods.....	106
1.1 Split Ubiquitin Yeast Two Hybrid System (DUAL membrane system).....	106
1.2 Cloning of AtXX4, the <i>Arabidopsis</i> orthologous gene of <i>CmXX4</i> into entry and destination vectors using Gateway® technology	109
1.2.1 PCR amplification of AtXX4 cDNA.....	110
1.2.2 Cloning of AtXX4 into the pENTR™/D-TOPO® vector	111
1.2.3 Rapid PCR-based colony screening for cloned inserts.....	112
1.2.4 Plasmid extraction from positive bacteria colonies and sequencing of the cDNA insert.....	113
1.2.5 Subcloning the AtXX4 gene from the Entry clone into a Destination Vector for expression of fluorescent-tag-fusion protein.....	113
1.3 Use of <i>Agrobacterium tumefaciens</i> for transient expression of proteins and virus inoculation in <i>N. benthamiana</i>	116
1.3.1. Viral and other molecular constructs cloned into binary vectors.....	116
1.3.2. Preparation of <i>Agrobacterium</i> cultures for infiltration	117

1.3.3 Confocal microscopy analysis	118
2. Results and Discussion	119
2.1 Four out of sixteen CmXXX candidates interact with WMV-6K2 in Yeast..	119
2.2 Confirmation of the interaction between AtXX4 and TuMV-6K2 <i>in planta</i> using BiFC	122
2.2.1 <i>AtXX4 and TuMV-6K2 interact in healthy plants</i>	122
2.2.2 <i>AtXX4 /TuMV-6K2 interaction occurs at the level of the viral replication</i> <i>complex in infected cells</i>	126
2.3 Observation of AtXX4 self-interaction <i>in planta</i> by BiFC	128
2.4 Subcellular localization of AtXX4 in healthy and infected plants	130
General Conclusions and Future Perspectives	132
Acknowledgements.....	135
Reference.....	136
List of figures	165
List of tables.....	174

Abstract

Allium cepa L. is the most cultivated species of the *Allium* genus and one of the largest crops worldwide. Among viruses, the *Onion yellow dwarf virus* (OYDV) species (genus *Potyvirus*) represents the most limiting biotic stress for the crop. One of the most effective tools for controlling viral diseases is detecting virus resistant or tolerant varieties for the genetic improvement of host plant.

Thus, 25 Italian varieties/ecotypes, and a cultivar reported to be resistant to OYDV, namely ‘Texas early Grano 502’, were characterized by evaluating their response to potyvirus for intensity of symptoms, morphological traits and bulb water losses during storage. ‘Rossa di Tropea’ and ‘Texas early Grano 502’ were the most tolerant cultivars to OYDV, while ‘Acquaviva 7’ appeared the most susceptible, followed by ‘Pera sanguigna di Peschici’. The effects of virus infection led to a water accumulation increase in the bulb tissue with consequent significant water losses during storage. A genetic characterization of 15 tested onion varieties/ecotypes was carried out by using 12 SSR markers, highlighting that the tolerant varieties ‘Texas early Grano 502’ and ‘Rossa di Tropea’ are significantly distant from those susceptible ‘Acquaviva 7’ and ‘Pera Sanguigna di Peschici’. Furthermore, the varieties selected as the most sensitive and tolerant to OYDV were tested for eIF4E and eIF4G gene expression, which are reported as genes involved in the replication of many potyviruses, and thus possible targets in the development of plant virus resistance. Although a significant difference in the expression between susceptible and/or tolerant plants and between healthy and infected plants was highlighted, compared to the literature it could be suggested that OYDV could utilize a different path for its replication processes.

The RNASeq analysis carried out on healthy and OYDV infected samples allowed us to obtain interesting results on the virus infection effects by analysing the differentially expressed genes (DEGs). This approach was able to hypothesize the role of genes belonging to the *WRKY* transcription factor (TF) family in *A. cepa*. Infected samples showed only a few DEGs related to dormancy during storage, that appeared related to the virus infection, unlike healthy samples, which exhibited a high number of DEGs. Furthermore, the transcriptomic profiles and the analysis of

the co-expression allowed us to identify a TF (*AcWRKY32*) that potentially drives the release of dormancy in onion bulbs.

The study of protein-protein interactions, focused on the identification of plant factors involved in the movement of the *potyvirus*, was carried out by screening for melon proteins related to the ESCRT system and for the viral protein WMV 6K2 by SUY2H. Then, the *in-planta* interaction based on the *Arabidopsis* XX4 vs. TuMV 6K2 protein by BiFC analysis, led to confirm the involvement of the ESCRT AtXX4 protein in TuMV replication and movement processes. GFP analysis was useful to characterize the subcellular localization of AtXX4.

Our results have broadened the knowledge on the infectious process implemented by OYDV within the plant and leading to the following conclusions. The traits of tolerance/susceptibility to OYDV recovered in the biodiversity of local varieties and ecotypes were highlighted. An explanation on how OYDV infections are the primary factor to create optimal conditions for secondary pathogens was furnished. The role of OYDV in breaking dormancy in the infected bulb was identified by differential expression of some TF belonging the WRKY gene family in onion. The foundations have been laid to understand the pathway for the translocation of OYDV along the plant, to determine whether the XX4 protein may also have a biological role in the onion-OYDV system.

Keywords: *Allium cepa*, OYDV resistance, SSR genetic characterization, WRKY, RNAseq, DEG, BiFC.

Riassunto

“Caratterizzazione di popolazioni italiane di cipolla, analisi della risposta delle piante all'infezione del virus del nanismo giallo della cipolla (OYDV) e delle interazioni pianta-potyvirus”

Allium cepa L. è la specie più coltivata del genere *Allium* ed è una delle colture più diffuse al mondo. L'Italia ha una ricchezza di germoplasma di cipolla con oltre 80 varietà. Tra i virus, *Onion yellow dwarf virus* (OYVD) (genere *Potyvirus*) rappresenta lo stress biotico più importante della cipolla. Uno degli strumenti più efficaci per controllare le malattie virali è individuare cv resistenti o tolleranti da utilizzare nel miglioramento genetico delle piante.

Pertanto, 25 cv/ecotipi italiani ed una cv Texas early grano 502 (resistente a OYDV), sono stati caratterizzati valutando la loro risposta a OYDV per intensità dei sintomi, caratteri morfologici e perdita d'acqua del bulbo durante lo stoccaggio. 'Rossa di Tropea' e 'Texas early Grano 502' sono risultate le più tolleranti, mentre 'Acquaviva 7' la più suscettibile, seguita dalla 'Pera sanguigna di Peschici'. Gli effetti dell'infezione hanno portato ad un aumento dell'accumulo di acqua nei bulbi con conseguenti perdite d'acqua significative in conservazione. Su 15 delle cv/ecotipi in esame è stata effettuata una caratterizzazione genetica mediante 12 marcatori SSR, evidenziando che le cv tolleranti 'Texas early Grano 502' e 'Rossa di Tropea' sono filogeneticamente distanti dalle suscettibili 'Acquaviva 7' e 'Pera Sanguigna di Peschici'. Inoltre, sulle cv più sensibili e sulle più tolleranti a OYDV, si è valutata l'espressione dei geni eIF4E ed eIF4G, che la letteratura riporta come geni coinvolti nei processi di replicazione di molti potyvirus e quindi possibili target da utilizzare nello sviluppo della resistenza ai virus delle piante. Sebbene si siano evidenziate differenze significative nell'espressione tra cv suscettibili e/o tolleranti e tra piante sane ed infette, si può ipotizzare che OYDV nel suo processo di replicazione adotti percorsi diversi rispetto a quelli di altri potyvirus.

L'analisi RNASeq effettuata su campioni sani e infetti da OYDV ha consentito di ottenere risultati interessanti sugli effetti dell'infezione virale analizzando i geni

differenzialmente espressi (DEGs). Questo approccio ha evidenziato il potenziale ruolo dei geni appartenenti alla famiglia dei fattori di trascrizione (TF) WRKY in cipolla. I campioni infetti hanno mostrato pochi geni espressi in modo differenziale correlati alla dormienza durante lo stoccaggio a differenza dei campioni sani che hanno evidenziato un gran numero di DEGs. Inoltre, i profili trascrittomici e l'analisi della co-espressione hanno permesso di identificare nel WRKY-TF (*AcWRKY32*), un gene che potenzialmente guida il rilascio di dormienza nei bulbi di cipolla.

Lo studio sulle interazioni proteina-proteina, incentrato sull'identificazione dei fattori vegetali coinvolti nel movimento dei potyvirus, è stato effettuato mediante screening di proteine del melone correlate al sistema ESCRT e per la proteina virale WMV 6K2 mediante SUY2H. Successivamente, l'interazione *in-planta* della proteina XX4 di *Arabidopsis* vs la TuMV 6K2 mediante analisi BiFC, ha permesso di confermare il coinvolgimento della proteina ESCRT AtXX4 nei processi di replicazione e movimento di TuMV. L'analisi GFP ha permesso di caratterizzare la localizzazione subcellulare di AtXX4.

I nostri risultati hanno ampliato le conoscenze su OYDV in cipolla, consentendo le seguenti conclusioni. Sono stati evidenziati caratteri di resistenza/suscettibilità ad OYDV nella biodiversità delle varietà e degli ecotipi locali. È stata fornita una spiegazione su come le infezioni di OYDV siano il fattore principale per creare condizioni ottimali per i patogeni secondari. È stato dimostrato il ruolo di OYDV nell'interruzione della dormienza nel bulbo infetto grazie all'individuazione e caratterizzazione di alcuni TF della famiglia WRKY in cipolla. Infine, si sono poste le basi per comprendere il percorso di traslocazione di OYDV nella pianta, e per determinare se anche nel sistema cipolla-OYDV la proteina XX4 possa avere un ruolo biologico.

Parole chiave: *Allium cepa*, resistenza a OYDV, caratterizzazione genetica SSR, WRKY, RNAseq, DEG, BiFC.

General Introduction

1. *Allium* genus

1.1 General characteristics

The genus *Allium* has a significant economic importance since it includes a considerable number of vegetable species for human consumption and ornamental species. Is a large, monocotyledonous genus with more than 850 species (Deniz, 2015) of mostly perennial bulbs; the majority are found in the northern Hemisphere cross the Holarctic region from the dry subtropics to the boreal zone (Fritsch *et al.*, 2010). The second place for the richness of biodiversity is located in western North America, the only exception is *Allium dregeanum* which is native to south Africa (De Wilde-Duyfjes, 1976; de Sarker, 1997), obviously in these places a considerable number of subgroups with taxonomic characteristics often very different from each other has differentiated.

It is a large genus of perennial, mostly bulbous plants sharing some characteristics: rhizomes or bulbs with several tunics membranous, fibrous or coriaceous; basally arranged leaves that frequently covering the floral scape, umbellate inflorescences composed of few or many flowers, the flower colour usually is withe or rose to violet, and sometimes blue or yellow.

The superior ovary has three cells (locules) with two or more ovules per locule; there are often nectaries at the base of the ovary. Tepals are slightly differentiated in spirals, the stamens are in two whorls, sometimes basally connected, the style is single with slender, capitate or, rarely, trilobate stigma, rhomboid or spheroidal black seeds.

The reserve compounds consist of sugars, mainly fructans, and no starch.

Characteristic is an onion-like smell and taste due to the enzymatic decomposition products of several cysteine sulphoxides (Fritsch and Friesen, 2002).

The genus is diverse in cytology. predominant basic chromosome numbers $x = 8$ and $x = 7$ but other numbers ($x = 9, 10, 11$) and variation in ploidy also occurs (Xu *et al.*, 1998; Zhou *et al.*, 2007; Huang *et al.*, 1995; Traub, 1968; Friesen, 1992).

Most of which, are wild plants, and among the edible ones many are still harvested spontaneously, only a few, instead are cultivated and commercialized.

Evolution of the genus has been accompanied by ecological diversification. Most part of species grow in open site, with arid or moderately humid climates, some *Allium* species have adapted to many environments, from steppes to rocky soils, European forests, high mountain pastures in the Himalayas and central Asia, even some saline and alkaline environments are tolerated by some taxa (Hanelt, 1990). They are weakly competitive and therefore it is rare to find them in dense vegetation, however, there are some forest species - such as *A. ursinum* and also some pasture species, including *A. vineale* and *A. carinatum*.

The adaptation of *Allium* species in these different habitats has led to a large change in their growth rates in terms of growth, flowering and seed germination.

There are species with spring, summer or autumn flowering, with one or more annual cycles of leaf formation and also with continuous formation. The species can show summer or winter dormancy as an adaptation to arid or cold climates (Brewster, 2008).

For many species (“ephemeroids”), annual growth is limited to a very short period between spring and early summer, when the cycle from leaf sprouting to seed ripening is completed in 2 to 3 months.

For most species, seed germination appears to be limited to a few years, unless the seed is stored in cold and very dry conditions, where its life can be significantly extended (Fritsch and Friesen, 2002).

The *Allium* genus has a great economic importance and includes both ornamental and horticultural plants, with the exception of the seeds, all parts of the plants can be consumed. Harvesting in the past has caused a decline in wild resources, probably the use of wild plants and the introduction in orchards were among the main factors of the domestication process, and subsequently the selection led to the current plants (Hanelt, 1990).

Are part of the genus *Allium*, some bulbs of daily food use such as: shallot (*A. ascalonicum* L.), leek (*A. ampeloprasum* L.), onion (*A. cepa* L.), Welsh onion (*A. fistulosum* L.), garlic (*A. sativum* L.), chives (*A. schoenoprasum* L.).

As with many ancient cultivated plants, the amount of information regarding the evolutionary history of cultivated alliums is very limited. Some archaeological finds support the hypothesis that some species of *Allium* were cultivated in antiquity. However, it is impossible to follow these tracks because many plant names from that era cannot be assigned to particular plant species with certainty (Fritsch and Friesen, 2002).

1.2 Phylogenies and classification

The taxonomy of the genus *Allium* is still very confused with descriptions often incorrect (Li *et al.*, 2010), nowadays there are more than 850 species distributed in the northern hemisphere and 650 species synonymous, to which new ones are always added (Deniz,2015) (Gregory *et al.*, 1998). The *Allium* is one of the largest genera of monocots, also has a great variability (Li *et al.*, 2010), which greatly complicates the classification process (Storsberg *et al.*, 2003; Mabberley, 2008), a further difficulty derives from the fact that the genus has a remarkable polymorphism linked to an adaptation to different habitats. In addition, the traditional classifications were based on homoplasious characteristics (convergent evolution of similar characteristics in different species caused by the push of the same environmental pressures). Therefore, it is important to classify this huge number of species into smaller units or groups for practical purposes.

Some progress has been made using molecular phylogenetic methods, through the analysis of the internal transcribed spacer ITS1 and ITS2, one of the most commonly used markers in the study of the differentiation of *Allium* species (Li *et al.*, 2010; Deniz *et al.*, 2015).

In old classification systems, the *Allium* genus has been placed in the Liliaceae and Alliaceae but has recently been repositioned in the *Amaryllidaceae*. In the APG III classification system, *Allium* is placed in the family Amaryllidaceae, subfamily *Allioideae* (Reveal and Chase, 2011).

Linnaeus originally grouped his 30 species into three alliances (1753). Since then, numerous attempts have been made to divide the growing number of species into smaller groups.

Regel's subsequent treatise (1875) of *Allium*, divided his 262 species among the six sections proposed by Don (1832).

Subsequent studies have recognized an increasing number of infrageneric groups together with a greater number of species: 3 subgenera, 36 sections and subsections and about 600 species (Traub, 1968); 6 subgenera, 44 sections and subsections (Kamelin, 1973); in 1992 Hanelt *et al.* proposed a classification based on morphological, karyological, serological and ecological studies, it included 6 subgenera, 50 sections and subsections for 600-700 species (Hanelt *et al.*, 1992).

In 2006 has been described a new classification with 15 subgenera, 56 sections and about 780 species based on internal transcribed spacers of nuclear ribosomal gene (ITS) (Friesen *et al.*, 2006).

Subsequent studies have shown that compared to previous classifications, this classification is a significant improvement.

Banfi *et al.* (2011) resumed a classification based on three main monophyletic groups, believing that these are more immediate and appropriate for the identification of the main monophyletic taxa, suggesting that the phylogenetic trichotomy of the genus *Allium* sensu lato is sufficiently distinct to justify its subdivision into three separate genera.

The evolutionary lines correspond to the three main clades. The first clade (the oldest) *Nectaroscordum* Lindl. (type: *N. siculum*) with three subgenera is mainly bulbous, the second *Caloscordum* Herb. (type: *C. neriniflorum*) with five subgenera and the third *Allium* L. sensu stricto (type: *A. sativum*) with seven subgenera contains bulbous and rhizomatous taxa (Li *et al.*, 2010).

1.2.1 Evolutionary lineages and subgenera of *Allium* genus

Three evolutionary lineages and 15 subgenera are described according to the following classification scheme (Figure 1) (Friesen *et al.* 2006; Li *et al.*, 2010; Choi *et al.*, 2011).

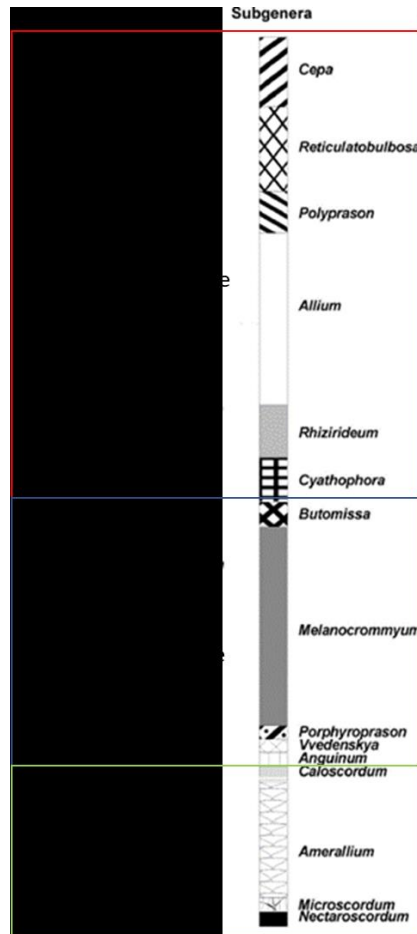


Figure 1. Evolutionary line of *Allium* genus (Friesen *et al.*, 2006)

First evolutionary line

This lineage is considered the oldest *Allium* line and most of the species are mainly bulbous, the other two have bulbous and rhizomatous taxa.

It is composed of three subgenera, but almost all belong to the subgenus *Amerallium* which is the third largest subgenus of the genus *Allium*.

With the exception of the subgenera *Nectaroscordum* and *Microscordum*, which have exclusively bulbous species, the *Amerallium* contains also some rhizomatous elements.

Second evolutionary line

Almost all the species in this lineage consisting of five subgenera are part of the subgenus *Melanocrommyum*, which is more closely associated with the subgenera *Vvedenskya* and *Porphyroprason*, the remaining two subgenera are *Caloscordum* and *Anguinum*. Of the five subgenera, *Melanocrommyum*, *Caloscordum*, *Vvedenskya* and *Porphyroprason* are bulbous and the remaining small subgenus *Anguinum* is rhizomatous (Fritsch *et al.*, 2010).

Third evolutionary line

The third evolutionary line contains seven subgenera and among them, there is the largest of the genus *Allium*: the subgenus *Allium*, which in turn also contains most of the species in its lineage (Figure 2).

The subgenera *Butomissa* and *Cyathophora* form a clade for the remaining five subgenera. Of the remaining five subgenera, *Rhizirideum* forms a medium sized subgenus which is the sister of the other four, *Allium*, *Reticulatobulbosa*, *Cepa* and *Polyprason* (Li *et al.*, 2010).

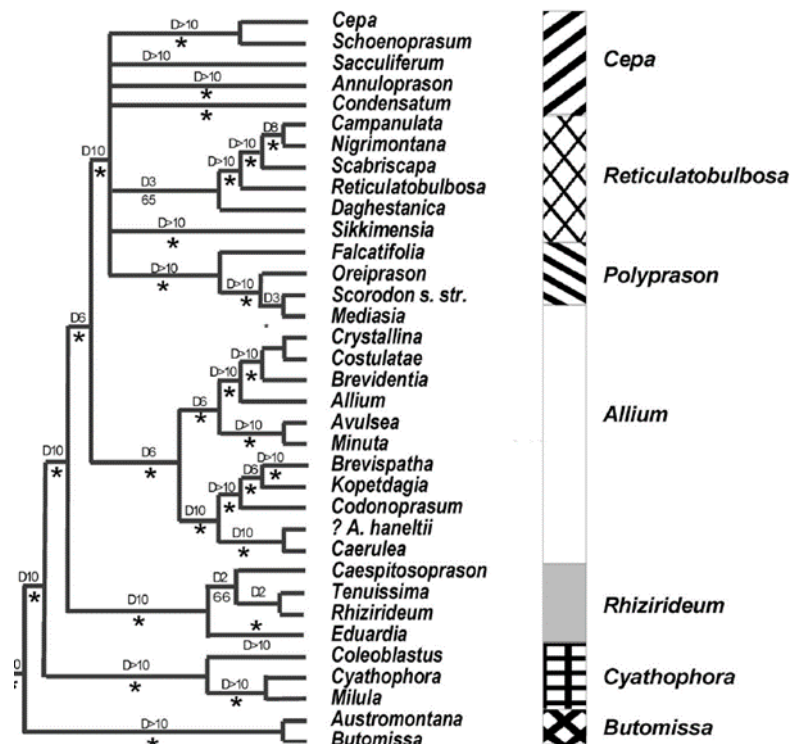


Figure 2. Third evolutionary line of *Allium* genus (Friesen *et al.*, 2006)

1.2.2 The *Cepa* section

Cepa section is part of the *Cepa* subgenus, the most divergent or advanced among the *Allium* subgenus, which includes the main onion crops, *A. cepa* and *A. fistulosum*; the *Sacculiferum* section, *A. chinense*; and the *Schoenoprasum* section *A. schoenoprasum* (Brewster, 2008).

It includes species with cylindrical and opposite fistulous leaves, some species have more or less flattened leaves.

The scape is fistulose and terminates with a head-like inflorescence. Flowers are campanulate, with capitate stigma. The ovary is trilobate with two ovules per locule, which develop into angular seeds (Agati, 1952).

The bulbs are mainly well developed, formed from several leaf bases covered by thin, dry skins with short vertical rhizomes, have not tunics reticular or fibrous.

During the growth a gradual reduction of the rhizome can be noticed, which finally leads to the basal plate, typical of the common onion (Fritsch and Friesen, 2002).

The wild species of this section grow within the Irano-Turanian floristic region, except *A. altaicum* and *A. rhabdotum*, which grow in the mountains of southern Siberia and Mongolia and in the eastern Himalayas, respectively (Hanelt, 1985; Friesen *et al.*, 1999b). The wild species of section *Cepa* are petrophytes, means they prefer, rocks, stony slopes, riverbanks, gravelly deposits and similar sites with a shallow soil layer. Their presence is not strongly correlated either to the soil's PH or mineral content of the soil.

This distribution pattern usually leads to the formation of small populations (Levichev and Krassovskaja, 1981; Hanelt, 1985), but cases of large populations have been reported (Hanelt, 1990).

Unlike some other *Allium* species in the same area, the species of the *Cepa* section are not ephemeroids, they have a fairly long annual growth period from spring to autumn, but in arid areas, induced by drought, they can show a weak summer dormancy. The growth of the leaves begins in the spring but could be limited by the low temperatures in the following autumn and winter.

All wild taxa in this section have a long juvenile phase, lasting 3-10 years, before flowers are produced (Hanelt, 1985).

These species have long been collected by local populations, who used bulbs and leaves for fresh consumption or as reserves for the winter. The continuous collection has led to the disappearance of local species and a reduction in the size of the population (Hanelt, 1990), leading to many endangered species. It is important that these species do not disappear, as they are a source of variability that could bring precious genes to crops, since all the wild species of the *Cepa* section are the secondary gene pool of *A. cepa* and *A. fistulosum* (Hanelt, 1985).

The evaluation and use of these genetic resources could significantly contribute to the genetic improvement of these species (Kik, 2002).

Grouping of the species

The *Allium cepa* section is composed of 12 species, most of which are used by man as a fresh or dried food, or for medical purposes. Most of the species except *Allium cepa* and *A. fistulosum* are not cultivated but are spontaneous species collected in nature (Gurushidze *et al.*, 2007), the *Cepa* Section has been carefully described at a morphological, biochemical and cariological level (Klaas, 1998), and with molecular analyses which have further demonstrated its classification (Pich *et al.*, 1996). The main specific morphological characteristics of the section have been described by van Raamsdonk and de Vries (1992 a, b).

On the basis of morphological and geographical differences, the species of the section were divided into 3 groups (Hanelt, 1985). However, the results of the crossing experiments (van Raamsdonk and de Vries, 1992a) and of the molecular analyses show *A. oschaninii* is a separate group from *A. cepa* / *A. vavilovii* evolutionary lineage (Friesen and Klaas, 1998).

Therefore, in 2002 the *Cepa* section was divided into four alliances: the *Cepa* alliance, the *Altaicum* alliance, *Galanthum* alliance and the *Oschaninii* alliance (Fritsch and Friesen, 2002).

1.2.3 The *Cepa* alliance

The species in this group have many characteristics in common with the species of the *Oschaninii* alliance such as white flowers with wide open tepals, but the flowers can also be greenish, there are a large number of cylindrical leaves, usually four to nine, initially flat or semi-cylindrical.

The plants of this alliance are mainly distributed in the Turkmen-Iranian region. This alliance includes *A. cepa* (the common onion), *A. vavilovii* and *A. asarense*.

Allium vavilovii M. Pop. et Vved. is an endangered species located in northeastern Iran and in the central region of Turkmenia. Like *A. oschaninii* it has a bubble-shaped hollow stem in the lower half, but the leaves are completely flat and crescent-shaped.

Molecular analysis has revealed that it is the closest known relative of the common onion and is completely interfertile with it (Kik, 2002; Friesen and Klaas, 1998; Fritsch *et al.*, 2001).

Allium asarense R.M. Fritsch et Matin. is among the most recently discovered species, identified in a single place west of Tehran, on rocky and steep terrain.

The leaves are semi-cylindrical, not swollen, a stem with a bubble-shaped hollow and small semi-globular umbel with small greenish brown flowers. Initially it was believed to be a subspecies of *A. vavilovii*, but through molecular analysis has been defined as a basal group of *A. cepa* / *A. vavilovii* evolutionary lineage (Friesen and Klaas, 1998; Fritsch *et al.*, 2001).

Allium cepa L. also known as onion bulb or common onion is the most important plant of the *Allium* genus grown worldwide.

2. *Allium cepa* L.

The onion, according to the APG (Angiosperm Phylogeny Group III), is classified as follows: Kingdom *Plantae*, Class *Monocotyledones*, Order *Asparagales*, Family *Amaryllidaceae*, Subfamily *Allioideae*, genus and species *Allium cepa* L.

Although it is the most important crop within the *Allium* genus, the origin and its wild ancestor is still unknown.

2.1 Historical information

Since the wild onion is extinct, the ancient testimonies on the use of onions embrace western and eastern Asia, but the geographical origin of the onion is still uncertain (Ansari, 2007; Cumo, 2015), with probable domestication throughout the world. Onions have been described in various ways as originating in Iran, from the subcontinent of western India and central Asia, it is assumed that our ancestors discovered and started eating wild onions long before agriculture or even writing was invented.

Since ancient times onion was an important vegetable for people around the world, used for both fresh food, cooked and dried; but also, for religious and medical practices. Traces of onions recovered in China in Bronze Age settlements suggest that onions were already used in 5000 BC, not only for their taste, but for the durability of the bulb in storage and transport, constituting part of the diet of those populations. The ancient Sumerians have cultivated and cooked onions 4000 years ago, as shown by the plant remains discovered in the royal palace of Knossos in Crete (Estes, 2000). More consistent evidence dates bring back to its domestication in ancient Egypt (3000 BC) (Maksouda *et al.*, 2011) where spherical shape and concentric rings of the bulb were symbols of eternal life and used in burials, as evidenced by traces of onion found in the orbits of Ramesses IV.

During the 1st century AD Pliny the Elder wrote on the use of onions in Pompeii, documenting that the Roman people believed in the onion's ability to improve eye ailments, help sleep and cure various pathologies, from oral sores and toothache to dog bites, low back pain and even dysentery.

Alexander the Great in the 4th century BC transported onion from Egypt to Greece, and from there it has been spread in Europe (Platt, 2003). In the following centuries, onions were grown all over Europe and at the beginning of the Middle Ages they became part of popular cuisine in places like Germany (Jones and Mann, 1963).

In the discovery's era, onion was brought to North America by European colonists, which found that the plant was already available and widely used in Native American gastronomy.

Onion is now grown all over the world in many varieties, sizes and flavors and has gained a permanent place in our current cuisine both raw and cooked and as a medicinal.

Genetic studies carried out more recently have only reported one species, *A. vavilovii* Popov & Vved, as a possible ancestor; it also seems possible that *A. cepa* is originated through the hybridization of *A. vavilovii* Popov et Vved. with *A. galanthum* Kar. et Kiror or *A. fistulosum* L (Fritsch e Friesen, 2002; Gurushidze *et al.*, 2007). Some evidence, points to Southwest Asia as the primary centre of differentiation of the *Allium cepa* L species, while the Mediterranean basin is only a secondary centre (Hanelt 1990; Fritsch e Friesen, 2002).

The wide variability within the *cepa* species suggested the use of different methods for subdivision into intraspecific groups; therefore a simple and informal classification was applied, similar to that proposed by Jones and Mann (1963), based on the division into three groups: Common onion group, Aggregatum group, and Ever-ready onion group (*proliferum* onoin). This approach is simpler and more advantageous than making exclusive reference to scientific taxonomy and nomenclature, characterized by rigidity.

The Common onion group includes the most economically important varieties of *Allium*, including local cultivars, ancient cultivars and modern F₁ hybrids spread in many regions of the world. Varieties in this group are seed or bulb reproduced and form a single large bulb. The demand for high quality and efficient production cultivars intensified the spread of F₁ hybrids, leading the increase of genetic

erosion. Nonetheless, there is still a large biodiversity in Northern India, Pakistan, Russia, Europe and the Mediterranean basin (Astley *et al.*, 1982).

The *Aggregatum* group includes varieties of less economic importance, they produce small and multiple bulbs that are aggregated together. The varieties of this group are grown mostly in private gardens in Europe, America and Asia, with the exception of the shallot which is the only cultivated for large-scale marketing and is the most important and representative of the *Aggregatum* group. In subtropical areas, some local types are cultivated to replace the real onion since they can be propagated vegetatively and have a very short growing cycle.

Ever-ready onion group includes plants with a remarkable vegetative growth and characterized by the quite absence of the dormancy period, in fact both bulbs and leaves can be harvested throughout almost all the year. They are eaten in salads and commonly grown in British gardens since the mid-20th century (Jones and Mann, 1963).

2.2 Botanical traits and agronomic techniques

Allium cepa is a bulbous, herbaceous, biennial cycle plant with a diploid chromosomal set ($2n = 2x = 16$). In the first year it develops leaves with sheathing shape at the base and tubular at the apical part. Vegetative growth depends on the photoperiod and is concluded by the bulb formation. During this process the reserve substances transferred to the base of leaves to constitute the bulb, the edible part, composed of a series of fleshy tunics strongly pressed together (4-8 mm thick).

Leaves and tunics are inserted on a very shortened stem (basal plate, disc, 1-2 cm wide), which inside the bulb has the vegetative apex who produce flower stems in the 2nd year.

The root system develops from the lower part of the disc, is mostly fasciculate and devoid of root hairs, the shape of the single root is tubular and white, most of them are found in the first 20-25 cm of soil.

The adult leaf consists of a tubular sheath that grows from a small ring on the disc and a slightly grooved hollow sheet. It has a circular section and is closed at the apex, provided with wax, and has a fleshy consistency and green colour.

Onion plant can form up to 14 leaves during vegetative growth, but due to natural senescence it loses up to 6 leaves, so it rarely has more than 8 leaves at the same time (Figure 3).

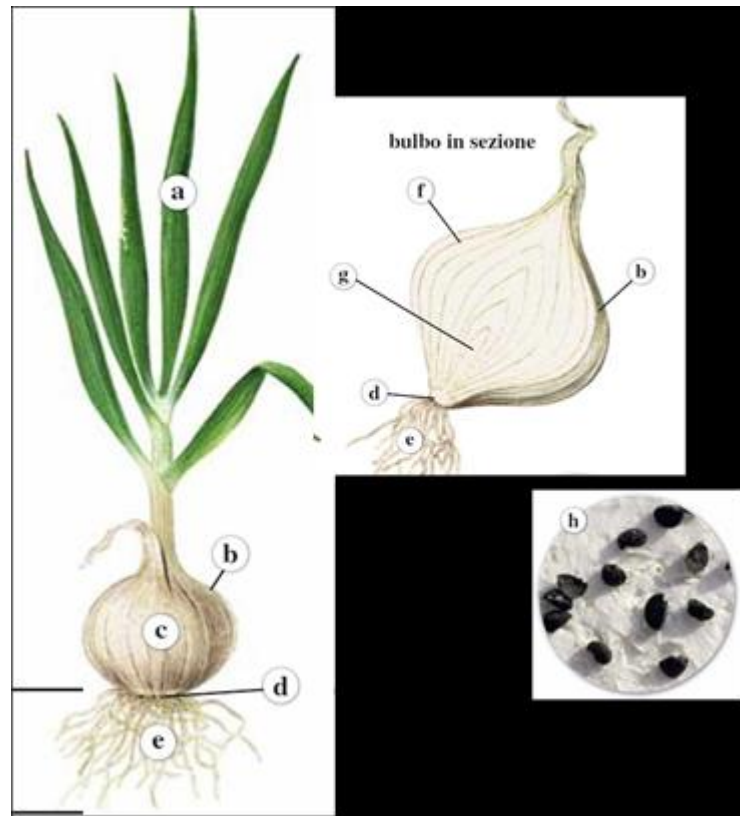


Figure 3. Onion morphology. a-leaves, b-outer tunics, c-bulb; d-disc, e-fasciculate roots, f-fleshy tunics, g-vegetative apex, h-seeds (Locatelli, 2009)

The reserve substances accumulated in the inner tunics nourish the buds during the first stages of their development when in the second year, they evolve into floral scapes with a variable height up to 1.5 m. Also, scapes are hollow, green in colour and end with a spathe.

The umbrella-shaped inflorescence is simple, dense and globular formed by a few hundred hermaphrodite flowers. The individual flowers consist of 6 petals, 6 stamens and 3 bilocular carpels. The fruit is a trilocular capsule containing 2 or 3 black seeds per locule.

Flowering is very gradual; it begins on the main scape and then continues on the lateral scapes. Onion is distinctly proterandry plant, that means a pollen formation anticipated to the stylus receptivity, therefore the fertilization is mainly allogamous and entomophilous by pollinating insects, mostly bees.

The formation of the bulb is essentially linked to the photoperiod, in general for the early varieties the critical minimum is about 12 hours of light, 13-14 for the medium-early and 15 for the late ones; with increasing temperature, the minimum critical decreases. This process continues for about 6-8 weeks simultaneously with the gradual drying of the first leaves. During bulb formation, the internal leaves remain in the form of fleshy tunics, contributing to the bulb's enlargement. In the final phase of the cycle there is the maturation of the bulb with the drying out of external protective tunics and the complete senescence of leaves. The plant folds on itself and although there is no more photosynthetic activity, the bulb can further increase in weight thanks to the translocation of the substances accumulated in the leaves.

Pedo-climatic needs and cultivation methods

Onion prefers medium-textured or even clayey soils, with a good amount of organic substance, well drained, with pH around neutrality. Sandy soils can be used under conditions of adequate pH and regular water supply. The depth of the soil, on the other hand, is not a limiting factor for the reduced development of the root system. It adapts to different thermal conditions, although in the case of low temperatures all the activity of the plant slows down. In fact, germination begins even with temperatures just above 0 °C while optimal temperatures range from 13-28 °C. For vegetative development, the minimum temperature is -8 / -11 °C.

The preparation of the soil is essential to avoid water stagnation that favours the development of root rot. The tolerance of onion to salinity is low, so acid soils (that do not make calcium available) and those that are too compact (that cause deformations of the bulb) are to be discarded. The phosphoric and potassium fertilization is carried out in pre-transplantation, while for the nitrogen fertilizations some distributed interventions are carried out, shortly after the transplantation and

in cover. Nitrogen deficiency is manifested by yellowing, and reduced size of the leaves and bulb.

The type of planting system depends on the surfaces used, the production area and the destination of the product.

Direct sowing is the most widespread technique in central and northern Italy and is carried out on large surfaces while the transplanting of seedlings is mostly used in the southern production areas. Transplantation in general allows more uniform productions, thanks to greater plant regularity, uniformity of growth and development of plants.

The use of small bulbs to obtain the more enlarged ones is the most widespread and appreciated agronomic technique; it is reserved for particularly valuable productions and crops in small areas. This technique reduces the crop cycle of one month and allows to obtain more uniform bulbs (MCP, <http://www.parco3a.org>).

2.3 Economic and nutritional importance

Onion is widely cultivated and used in the daily diet in different parts of the world. It is widely used in cooking, both raw and cooked, and is highly valued for its flavors and nutritional properties.

The medical uses, supported by clinical data, of onion are mainly linked to the prevention of senile cardiovascular alterations and in cases of inappetence. Onion is also rich in quercetin, an antioxidant flavonoid, the strong antioxidant action has been experimentally confirmed: it reduces the effect of free radicals and helps to prevent the damage associated with them. It also appears that it can stabilize cells in releasing histamine in the body.

Many studies have been carried out in the medical field regarding the beneficial effects of quercetin against diseases such as: asthma, allergies, heart disease, high cholesterol, hypertension, prostatitis, rheumatoid arthritis and cancer. Moreover, antiviral, antibacterial and antifungal properties of onion contents have been reported (National Onion Association, 2020; Suleria *et al.*, 2013). Onion is also rich in vitamin C, folic acid and proteins.

The onion is a crop of economic importance on a world scale, grown in about 175 countries, in a temperate, subtropical and tropical climate, with a positive trend in recent years both in terms of surface area and in terms of production.

In 2018 the world surface covered by this crop was 5.039.908 ha with a production of 96.773.819 tons (Figure 4).

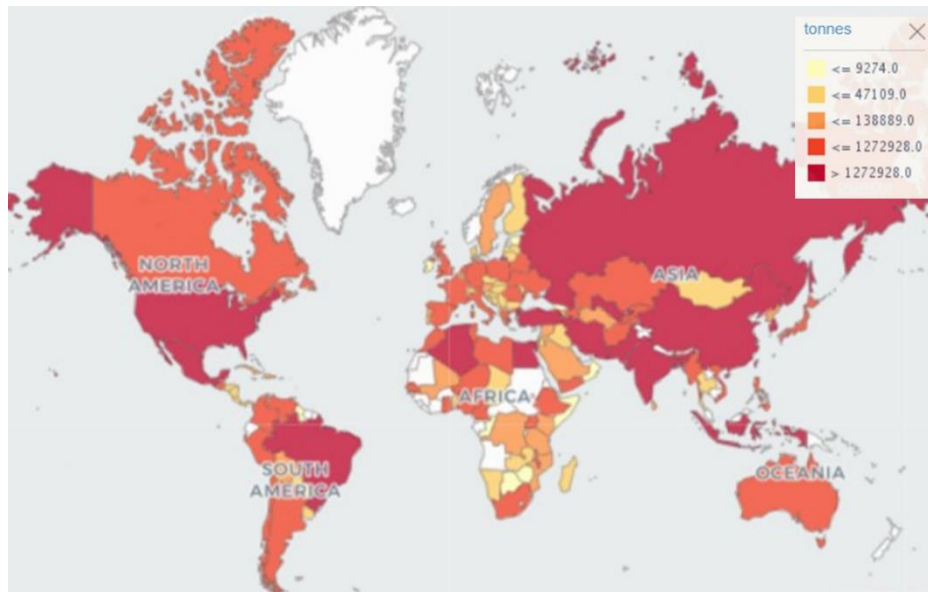


Figure 4. Onion world production (t) (FAOSTAT, 2018)

More than 67% of world onion production occurs in Asia, in particular the largest producer is China, followed by India and the United States; in Europe production is 9.3% with 8.953.700 tons (Figure 5) (FAOSTAT, 2018).

Production share of Onions, dry by region

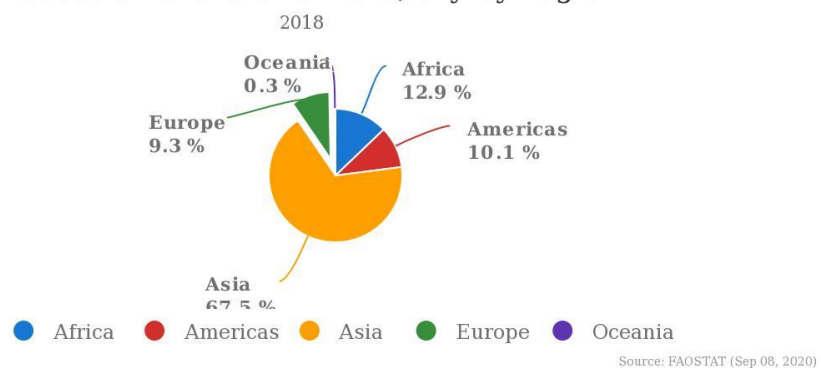


Figure 5. Top 5 Onion producers (FAOSTAT, 2018)

It is mainly marketed as a fresh or canned product but also as a preserved, frozen or dehydrated product.

In Italy, the onion represents an important vegetable crop with a production of about 372.183 tons on an area of about 13.224 ha which is located more in the north; Emilia Romagna is the region with the greatest production, followed by Molise, Puglia, Calabria and Veneto (ISTAT, 2020).

In Italy, there is a large number of local varieties and ecotypes and there are over 80 varieties registered in the National Register while more than 700 are registered in the European Register (Schiavi, 2012).

The varieties of onions differ one from each other for various criteria such as: morphological characteristics (shape, size of the bulb, color of the bulb); the photoperiodic needs necessary for the induction of bulb formation (short day, intermediate day, and long day varieties); the destination of the product (fresh, pickled or dehydrated).

Italy has a high wealth of germplasm with regard to local cultivars which differ both in the morphological and intrinsic characteristics of the bulb and in the cultivation areas (sometimes very restricted). Some cultivars of local importance are: Cipolla Ramata di Montoro (Campania), Cipolla Giarratana (Sicilia), Cipolla Rossa di Acquaviva delle Fonti (Puglia), Cipolla Borettana (Emilia-Romagna), Cipolla di Breme (Lombardia), Cipolla di Cannara (Umbria) and Cipolla Rossa di Tropea (Calabria).

3. Onion diseases

The onion crop is subject to various pathologies induced by abiotic or biotic agents that cause damage to production, which vary according to the location, the environment, the cultivar and the causal agent (Agosteo and Magnano di San Lio, 2005; Schwartz and Mohan, 2008).

The fungal diseases associated with onion are caused by fungal parasites that can affect the host both in the field and in post-harvest. The most important fungal diseases are, fusarium basal rot (*Fusarium oxysporum* f.sp. *cepae*); botrytis or leaf blight (*Botrytis* spp., *Botryotinia squamosa*); white rot (*Sclerotium cepivorum*); downy mildew (*Peronospora destructor* Berk).

Regards diseases caused by bacteria, most are associated with various types of bulb rot such as: soft rot (*Pseudomonas gladioli* pv *alliicola*); slippery skin (*Pseudomonas cepacia*) although some bacteria can cause wilting of the aerial part of plants such as bacterial blight (*Xanthomonas axonopodis* pv. *allii*) or affect both the aerial part and the bulbs such as leaf streak and bulb rot (*Pseudomonas viridiflava*).

Viruses are certainly among the most problematic pathogens since their control is mainly based on the use of preventive agronomic strategies and the use of virus-free propagation material.

3.1 General description of plant viruses

Viruses can be defined as infectious entities characterized by one or more molecules of a single type of nucleic acid that contain the information necessary for the synthesis of viral proteins and act as a template for the synthesis of new nucleic acid molecules. Nucleic acid, coated with a capsid protein, is capable of multiplying in living cells and causing infectivity (Luria and Darnell, 1970).

Viruses are devoid of ribosomes and enzymes, therefore they do not have their own biochemical and physiological activity, for this reason they are not considered living beings but macromolecules and are defined 'obligate parasites'. This means that they totally depend on the host cell for their life cycle, using systems metabolites of the plant itself. For this reason, viruses are a realm of their own.

Their replication is entirely due to the protein synthesis mechanisms of the host cell, the two constituents (nucleic acid and protein coating) are synthesized separately and only subsequently assembled to form new viral particles (Giunchedi *et al.*, 2007).

Once the viral particles of the pathogen have penetrated into the plant, they replicate quickly and colonize it. Some viruses are latent (do not induce symptoms), others are pathogens because cause mild or severe diseases, determining various morphological alterations (symptoms) and yield reductions.

The spread of the virus inside the plant induces alterations of its metabolism causing, after the incubation period, the appearance of symptoms, that is the effect of pathogen viruses (Walkey, 1985).

Symptoms appearance also depends on plant immunity, resistance or tolerance towards a virus.

In case of susceptible plants, symptoms caused by viruses are generally evident in all or some organs and they can vary intensity in relation to host plant (species and cultivar), virulence of viral strains and environmental conditions. In fact, in summer the symptomatic manifestations are less evident because high temperatures interfere negatively on virus replication. Virus infection in some cases can reach also reproductive organs as pollen and seed. In many plant species, symptoms may appear many years after infection if virus has a very long incubation period.

Normally, plant infected by virus shows mild or severe decline and all organs smaller than normal. The most common alterations caused by viruses are: stunting, yellowing, mosaic discolorations, dwarfing, leaf malformations, curling, blistering, mottling, variegations, necrosis.

While the absence of symptoms is a positive aspect, on the other hand plants with latent infections are sources of inoculum for susceptible species and, since are not easily identified in the field and or in a germplasm collection, they represent a serious threat.

In nature and in agricultural practice, the transmission and spread of viruses occurs by infected plant propagation and / or through vectors.

Transmission by plant parts

In this type of transmission virus passes directly without intermediaries from cells of infected plants to cells of healthy plants. The inoculation can occur directly by grafting an infected plant onto a healthy plant, during pollination (by infected pollen), through the use of infected propagation material (bulb, cutting, etc.) or indirectly through the use of non-sterilized tools.

Virus transmission can also occur by seed; in the past it was considered rare and of little importance for epidemiological purposes, but today it is considered an important way of spreading because virus remains infectious for years inside the seed and can be spread for large distances through trade.

Transmission by seed affects at least 20% of known viruses. Most viruses are localized in the embryo (embryonic transmission), less frequently they are localized on the seed coat or in the endosperm (Sastry, 2013). Those present on the seed coat can penetrate inside the seed through micro-lesions or in the germination phase.

Although in some cases the percentage of seed transmission seems of irrelevant epidemiological importance, a very few infected seeds can generate important epidemiological events. For example, pepino mosaic virus (PepMV), despite the rate of transmission by seed is rather low, equal to 0,057% (Hanssen *et al.*, 2010), is able to cause infection by simple contact during cultivation operations (Faggioli *et al.*, 2012).

Transmission by vectors

It occurs through different vectors, among which the most representative are insects, it can also occur through mites, nematodes, fungi (Hull, 2002).

A vector is an organism able of acquiring a virus from an infected plant, retaining it in its infectious form for a short or long time and inoculating it in other plants during its feeding preserving its biological functions (Giunchedi *et al.*, 2007).

The phytophagous insects come into contact with the virus during the tasting and feeding bites on infected plants and acquire it, subsequently the retention of the virus occurs in specific sites such as the oral apparatus or digestive system, finally the insect going to feeding will inoculate the virus on healthy plants. Depending on

the persistence of the virus and therefore on its ability to inoculate it, the vector can be non-persistent, semi-persistent and persistent.

Non-persistent viruses are transmitted exclusively by aphids, the acquisition and inoculation take place through trophic stings in few seconds, without a latency period. The infectious period is very short, and the ability to infect is rapidly lost unless the vector frequently feeds on infected plants.

In persistent transmission, viruses require long acquisition and inoculation times. In this type of transmission, a latency period is always required, and the infectious capacity of the vector can vary from several days to the remaining life of the insect. Persistent transmission is divided into circulatory or propagative. In circulatory transmission, the virus that has reached the alimentary canal overcomes the barriers of the intestine, penetrates the insect's body and accumulates in the salivary glands without increasing its concentration. Since in propagative transmission viruses multiply in the insect's body, increasing their concentration after acquisition, some of them can be transmitted to the insect progeny through eggs; in this case the transmission is called transovarian (Gray and Banerjee, 1999).

Semi-persistent viruses are transmitted by aphids, whiteflies, leafhoppers and coccidia, with intermediate modalities of the first two types. As for non-persistent, there is no latency and infectivity after a few days of acquisition; the virus is localized in the upper part of oral apparatus and it is lost after the moulting.

Usually there is a specificity between vector and virus; in fact, insects are able to transmit a limited number of viruses, sometimes even only one (Andret-Link and Fuchs, 2005).

3.2 Main viruses of Onion

The viral species, known to date, able to infect onion belong to the genera *Potyvirus*, *Tospovirus*, *Carlavirus* and *Allexivirus*. The species belonging to the genus *Potyvirus* and *Tospovirus* are the most relevant as they cause the greatest economic damage (Katis *et al.*, 2012).

Tospovirus

The *Tospovirus* genus is part of the *Tospoviridae* family and is the only genus of the family able of infecting plant species.

Members of the *Tospovirus* genus are among the most harmful viruses, causing significant production losses in a wide range of agricultural and ornamental crops worldwide (Mumford *et al.*, 1996). Their distribution is closely linked to the diffusion of their vectors (thrips), which also occurs through the commercial exchanges of plants and propagation material infested by these very small insects that easily hide inside the flowers and among the young leaves.

Tospoviruses are characterized by spherical viral particles, with a diameter of 80-120 nm, surrounded by an envelope of a lipid membrane in which two glycoproteins are incorporated, inside the virion is enclosed a genome consisting of three single filaments of RNA.

The most important Tospoviruses infecting onion are described below.

Tomato spotted wilt virus (TSWV) was first identified in tomato plants (Samuel *et al.*, 1930). On onion has been reported only in Georgia (USA) in mixed infection with IYSV, but its role remains to be determined (Mullis *et al.*, 2004; Gent *et al.*, 2006).

Impatiens necrotic spot virus (INSV) is the second identified species of the genus *Tospovirus* (Law and Moyer, 1990). It mainly affects ornamental plants and has been found sporadically in onion crops.

Iris yellow spot virus (IYSV), was first reported in *Iris hollandica* in the Netherlands (Cortes *et al.*, 1998), but in onion causes severe economic damage. It has been reported in several countries including Italy (Tomassoli *et al.*, 2009).

The virus is transmitted by onion thrips, *Thrips tabaci* Lindeman (Nagata *et al.*, 1999; Krizman *et al.*, 2001), no seed transmission has been reported (Bulajić *et al.*, 2009).

IYSV does not move systemically within the onion plant, but remains localized in limited portions (Smith *et al.*, 2006; Boateng and Schwartz, 2013) in

correspondence with the thrips bites, where it causes the characteristic rhomboid spot (diamond shape) chlorotic or necrotic, furthermore the lesions caused by the virus facilitate the establishment of other pathogens such as *Peronospora destructor* (Tomassoli and Turina, 2012). IYSV has been found in Calabria (Manglli *et al.*, 2012); even if caused damages were not important (Manglli *et al.*, 2020) it represents a serious threat for onion cultivations.

Potyvirus

Potyviruses represent one of the most important genera of plant viruses, with a wide geographical distribution, able to infect numerous crops and causing considerable economic damage. About 15% of known viral species belong to this genus. Potyviruses are transmitted in a non-persistent manner by more than 200 aphid species: each virus can be transmitted by more than one aphid species and each aphid species can transmit more than one viral species, thus making their control difficult (Gibbs *et al.*, 2008).

The genome of potyviruses consists of a single strand of RNA, 10.538 nucleotides long with positive polarity, which encodes a single polyprotein, divided into ten mature proteins (Gibbs and Oshima, 2010). There is also an additional and superimposed ORF called, PIPO “pretty interesting potyviridae ORF”, which plays an essential role in the intercellular movement of the virus together with the Cylindrical Inclusion helicase (CI), and the second 6K2 molecular-weight membrane anchoring protein (6K2) proteins (Chung *et al.*, 2008; Movahed *et al.*, 2017) (Figure 6).

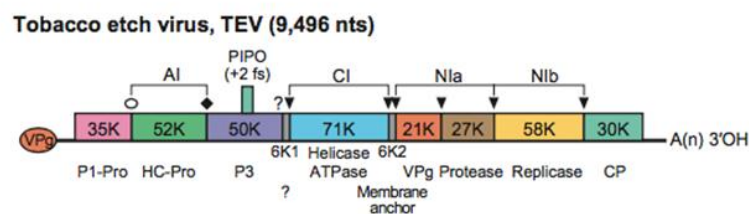


Figure 6. Genomic map of a member of the genus *Potyvirus*, using a strain of Tobacco etch virus as an example (Virus Taxonomy 9, ICTV)

The potyviruses that infect species belonging to the genus *Allium* are: *Onion yellow dwarf virus* (OYDV), *Leek yellow stripe virus* (LYSV), *Shallot yellow stripe virus* (SYSV) and *Turnip mosaic virus* (TuMV) (Van Dijk, 1993; Katis *et al.*, 2012).

Among these, OYDV is considered the most important as it causes the greatest economic damage (Van Dijk, 1993). It was first found in the United States of America in 1929 (Melthus *et al.*, 1929), with infection rates in the field above 90% in several countries (Conci *et al.*, 1992; Dovas and Volvas 2003; Hoa *et al.*, 2003). The first report of symptoms associated with OYDV in Italy occurred in 1993 (Marani and Bertaccini, 1993), confirmed by laboratory analyses in 2003 (Dovas and Vovlas, 2003). A recent survey showed that it is widely present in Calabria (Manglli *et al.*, 2020).

The host plants of this virus are limited to mainly onion and garlic (*A. sativum* L), but it can also infect shallots (*A. ascalonicum* L.), leek (*A. ampeloprasum* L) and other species. The virus survives in onion sprouts, plant residues and bulbs (Schwartz and Mohan, 2008; Katis *et al.*, 2012), is transmitted in a non-persistent manner by more than 50 aphid species (Drake *et al.*, 1993). Including *Myzus persicae* (Sulzer) (62.5%), *Aphis craccivora* (Koch) (46.87%) and *A. gossypii* (Glover) (53.31%) (Abd El-Wahab, 2009a, b; Kumar *et al.*, 2011).

It induces the folding, curling and twirling of the leaves and flattening, as well as longitudinal chlorosis; growth is stunted, it can cause dwarfing (Figure 7). The flower scapes also show similar symptoms of leaves, producing small inflorescences with a reduced number of seeds (Kumar *et al.*, 2012). Furthermore, on onion there is a reduction in the size and weight of the bulb up to 40% and loss of seeds up to 50% with a reduction in quality and germination (Kumar *et al.*, 2012; Elnagar *et al.*, 2011).

Two strains were isolated based on the specificity of the host, the first groups isolates referred to as OYDV-G that infect only garlic (Barg *et al.*, 1995). The isolates of the second group infect only onion and cannot be transmitted even artificially to garlic (Celli *et al.*, 2013). Molecular characterization demonstrated that the two strains are the same viral species (Manglli *et al.*, 2014).



Figure 7. Symptoms caused by OYDV (<https://www.plantevernleksikonet.no/l/oppslag/1521/>)

4. Molecular analyses on plant responses to OYVD

4.1 EIFs gene family expression

Most eukaryotic cellular mRNA harbor a 5' end cap (m⁷GpppN-) and a poly (A) tail, which leads to higher translation efficiency and greater stability of the mRNA. The cap structure serves as the binding site for eukaryotic translation initiation factor 4F (eIF4F).

The eIF4F consists of two subunits: eIF4E cap-binding subunits and eIF4G (Gingras *et al.*, 1999). In plants, an eIF4F isoform was identified, called eIFiso4F. eIFiso4F consists of a cap-binding subunit eIFiso4E and eIFiso4G (Browning *et al.*, 1996).

The eIF4G and eIFiso4G interact not only with eIF4E and eIFiso4E, respectively, but also with eIF4A, eIF3 and the poly (A) binding protein. As well, the eIF3 recruits the 40S ribosomal subunit, while eIF4A is a DEAD-box RNA helicase that carries out the 5' UTR of the mRNA to facilitate binding of the 40 S ribosomal subunit to the 5' UTR. After binding to the 5' UTR, the 40S ribosomal subunit migrates in a 5' to 3' direction towards the initiation codon, where the 60S ribosomal subunit binds and translation begins (Browning *et al.*, 1996, Gingras *et al.*, 1999). Through the association of the poly (A) tail, the poly (A) binding protein, eIF4G, eIF4E and the 5' capped polyadenylated mRNA is thus circularized (Wells *et al.*, 1998; Sachs, 2000). This mRNA circularization is believed to contribute to the improvement of synergistic translation by the cap and poly (A) structures.

Plant viruses encode several essential proteins (e.g., coat proteins, movement proteins, replication enzymes), but their coding capacity is limited and they must rely on host factors for every stage of the infection cycle (Sanfacon and Jovel, 2007; Nagy and Pogany, 2012; Wang, 2015). In particular, since viruses do not normally encode canonical translation factor, they developed a wide spectrum of strategies to hijack translation factors from their hosts favouring the translation of viral RNAs to the detriment of endogenous mRNAs (Zhang *et al.*, 2015; Simon and Miller, 2013).

The mRNAs of many RNA viruses lack the 5' cap, the 3' poly (A) tail or both, but they are stable and efficiently translated into the host cell cytoplasm through mechanisms that have evolved for each virus (Gallie, 1996). For example, genomic RNAs from cucumber mosaic virus (CMV), tobacco mosaic virus (TMV), and bromine mosaic virus have a 5' cap but lack a 3' poly tail (A), by contrast their 3' UTRs contain structures similar to typical tRNA loops. The 3' UTRs of TMV RNA and bromine mosaic virus contain sequence elements that increase translation efficiency.

RNA translation of some viruses is highly dependent on a sequence that functions as a cap-independent translation enhancer (TE) in the 3' UTR, and eIF4F is involved in this' enhanced translation 'by 3' TE in vitro (Wang *et al.*, 1997).

The virus replication depends on the host translation system and many other of their functions. The loss of one of these factors results into resistance to the virus (Yoshii, *et al.*, 2004).

Indeed, several wild-type genes corresponding to recessive mutations that confer resistance to viruses were identified, and they are considered necessary for viral replication (Tsujiimoto *et al.*, 2003, Yamanaka *et al.*, 2000).

Several studies showed that preferred factors involved in virus replication are the eukaryotic translation initiation factor (EIF), in particular the isoforms *eIF4E* and *eIF4G* (Wang and Krishnaswamy, 2012; Le Gall *et al.*, 2011; Robaglia and Caranta, 2006; Maule *et al.*, 2007; Duprat *et al.*, 2002, Lellis *et al.*, 2002, Ruffel *et al.*, 2002). Translation of eukaryotic mRNAs depends on the binding of *eIF4E* to their 5' m⁷G cap structure and it is also enhanced by interaction of the polyA-binding protein (PABP) with their 3' polyA tail. The large *eIF4G* scaffold protein binds to both *eIF4E* and PABP promoting circularization of mRNA. The tight association between *eIF4E* and *eIF4G* constitute the core of the eIF4F complex, despite other interaction with other *eIF4* isoforms occurred (Sanfaçon, 2015).

The family *Potyviridae* is one of the largest families of plant viruses and includes many economically important pathogens of cultivated crops, especially members of the genus *Potyvirus* (Gibbs and Ohshima, 2010). Cultivated crops and wild plant species have co-evolved with potyviruses, resulting in development of recessive resistance in plants and/or virulent isolates that have adapted to circumvent the

recessive resistance, in both cases involving mainly the eIF4F complex (Charron *et al.*, 2008; Moury *et al.*, 2014).

Thus, one strategy to select resistant/tolerant crop varieties to potyvirus involved the smart design of new resistances based on disrupting the interaction between potyviruses and *eIF4E/iso4E* (Truniger and Aranda, 2009).

Natural recessive resistance to potyviruses is generally associated with mutations of *eIF4E* or *eIFiso4E* that hinder their interaction with the viral protein genome-like (VPg). Most of these mutations have been mapped to two surface-exposed regions of *eIF4E* near the cap-binding pocket (Charron *et al.*, 2008; Moury *et al.*, 2014).

Indeed, silencing the *eIF4E* isoform by transgenic expression of small intron-spliced hairpins with homology to the endogenous gene resulted successfully used as an alternative approach to engineer resistance to one or several potyviruses (Mazie *et al.*, 2011; Rodriguez-Hernandez *et al.*, 2012; Wang *et al.*, 2013). Overexpression of mutated *eIF4E* (or *eIFiso4E*) alleles has been validated as an efficient technology to transfer resistance from one crop to another (Cavatorta *et al.*, 2011; Duan *et al.*, 2012; Kang *et al.*, 2007; Kim *et al.*, 2014), it is also reported that the overexpressed recessive allele conferred dominant resistance (Kang *et al.*, 2007). The potyvirus VPg protein interacts exactly with either eIF4E or eIFiso4E and this specificity is influenced by the specific host-virus combination and can even vary from one virus strain to another (Estevan *et al.*, 2014; Nicaise *et al.*, 2007; Sato *et al.*, 2005; Schaad *et al.*, 2000). As a result, mutation of a single eIF4E isoform is often sufficient to provide resistance to a target potyvirus.

Nevertheless, virulent potyvirus isolates have been described that overcome recessive resistance genes corresponding to *eIF4E/iso4E* alleles. In most cases, virulence has been mapped to mutations in the VPg protein (Ayme *et al.*, 2006; Ayme *et al.*, 2007; Moury *et al.*, 2004). Although in some cases, mutations in the VPg increase its binding affinity to the resistant *eIF4E/iso4E* protein (Charron *et al.*, 2008), in other cases it does not (Gao *et al.*, 2004). In at least one case, mutation of VPg does not increase its affinity for other *eIF4E* isoforms either, eliminating the possibility that other isoforms of *eIF4E* are used by the virulent virus (Gallois *et al.*, 2010).

One of the main challenges for plant breeders is to identify new sources of resistance to pathogens. Wild crops are the main source of these resistances, which can be monitored through direct phenotyping of core collections with the pathogen. However, this approach takes more time and resulted very expensive thus, allele isolation, which involves the search for “polymorphism within the genes of interest”, represents a complementary approach to plant phenotyping to isolate new sources of resistance to pathogens in natural variation (Lebaron *et al.*, 2016). Viruses harbor a particular small genome and rely on host factors for infecting them (Fraser, 1990). Hence, the polymorphism within those host factors could be linked with plant resistance, a mechanism defined as loss of susceptibility (Pavan *et al.*, 2010; van Schie and Takken, 2014).

4.2 Differential gene expression (DEG) analysis after bulbs OYVD infection

Onion bulb quality as flavour and pungency can change during time due to bulb dormancy, water loss and disease susceptibility. Mainly, bulb dormancy is one of the main factors of postharvest life, thus an early sprouting during storage can cause a drastic loss of quality (Kopsell and Randle, 1997).

Onion dormancy includes three major stages, rest, dormancy, and regrowth (sprouting) (Sharma *et al.*, 2016). After harvest, onions show a rest period without any responses to rapid environmental change, with a break in the cellular activity and low activity of endogenous hormones (Sharma *et al.*, 2016). Later, as the bulb matures the development and expansion of new leaves is blocked, the pseudo stem becomes soft by collapsing, and the onion bulb enters into its dormancy stage, responding in a differential manner to environmental change during early and later stage. Dormancy can be considered as a physiological stage in the bulb life cycle from flowering to the sprouting start, showing two different phases: the endo-dormancy (during spring), subject to the conditions within the bulb and, once the endo-dormancy period is over, the eco-dormancy (during summer), depending on external environmental factors (Chope *et al.*, 2012), prevents the sprouting. Dormancy release is characterized by nutrient mobilization and cell elongation of

sprout leaves (Pak *et al.*, 1995), while the regrowth (external sprouting) starts when the sprout grows over the neck of the mature bulb harvested (Brewster, 2008).

Significant differences about dormancy timings among and within *Allium* species were reported (Kopsell and Randle, 1997). Among others, pathogens infection showed a key role in modulating and altering bulb dormancy, causing a premature sprouting and bulbs rooting, with a rapid decay during storage and shorter shelf life (Davidson, 1958; Dafni *et al.*, 1981; van Dijk, 1993; Kamenetsky and Rabinowitch, 2006; Katis *et al.*, 2012; Sharma *et al.*, 2016).

Among viruses, onion yellow dwarf virus (OYDV) is a potyvirus that infects various plants from the *Allium* genus, causing a high number of symptoms like leaf striping and growth reduction that lead to high yield loss. Thus, OYDV is considered one of the most economically important virus diseases causing loss of storage quality in onion bulbs worldwide (Katis *et al.*, 2012).

Several studies described the cross-talk among different hormones related to dormancy release, non-structural carbohydrate reserves mobilization, and external sprouting (Davis *et al.*, 2007, Cools *et al.*, 2011; Chope *et al.*, 2012). Particularly, sprout elongation is promoted by cytokinins (CKs) and gibberellins (GA) whilst abscisic acid (ABA) shows an antagonist action. Matsubara and Kimura (1991) highlighted the ABA accumulation during bulb growth followed by a progressive depletion just after harvest, with the lowest level recorded with beginning of sprout elongation (Chope *et al.*, 2006). However, although many physiological and biochemical changes take place during bulb dormancy, the key molecular mechanisms and transcriptional factors involved are not well understood in onion. Transcription factors (TF) family genes showed a central role in plants responses to stress allowing to refashion gene expression patterns throughout the bind to specific DNA sites frequently in gene promotor region (van Verk *et al.*, 2008). Among others, *WRKY* gene family is an important class of transcriptional regulators harbored a highly conserved domain of 60 amino acid residues (Eulgem *et al.*, 2000; Zhang and Wang, 2005). Many *WRKY* family members play a key function into biotic and abiotic stress responses (Tao *et al.*, 2009; Wang *et al.*, 2014; Li *et al.*, 2016; Viana *et al.*, 2018; Wang *et al.*, 2019). Besides, *WRKY* genes have a pivotal role also in important plant physiological processes, such as embryogenesis (Lagacé

and Matton, 2004), seed germination and dormancy (Xie *et al.*, 2007; Ding *et al.*, 2014; Chen *et al.*, 2016), flowering time (Li *et al.*, 2016) and fruit ripening (Cheng *et al.*, 2016). In *Arabidopsis* *AtWRKY18* and *AtWRKY53* mediated a signaling pathway driving the leaf senescence (Potschin *et al.*, 2013); Ding *et al.* (2014) demonstrated that *WRKY41* regulate *ABI3* expression and seed dormancy in collaboration to abscisic acid. Up to now, large efforts were focused to identify the members of *WRKY* gene family in several plant species (e.g. Guo *et al.*, 2014; Yang *et al.*, 2017; Wang *et al.*, 2019), but the characterization and organization of *WRKYs* in onion and their involvement in bulb dormancy is until now unknown.

5. Molecular plant-virus interactions

5.1 Replication and cell-to-cell movement of potyviruses are connected processes

In order to spread throughout the plant, plant viruses must move from the site of replication within the cell to reach plasmodesmata (PD, typical membranous nano-channels connecting nearly all plant cells), cross them to enter the adjacent cells (cell-to-cell movement), to finally reach the elements of the phloem for systemic movement (Schoelz *et al.*, 2011). Although a distinction is generally made between intra- and intercellular movement, it is difficult to separate both. For example, since the endoplasmic reticulum (ER) network stretches from the cytoplasm, through the PD, and into the next cell, a virus may utilize this network for both intra- and intercellular transport (Pitzalis and Heinlein, 2018). However, despite this continuity, the SEL (Size Exclusion Limit) of PD constitutes a physical barrier that must be overcome by a virus to successfully move from cell-to-cell.

Since the viral nucleic acid or viral particles are too large to passively cross the PD autonomously, plant viruses encode a class of proteins called movement proteins (MP) that interact with host proteins to modify the PD for cell-to-cell transport of the viral genome (Heinlein, 2015).

Few information is known about the movement process of *Potyviridae* and of the genus *Potyvirus* in particular. Unlike other viral genera, no specific potyviral MP dedicated to movement has been identified, but several viral multifunctional proteins were reported to participate in the movement of potyviruses (Sorel *et al.*, 2014). Genetic, biochemical and ultra-structural studies have shown in particular the fundamental role in the cell-to-cell movement of potyvirus of three viral proteins: Cylindrical Inclusion helicase (CI), P3N-PIPO (Pretty Interesting Potyviridae ORF) and the second 6K molecular-weight membrane anchoring protein (6K2). Vijayapalani *et al.* (2012) showed that P3N-PIPO is located at the PD and is able to promote its movement through cells. Moreover, it can also direct the CI protein towards the plasmodesmata through the secretory pathway (Wei *et al.*, 2010).

The CI is a multifunctional scaffolding protein that participates in different stages of potyvirus infection (replication, translation, virus movement) (Sorel *et al.*, 2014). This protein forms cylindrical inclusions in the cytoplasm near PD in infected cells and is associated with nearby cone-shaped structures. For turnip mosaic virus (TuMV), cellular studies confirmed the crucial role played by CI, P3N-PIPO and 6K2 proteins in the cell-to-cell movement of potyvirus (Movahed *et al.*, 2017). In particular, the protein 6K2 of TuMV is a membrane protein involved in endomembrane rearrangements for the generation of viral compartments important not only for replication (Beauchemin *et al.*, 2007), but also for intracellular and intercellular movement (Cotton *et al.*, 2009; Grangeon *et al.*, 2013; Jiang *et al.*, 2015). TuMV therefore represents one rare example of plant viruses able to utilize the host endomembrane system to develop membranous complexes mobile between cells, reminding of animal viruses that utilize membrane-derived vesicles for budding from an infected cell and entry into healthy cells. In particular, TuMV infection reorganizes the host cell endomembrane system with the formation of at least two types of structures: *i*) a large perinuclear globular structure which is an amalgamation of ER, Golgi bodies, COPII coatomers, and chloroplasts. This contains also vRNA as well as viral proteins (6K2, VPg-proteinase, the RNA-dependent RNA polymerase CI) and host proteins, such as eukaryotic translation initiation factors; *ii*) peripheral motile ER-derived vesicles that traffic on transvacuolar strands and actin filaments toward PD and move through these channels to the neighbouring cells (Cotton *et al.*, 2009; Wan *et al.*, 2015). Altogether those results suggest that the replication and movement are processes probably acting in a coordinated way for TuMV. Indeed, Tilsner and Oparka (2012) proposed a model for coupling of movement and replication of viruses. Their review gathers multiple examples of viral MPs associated with vesicle replication complexes (VRCs) and shows how this localization is correlated with viral cell-to-cell movement.

5.2 Components of the vesicle trafficking machinery are implicated in the replication and movement of plant viruses

During plant infection, positive-stranded RNA viruses use the membranes of various host organelles, such as ER, chloroplasts and mitochondria, to induce the formation of a specialized compartment, the viral replication complex (VRC). This compartment protects viral RNA transcription and replication activities (Nagy and Pogany, 2012; Laliberté and Zheng, 2014; Romero-Brey and Bartenschlager, 2014; Shulla and Randall, 2016). Several plant viruses are known to interact with components of membrane trafficking complexes for their own benefit, facilitating the transport and replication of the viral material. For example, the tombusvirus tomato bushy stunt virus (TBSV) interacts through its replicase protein with members of ESCRT (endosomal Sorting Complex Required for Transport), a complex involved in endosome life cycle mediating vesicle formation (Panavas *et al.*, 2005; Jiang *et al.*, 2006). The recruitment by TBSV of the proteins of the ESCRT complex seems fundamental for the formation of VRC, which could allow the virus to avoid recognition by the host defense system and / or prevent the destruction of RNA viral by the gene silencing mechanism (Barajas *et al.*, 2009). The endosomal sorting complex required for transport (ESCRT) is involved in the multi-subunit membrane remodelling. It plays essential roles in the formation of multivesicular bodies (MVB) and the sorting of ubiquitinated membrane proteins into their intraluminal vesicles for degradation upon the fusion of the MVB and the vacuole (Raiborg and Stenmark, 2009; Henne *et al.*, 2011; Cui *et al.*, 2016).

Vesicular traffic controls the communication between the cells and the extracellular environment also controls the structures of the intracellular compartments (Reyes *et al.*, 2011; Paez Valencia *et al.*, 2016).

Very interestingly, vesicular endocytosis and plasmodesmata may share some regulatory mechanisms regarding virus movement. Indeed, Giner *et al.* (2017) showed that a mutation in the *Vacuolar Protein Sorting 41* gene (*VPS41*) in cucumber prevents the systemic infection of the cucumovirus cucumber mosaic virus (CMV) by restricting the virus to the bundle sheath cells and impeding CMV loading to the phloem. VPS41 protein is involved in vesicle trafficking from late

Golgi to the vacuole and therefore could be involved in the systemic movement of CMV (Giner *et al.*, 2017).

For potyviruses and TuMV in particular, two recent publications showed that the 6K2-induced TuMV replication vesicles could take an unconventional cellular pathway that may involve prevacuolar/MVB for virus infection (Cabanillas *et al.*, 2018). In particular, a MVB-localized VPS10-interacting protein 11 (Vti11) was shown to play a critical role in TuMV replication and systemic infection in Arabidopsis. This protein was also found within the proteome of extracellular vesicles (EVs) isolated from Arabidopsis. The EVs can be derived from MVB intraluminal vesicles that are released upon fusion of the MVB boundary membrane with the plasma membrane (Rutter and Innes, 2018). The hypothesis proposed by Cabanillas *et al.* (2018) is that given its localization to MVBs, Vti11 would allow the release of TuMV-vesicles in the extracellular space. This would represent a big change of paradigm and a novel pathway for intercellular movement of plant viruses. This hypothesis was supported by the recent study of Movahed *et al.* (2019) who showed that TuMV-EVs (containing replication complexes) are released in the extracellular space. Proteomic analyses of these EVs revealed the presence of TuMV and host proteins. This discovery makes a new point of view about the presence of viral component located outside plant cells and highlights the implications of extracellular vesicles in viral infection (Movahed *et al.*, 2019). How exosomes contribute to systemic viral infection in plants and which are the molecular players involved in this vesicle transport pathway in plants is still an exciting domain of investigation.

Organization and Aims of research

The onion (*Allium cepa* L.) is the most cultivated species of the genus *Allium*. It is one of the oldest crops and the third largest crop in terms of cultivated hectares in the world (FAOSTAT, 2018). Italy has a high wealth of germplasm about the local cultivars that differ both for the morphological and organoleptic traits of the bulb and for the cultivation areas (sometimes very restricted). There are over 80 varieties recorded in the Italian National Register, while more than 700 are registered in the European Register (Schiavi, 2012).

Onion cultivations are threatened by abiotic (salinity, heat, etc.) and biotic stresses (insect pests, fungi, viruses, etc.) that greatly reduce crop yield. Mahy and van Regenmortel (2009) reported that each year global crop suffers of 10–15% yield reduction due to pathogenic viruses.

Onion yellow dwarf virus (OYDV), belonging to the *Potyvirus* genus, has been reported as the most common virus on onion and *Allium* species, causing harmful effects on the yield and quality of the bulb (Kumar *et al.*, 2012; Elnagar *et al.*, 2011). In Calabria (southern Italy), it was detected for the first time on ‘Rossa di Tropea’ onion (Parrella *et al.*, 2005), more recent research highlighted its presence in the same area showing severe damages caused by this virus (Manglli *et al.*, 2020).

Among the main agronomic means to control OYDV infections (as to adopt crop-free periods, rotations, vector management and the removal of infected plants), the virus-free propagation material (bulbs and seeds) utilization appears the most important. However, virus management strategies are difficult to be effective for long time because of particular factors associated with virus disease epidemiology, such as unpredictable vector migration and virus host-range expansions (Loebenstein and Katis, 2014).

Thus, the efforts to search virus-resistant or tolerant varieties of cultivated species and the improvement of host plant resistance against plant viruses are strongly pursued. Indeed, the use of genetic resistance by increasing plant cellular immunity against pathogens is wisely the most effective strategy, mainly for viral diseases (Whitham and Hajimorad, 2016).

In view of above, the first aim of the PhD thesis was to evaluate the response of several Italian varieties/landraces towards OYDV infection in terms of resistance/susceptibility phenotype.

The selected Italian onion local cultivars/biotypes, including the only known resistant cultivar 'Texas early grano 502', were characterized evaluating their response towards OYDV by symptomatology, morphological features and bulb water losses.

Genetic characterization and cluster analysis of sixteen Italian varieties were also carried out to study their genetic similarity and eventually correlate it with their behaviour towards OYDV.

Since plant viruses have a limited coding capacity, they strongly depend on host factors (Sanfacon and Jovel, 2007; Nagy and Pogany, 2012; Wang, 2015). Viruses do not normally encode translation factors to translate their RNAs, but the use of these factors from their hosts have been reported (Zhang et al., 2015; Simon and Miller, 2013). Many recessive resistance genes have been mapped to the isoforms of the eIF4E and eIF4G genes that generally interact with RNA or viral proteins (Wang and Krishnaswamy, 2012; Le Gall *et al.*, 2011; Robaglia and Caranta, 2006; Maule *et al.*, 2007). Failure of host resistance has also been attributed at viruses and cellular translation factors incompatibility (Calvo *et al.*, 2014; Nieto *et al.*, 2011). Mutation or down-regulation of translation factors have been reported as new sources of resistance to plant viruses (Sanfacon and Jovel, 2007; Wang and Krishnaswamy, 2012).

Therefore, the gene expression analysis of the eukaryotic translation Initiation Factors, eIF4E and eIF4G, was carried out on onion leaf and bulb from the varieties selected as tolerant/susceptible in this research.

Furthermore, a RNA-seq experiment was carried out between virus-free and OYVD-infected onion bulb to detail the Differentially Expressed Genes (DEGs) involved in the virus-infection that laid to underline the differences in the post-harvest dormancy between onion infected and non-infected bulbs. More interestingly, for the first time WRKY family members in onion (*AcWRKY*), by using transcriptome data *de novo* assembled and mapped on draft onion genome were identified.

Finally, the isolation of *AcWRKYs* potentially involved in onion bulb dormancy release through uninfected/OYDV infected profiles comparison, exploiting the alteration induced by virus in the onion life cycle as filter.

The last year of the thesis was performed at the French National Research Institute for Agriculture, Food and Environment (INRAE) in the centre of Nouvelle-Aquitaine-Bordeaux, under the supervision of Dr. Sylvie German-Retana. The aim of this research period was to participate in the functional validation of candidate plant factors potentially involved in potyvirus movement, one of the key steps in viral infection, by notably focusing on the role of plasmodesmata (PD) and proteins involved in the secretory pathway in this process. The rationale was that the host genes encoding those factors could be excellent targets to develop resistance: their modification should be associated with limited expansion of the virus within the plants as well as reducing the risk of resistance-breaking viral isolates emergence. Since potyviruses have developed strategies to hijack the host secretory pathway and PD for their transport, one of the aims was to identify the host proteins among membrane and plasmodesmata proteins, that interact with key potyviral baits involved in cell-to-cell movement (here the 6K2), using the plant pathosystem *Arabidopsis*-TuMV.

In particular, in the frame of a collaboration between INRAE-Bordeaux and INRAE-Avignon together with a private company (Gautier Semences, France), a candidate approach focused on one ESCRT protein (named XX4 for confidentiality) was performed. This gene was reported in the literature as a good candidate potentially involved in the replication and movement of a melon-infecting potyvirus species, the watermelon mosaic virus (WMV).

In this context, the main aim of PhD internship were to perform functional assays: *i*) to check whether XX4 and other ESCRT proteins interact with the WMV-6K2 protein *in vivo* (Yeast) through Split Ubiquitin Yeast Two hybrid (SUY2H) system, *ii*) to analyse *in planta* the interaction of *Arabidopsis thaliana* XX4 (AtXX4) with TuMV-6K2 using Bimolecular fluorescent Complementation assay (BiFC) and confocal microscopy *iii*) to characterize the subcellular localization of AtXX4 protein in healthy plants and TuMV-infected plants using the model plant *Nicotiana benthamiana*.

Chapter 1. Genetic characterization and analysis of onion populations' response to OYVD

1. Materials and Methods

1.1 Plant material

Twenty-five Italian onion local cultivars retrieved from cooperatives, European and Italian germplasm collection, nurseries and Italian Universities were selected for this project focusing mainly on varieties coming from southern Italy, with major interest on local and typical variety (Table 1). Among them, twelve accession of 'Acquaviva' and two populations of 'Rossa di Tropea' (RC and VV) were analysed. 'Texas early grano 502', a commercial cultivar reported to be OYDV resistant (Idris *et al.*, 1997), was included in the analyses.

Table 1. Twenty-six onion cultivars/ecotypes/populations tested for OYVD infection

<i>Cultivar/ecotypes</i>	<i>Germplasm collection</i>	<i>Origin</i>
<i>Rossa di Tropea (RC)</i>	University of Reggio Calabria	Calabria
<i>Rossa di Tropea (VV)</i>	Azienda agricola Colace Domenico (VV)	Calabria
<i>Giarratana</i>	Private nursery	Sicilia
<i>Bianca di Castrovillari</i>	ARSAC – Castrovillari (CS)	Calabria
<i>Pera Sanguigna di Peschici</i>	University of Foggia	Puglia
<i>Rossa Margherita di Savoia</i>	University of Foggia	Puglia
<i>Bianca di Margherita</i>	University of Foggia	Puglia
<i>Rosa o Dorata di Monteleone</i>	University of Foggia	Puglia
<i>*Acquaviva 1-12</i>	University of Bari	Puglia
<i>Ramata di Montoro</i>	Coop.Rama	Campania
<i>Dorata d'Ozieri</i>	Genebank information system of the IPK Gatersleben	Sardegna
<i>Dorata di Voghera</i>	University of Pavia	Lombardia
<i>Rossa di Breme</i>	University of Pavia	Lombardia
<i>Paglierina di Sermide</i>	University of Pavia	Lombardia
<i>Texas early grano 502</i>	Private seller	Commercial variety

*Acquaviva 1-12 were twelve different ecotypes of the cultivar Acquaviva

1.2 Greenhouse experimental trials and OYDV inoculation

In experimental trial conducted during 2018 all onion populations listed in table 1 were tested including the twelve ecotypes (1-12) of ‘Acquaviva’ cultivar and with the exception of ‘Rossa di Tropea VV’. In 2019, the greenhouse experiment trial was repeated to confirm results obtained in the first trial. For this reason, the most tolerant ‘Rossa di Tropea RC’ and ‘Texas early grano 502’, and the two cultivars ‘Pera Sanguigna di Peschici’ and ‘Acquaviva 7’ showed to be more sensitive to OYDV infection were used; another ecotype ‘Rossa di Tropea VV’ was added. The plants were grown inside an insect-proof greenhouse equipped with a double access door and double insect net, to preserve their phytosanitary status, located at the Mediterranean University of Reggio Calabria (RC-Italy) (Figure 8).



Figure 8. Greenhouse used for the experimental trials

A seedbed was prepared for each trial and seeds of the 26 cultivars/ecotypes were sowed for germination on a substrate composed of purple peat and perlite (Figure 9).



Figure 9. Seedbed used for the germination phase

Seedlings of 10 cm height were manually transplanted (after removing foliar and root tips) in pots (2 plants per pot) composing an experimental design that included a number of treatments equal to 25 genotypes under evaluation, inoculated and control with at least 8 replications (Figure 10).

The pots used in the experimental test had a diameter of 20 cm and were filled with a mixture of sandy and clayey soil in a 3:1 ratio, suitable for growing bulbs. The fertilization was carried out by adding 5g / pot of mineral fertilizer, 18-46 bi-ammonium phosphate in granular form.



Figure 10. Ten cm tall seedlings transplanted in pots after foliar and root tips cut

Forty-five days after transplanting, the artificial inoculation was performed with an OYDV strain provided by the Department of Agraria (Mediterranean University of Reggio Calabria) previously characterized. The virus strain was periodically transmitted on fresh tissues of ‘Rossa di Tropea’ onion to maintain its infectious ability and tissues used as inoculum was previously tested both by serological and molecular assay.

The artificial inoculation was carried out by emulating the trophic stings of vectors based on OYDV natural transmission by aphids in a non-persistent manner. Fresh infected leaf tissues were soaked in 0,1 M phosphate buffer in 1:5 (w:v) ratio to keep the virion stable and the pH constant, in Universal, BIOREBA (Reinach, Switzerland) pouches (Figure 11).



Figure 11. Preparation of the inoculum from OYDV infected leaves with phosphate buffer

The syringe needle was dipped in the infected plant extract solution before making the individual punctures. Ten punctures were made to each plant on the cuticle layer of two medium-sized leaves along their vertical axis (Figure 12).

Twenty-two plants of each genotype under analysis were inoculated, according to the experimental design, and 8 plants per genotype were inoculated only with PO_4 buffer as negative control (virus-free). Each plant was labelled, attributing it a progressive alphanumeric code, replica number, name of variety and sanitary status (OYDV-inoculated or healthy).



Figure 12. Mechanical inoculation of two leaves /plant

1.3 Control of the inoculation success

To determine how many plants were really infected and if a causal infection occurred in not inoculated ones, one month after inoculation, all plants (inoculated and not inoculated) were analysed for OYDV by DAS-ELISA (Clark and Adams, 1977) using commercial kits (Bioreba Reinach, Switzerland) following manufacturer's instructions.

The plates were sensitized for 2h and 30 min at 37 °C, using the coating buffer, with the IgG antibodies in a 1: 1000 dilution. The buffer was prepared after dissolving a tablet of substrate in 100 ml of distilled water and brought to pH 9.8.

The samples were macerated in Bioreba extraction bags with Extraction Buffer, 10 ml of Extraction Buffer were used for every 0.5 g of plant tissue. The macerated samples were then loaded into the plates in duplicate, after washing the plates with Washing Buffer (PBS-T). In addition to the samples, control samples were inserted in each plate: healthy and infected supplied by the Company and a "blank" control consisting of the Extraction Buffer only. The plates were left to incubate at 4 °C overnight.

After the incubation period and after washing with Washing Buffer, the plates were loaded with Conjugate Buffer, containing the antibody conjugated with alkaline phosphatase (AP) and left to incubate at 37 °C for 2h.

After incubation with the conjugate and further washing operations (Washing Buffer), the immune-enzymatic reaction in the plates was triggered using the substrate buffer (Substrate Buffer), containing the substrate p-nitrophenyl phosphate (1 tablet of 5mg / 10ml of Substrate Buffer). The plates were left to incubate at room temperature in the dark for 60 min.

Reactions were measured by spectrophotometer Multiscan FC (Thermo Scientific, Carlsbad, CA) at 405 nm, and samples with an optical density twice of the healthy control were considered positive.

1.4 Assessment of symptoms intensity

The proportion of OYDV-positive plants among those which had been inoculated, was assessed per cultivar or ecotype. Moreover, in order to evaluate the degree of tolerance/susceptibility and to identify among tested cultivars which are the most tolerant and the most susceptible the response to the virus was evaluated.

OYDV symptoms intensity was investigated by means of repeated observations, at 15- and 30-days post-inoculation (DPI) (T1 and T2, respectively). The virus infection symptoms were accomplished using the following score: 0 = no symptoms, 1 = mild symptoms, 2 = mild-medium symptoms, 3 = medium symptoms, 4 = medium-severe symptoms, 5 = severe symptoms, according to intensity thereof for the following features, yellowing, twirling and dwarfing (Sholten *et al.*, 2016) (Figure 13).

Then, within each cultivar/ecotype the total score relieved at T2 was divided by the number of plants resulted OYDV-positive by DAS-ELISA, so to obtain a plant infection index (PII), which was further reported as percentage of the highest value.



Figure 13. Symptoms caused by OYDV: A, B yellowing; C, D twirling; E, F dwarfing

1.5 Effects on plant growth

At the conventional intervals of 15- and 30-days post infection (DPI) (T1 and T2, respectively), plants growth of each variety/ecotype/population was evaluated. All the infected (OYDV-positive by DAS-ELISA) and uninfected (control) plants of each variety were subjected to morphometric surveys such as leaf number and the height of the longest leaf (Figure 14) to verify the plant growth modifications due to OYDV infection. The surveys always started from healthy plants and then proceeded to infected ones, to avoid potential artificial contamination or viral transmission.



Figure 14. Measurement of the morphological parameters: height of the longest leaf and number of leaves

1.6 Effects of OYDV on bulb long-term storage and water losses

About 45 days after OYDV inoculation, at the almost complete bulb growth, all the plants of the experimental trial were eradicated.

To facilitate the action, each plant was eradicated by exerting a counterclockwise twist, starting from the healthy plants and proceeding to the infected ones.

Plants were left lying on the pots, overlapping them so that the leaves could cover and protect the bulbs, to simulate the normal agronomic practices carried out in the open field (Figure 15).



Figure 15. Bulbs uprooted and covered until the shoot was dry to simulate the open field agronomic conditions

Sixty DPI, when the green portion was completely dry, the bulbs were collected and stored in a warehouse for 60 days to simulate as much as possible the suitable storage conditions of the product.

In order to verify whether the presence of OYDV facilitates or hinders post-harvest infections during the storage phases, the bulbs were visually checked to assess the state of conservation and the possible presence of secondary pathogens.

Afterwards, to determine the relationship between bulb post-harvest phytosanitary and the ability to maintain or not a correct water balance after storage, bulb water losses were analysed. In detail, 1g from each bulb was inserted in an oven at 60 °C until complete dehydration (Figure 16) and then recorded the final weight.



Figure 16. One gr of fresh bulb tissue placed at 60 °C until complete dehydration

Percentage of weight reduction was obtained with the ratio: (fresh weight - dry weight)/fresh weight * 100. This parameter allows to compare the ability to contain water after storage between infected and healthy bulb and among tested varieties/ecotypes.

The fresh weight/dry weight ratio is essential for proper storage and to prevent the formation of secondary pathogens in post-harvest, because the higher value of this parameter corresponds the higher susceptibility of the bulbs to be attacked by pathogens.

1.7 Statistical analysis

All experiments were set up in a completely randomized design with at least six replications for each treatment. All data were checked for normality (Kolmogorov–Smirnov test) and tested for homogeneity of variance (Leven median test). The data were analysed by three-way ANOVA considering Variety, Time, and Treatment as main factors. Finally, the data were processed by using SPSS v.22.0 software (IBM Corp., Armonk, NY).

1.8 DNA extraction, PCR and fragment analysis (SSR)

SSR analysis to evaluate the genetic distance between the varieties used was performed; in this way variations even between closely related accessions could be detected including in the analysis 12 onion SSR markers already reported in the literature (Baldwin *et al.*, 2012; Mc Callum *et al.*, 2008) (Table 2).

The analysis was carried out on all varieties, despite only accession n° 7 in Acquaviva cultivar was included for as it resulted the most susceptible in the greenhouse trials. ‘Rossa di Tropea’ samples of both experimental tests and both origins (RC and VV) were analysed.

Table 2. SSR markers used in onion populations phylogenetic analysis

<i>Primer</i>	<i>Forward</i>	<i>Reverse</i>	<i>size</i>	<i>dye</i>
ACM 373	AGGTTAAGAAGTTGAATGGTCTG	AAATGGACAAGTGGCATTCA	145-159	FAM
ACM 101	CCTTTGCTAACCAAATCCGA	CTTGTTGAGAAGGAGGACGC	227-248	VIC
ACM 235	TGAGTCGGCACTCACCTATG	ACGCATTTTCAAATGAAGGC	292/304	PET
ACM 446	TCAAGAATTCTGTTGCATCTTGT	AATAAGACCGCAGAAACGAAA	122-124	FAM
ACM 449	GTAAAGGTGTAATAGGAATGAATCG	TACAAAGAAACACACGCGCT	133-148	VIC
ACM 045	AAAACGAAGCAACAAACAAAA	CGACGAAGGTCATAAGTAGGC	226-275	NED
ACM 138	ACGGTTTGATGCACAAGATG	CCAACCAACAGTTGATACTGC	242-286	NED
ACM 387	ACGCACACTATTTGGGAAGG	GAGGAATAGAGAAGGCTGCG	151-162	PET
ACM 134	ACACACACAAGAGGGAAGGG	CACACACCCACACACATCAA	198-212	FAM
ACM 119	TTTCAGCAACATAGTATTGCGTC	TCTTCGGGATTGGTATGGAG	241-259	PET
ACM 443	TGGTGCTTGCTATGTTTTGC	CCCTAGGCCAAGCTTACTTGT	154-179	NED
ACM 477	TGCAATTGGAACTTGGTTTT	CCGTCCTCTATTTGCAGC	160-165	VIC

Total DNA was extracted from young leaves using the DNeasy Plant Mini Kit (QIAGEN) according to the supplier's protocol. The amplification reaction was performed in a mastercycler nexus gx2 thermocycler (Eppendorf, Germany) with a temperature amplification profile reported in table 3 and a reaction mixture with a total final volume of 10 µl including a GoTaq G2 DNA Polymerase (promega) shown in table 4.

Table 3. PCR reaction steps for DNA amplification

Step	Temperature	Time	Cycle
Initialiation	95 °C	2 min	1
Denaturation	95 °C	30 s	40
Annealing	56 °C	30 s	
Elongation	72 °C	20 s	
Final elongation	72 °C	5 min	1
Hold	14 °C	∞	1

Table 4. PCR reaction mix used DNA amplification

Reagents	Volume µl
DNA (7-50 ng)	1
Primer F/R (0,075 µmol)	0,15/0,15
5X Go Taq Buffer	2
dNTPs (10 mM)	0.2
GoTaq G2 DNA Polymerase (5U/µL)	0.05
H ₂ O	6,6
Final volume	10 ul

PCR products were separated on a capillary electrophoresis system (ABI PRISM 3500 Genetic Analyzer (Applied Biosystem), using 1 µl amplicon, 0.5 µl of GeneScan™ 600 LIZ® Size Standard v2.0 (Applied Biosystems) as internal control and 8.5 µl of Hi-Di™ Formamide (Applied Biosystems) The data were analysed using Gene Mapper v.5 software (Applied Biosystem, Thermo Fisher Scientific Inc).

Estimation of the genetic distance (GD) between the varieties was performed by using the GenAlex software v. 6.5 (Peakall and Smouse, 2012).

2. Results and Discussion

2.1 Resistance/susceptibility of onion populations to OYDV and effects on plant growth

The infected plants out of the 22 inoculated plants in each cultivar/ecotype exhibited a percentage of infection ranging from 27% (in Bianca di Margherita cv) to 77% (Dorata d'Ozieri cv), whereas almost varieties/ecotypes (16/25) had 55-68% of infection (Table 5). In addition, PII values clearly showed that 'Rossa di Tropea' and 'Texas early grano 502' were the most OYDV-resistant cultivars with 0.13 and 0.62 of Plant infection index, respectively (Table 5). By contrast, 'Acquaviva 7' (9.53) was the most susceptible one, followed by 'Pera sanguigna di Peschici' (Table 5). Even if 'Acquaviva7' showed to be the most susceptible among the tested cultivars/ecotypes, it is important to underline that other ecotypes of the same variety had a % of PII ranging from 100% to 41.2% (Figure 17).

Table 5. Results of first trial symptom observations and DAS-ELISA analysis accomplished in susceptibility/resistance evaluation trial 30 days post OYDV-inoculation (T2)

<i>Cultivar/ ecotype</i>	<i>Total symptoms score</i>	<i>Infected plants (N)</i>	<i>Infected plants/22 inoculated (%)</i>	<i>Plant infection index (PII)</i>	<i>PII (%)</i>
<i>Acquaviva 1</i>	46	11	50	4.18	43.9
<i>Acquaviva 2</i>	89	12	55	7.42	7.88
<i>Acquaviva 3</i>	70	14	64	5.00	52.5
<i>Acquaviva 4</i>	107	14	64	7.64	80.2
<i>Acquaviva 5</i>	104	16	73	6.50	68.2
<i>Acquaviva 6</i>	55	14	64	3.93	41.2
<i>Acquaviva 7</i>	143	15	68	9.53	100
<i>Acquaviva 8</i>	88	14	64	6.29	66.0
<i>Acquaviva 9</i>	66	12	55	5.50	57.7
<i>Acquaviva 10</i>	78	14	64	5.57	58.5
<i>Acquaviva 11</i>	135	16	73	8.44	88.5
<i>Acquaviva 12</i>	72	13	59	5.54	58.1
<i>Rosa o Dorata di Monteleone</i>	50	16	73	3.13	32.8
<i>Bianca di Margherita</i>	20	6	27	3.33	35.0
<i>Pera sanguigna di Peschici</i>	112	12	55	9.33	97.9
<i>Bianca di Castrovillari</i>	74	14	64	5.29	55.5
<i>Rossa Margherita di Savoia</i>	99	13	59	7.62	79.9
<i>Dorata d'Ozieri</i>	99	17	77	5.82	61.1
<i>Giarratana</i>	44	9	41	4.89	51.3
<i>Rossa di Tropea (RC)</i>	1	8	36	0.13	1.3
<i>Ramata di Montoro</i>	74	13	59	5.69	59.7
<i>Texas early grano 502</i>	8	13	59	0.62	6.5
<i>Dorata di Voghera</i>	90	13	59	6.92	72.6
<i>Rossa di Breme</i>	38	8	36	4.75	49.8
<i>Paglierina di Sermide</i>	68	14	64	4.86	51.0

Figure 17, representing PII as percentage of the highest value, clearly shows the behaviour of tested onion varieties towards OYDV infection.

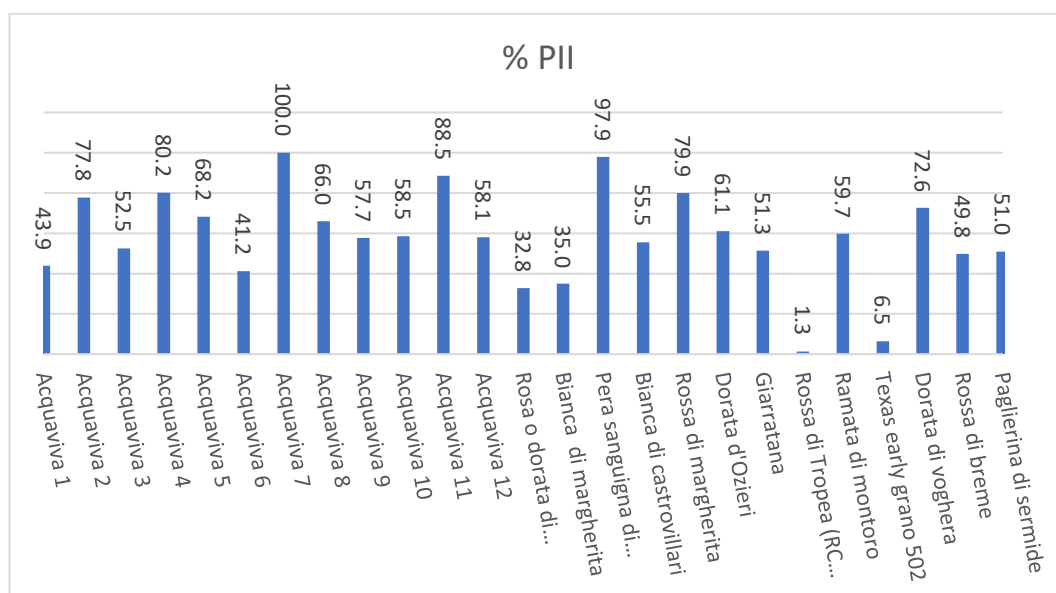


Figure 17. Percentage of plant infection index (% PII) during the first trial

The data from the second-year trial, performed using the most tolerant/sensitive cultivars above selected and adding the ‘Rossa di Tropea’ (VV) ecotype, confirmed the difference in tolerance/susceptibility of the varieties obtained in the first year. In particular, the ‘Rossa di Tropea’ (VV) ecotype supported the resistance of this cultivar (Table 6, Figure 18).

Table 6. Results of second trial symptom observations and DAS-ELISA analysis accomplished in susceptibility/resistance evaluation trial 30 days post OYDV-inoculation (T2)

<i>Cultivar/ ecotype</i>	<i>Total symptoms score</i>	<i>Infected plants (N)</i>	<i>Infected plants/22 inoculated (%)</i>	<i>Plant infection index (PII)</i>	<i>PII (%)</i>
<i>Acquaviva 7</i>	22	11	50	2.00	56.0
<i>Pera sanguigna di Peschici</i>	50	14	64	3.57	100.0
<i>Rossa di Tropea (RC)</i>	1	9	41	0.11	3.1
<i>Texas early grano 502</i>	0	6	27	0.00	0.0
<i>Rossa di Tropea (VV)</i>	1	8	36	0.13	3.5

The confirmation of susceptibility and resistance of onions previously tested towards OYDV infection in the second trial was showed in Figure 18.

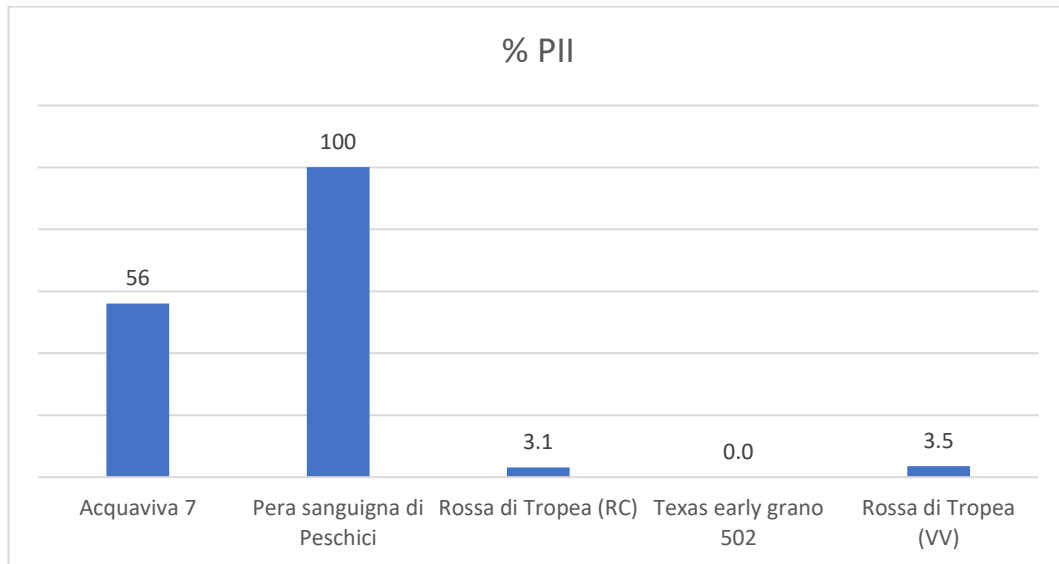


Figure 18. Percentage of plant infection index (% PII) in second trial

The statistical analysis carried out to evaluate the effects on plant growth highlighted significant differences in the plant height and number of leaves depending on the growth phase and the presence/absence of the virus in T1 - T2 range (measurement at 15 and 30 DPI, respectively) (Figure 19 - 1st year, Figure 20 - 2nd year).

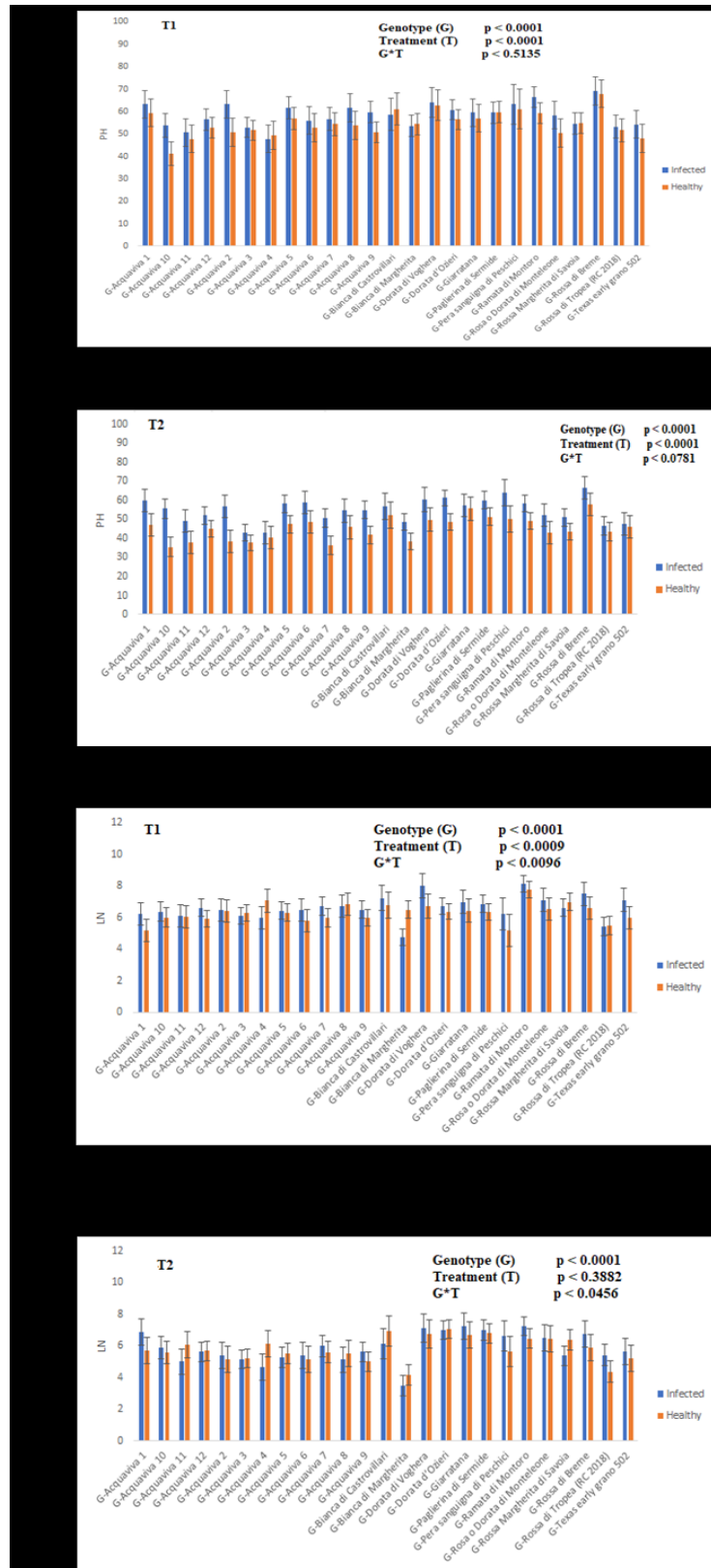


Figure 19. Results of the statistical analysis in the first year, plant height panel A) T1, B) T2; number of leaves panel C) T1, D) T2

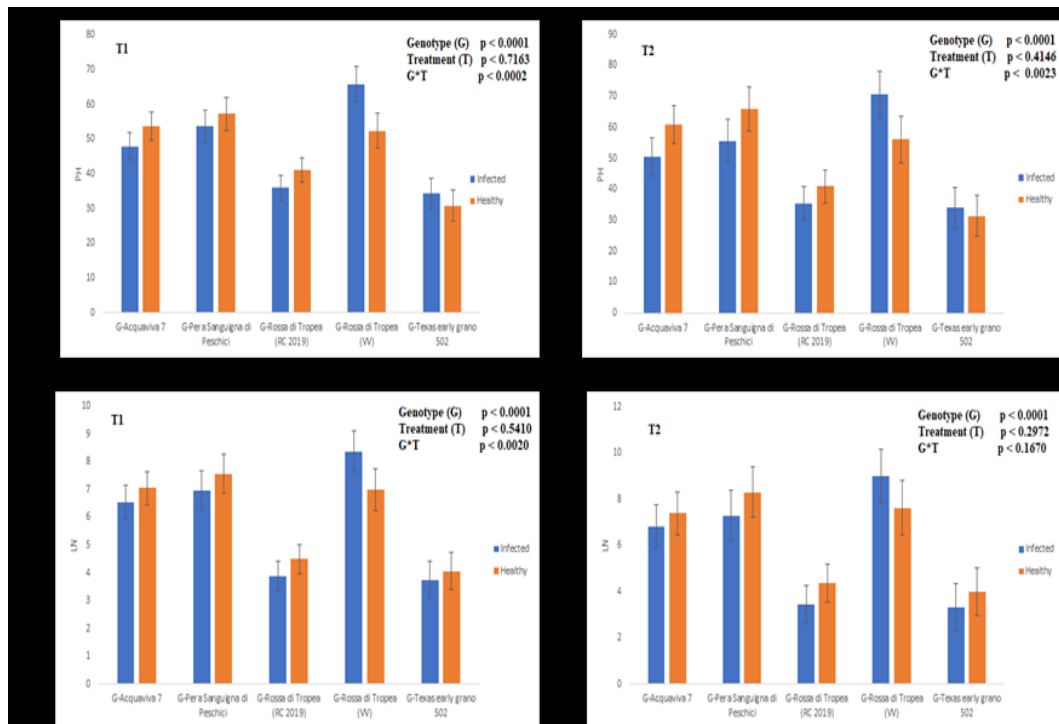


Figure 20. Results of the statistical analysis in the second year, plant height panel A) T1, B) T2; number of leaves panel C) T1, D) T2

The results showed significant different values for plant height and number of leaves in both year in relation to the growth stage (T1-T2), indicating a direct effect of the OYDV infection on plant growth and development (Figure 19 and 20). These effects could be explained by a water accumulation in the plant tissue as observed by Tiberini et al. (data not published).

Moreover, there were significant differences in the height and number of leaves in both years among tested varieties in relation to the infection condition. In fact, during the first year, statistically significant differences were detected among genotypes under evaluation and between healthy and infected plants over the time. In the second year, on the other hand, differences in height and number of leaves were observed among varieties, and for the same cultivar in relation to the time (Table 7).

Table 7. Analysis of Variance (ANOVA) for the first and second-year experiments

	<i>Year 1</i>	<i>Plant height</i>	<i>Number leaves</i>
<i>Variety</i>	.000*	.000*	
<i>Time</i>	.000*	.000*	
<i>Healthy/Inf</i>	.000*	.003*	
<i>Variety * Time</i>	.505	.000*	
<i>Variety * Healthy/Inf</i>	.006*	.000*	
<i>Time * Healthy/Inf</i>	.000*	.221	
<i>Variety * Time * Healthy/Inf</i>	.954	.951	
Year 2			
<i>Variety</i>	.000*	.000*	
<i>Time</i>	.000*	.093	
<i>Healthy/Inf</i>	.697	.533	
<i>Variety * Time</i>	.019*	.020*	
<i>Variety * Healthy/Inf</i>	.000*	.017*	
<i>Time * Healthy/Inf</i>	.090	.306	
<i>Variety * Time * Healthy/Inf</i>	.315	.961	

2.2 Effects of OYDV on bulb long-term storage and water losses

In the overall visual analysis on status of the bulbs after long term storage conditions it was possible to observe that most of bulbs collected from infected plants had a reduced tissue consistency. In addition, the presence of internal rots due to the establishment of secondary post-harvest pathogens, were recorded in both trials, resulting with a higher incidence in infected bulbs in comparison the respective healthy controls. Moreover, it could be observed that the incidence of the occurrences of internal rots in infected bulbs was higher in the cultivar established as sensitive in comparison to the tolerant ones. These results were confirmed in both year (Table 8) trials.

Table 8. Percentage (%) of bulbs affected by secondary pathogens observed (from infected and healthy plants) for each cultivar during the storage phase in the first and second year

<i>Cultivar/Ecotype Year 1</i>	<i>% inf</i>	<i>% health</i>
<i>Acquaviva 1</i>	0.0	40.0
<i>Acquaviva 2</i>	80.0	40.0
<i>Acquaviva 3</i>	60.0	20.0
<i>Acquaviva 4</i>	60.0	40.0
<i>Acquaviva 5</i>	60.0	0.0
<i>Acquaviva 6</i>	0.0	0.0
<i>Acquaviva 7</i>	62.5	0.0
<i>Acquaviva 8</i>	40.0	0.0
<i>Acquaviva 9</i>	20.0	20.0
<i>Acquaviva 10</i>	20.0	0.0
<i>Acquaviva 11</i>	0.0	20.0
<i>Acquaviva 12</i>	20.0	0.0
<i>Rosa o Dorata Di Monteleone</i>	40.0	0.0
<i>Bianca Di Margherita</i>	20.0	20.0
<i>A Pera Sanguigna Di Peschici</i>	14.3	0.0
<i>Bianca Di Castrovillari</i>	40.0	0.0
<i>Rossa Di Margherita</i>	60.0	0.0
<i>Dorata d'Ozieri</i>	40.0	20.0
<i>Giarratana</i>	0.0	0.0
<i>Rossa di Tropea (RC)</i>	0.0	0.0
<i>Ramata Di Montoro</i>	0.0	0.0
<i>Texas early grano 502</i>	0.0	0.0
<i>Dorata Di Voghera</i>	20.0	0.0
<i>Rossa Di Breme</i>	60.0	0.0
<i>Paglierina Di Sermide</i>	80.0	20.0

<i>Cultivar/ecotype Year2</i>	<i>% inf</i>	<i>% health</i>
<i>Acquaviva 7</i>	100.0	12.5
<i>A pera sanguigna di Peschici</i>	71.4	0.0
<i>Rossa di Tropea (RC)</i>	0.0	12.5
<i>Texas early grano 502</i>	0.0	12.5
<i>Rossa di Tropea (VV)</i>	37.5	14.3

Data obtained suggests that OYDV infection creates favorable conditions for the development of rot (caused by post-harvest pathogens).

In order to investigate if there was a correlation between major sensitivity to rot in OYDV infected tissues and water content, bulb water losses were determined after storage. Analyses on bulb water content were summarized in table 9 and 10. In particular, during the first year could be recorded a water content reduction in the infected bulbs of 94.66% in 'Rosa o Dorata di Monteleone' as maximum value to 76.49% in the 'Giarratana' as minimum value. In healthy bulbs the greatest water reduction was found in 'Giarratana' with a value of 92.82% whereas Acquaviva 4 variety showed the least reduction (83.98%).

The index of percentage of water losses comparing infected bulbs to healthy ones for each cultivar was also calculated. In view of this index, the 'Texas early grano 502' showed the smallest differences in water content between healthy and infected (-0.17), resulting in a stable water losses balance independently from the presence of OYDV, the population 'Rossa di Tropea', which resulted tolerant to OYDV infection, showed a reduction in water content of + 1.36. By contrast, the Acquaviva 7 and Pera sanguigna di Peschici varieties, considered sensitive to OYDV infection, showed among the highest differences in water content between healthy and infected samples (Table 9).

Table 9. Average reduction values of infected and healthy bulbs of the first year analysed after the storage, including the percentage of water reduction comparing infected to healthy bulbs

<i>Cultivar/ecotype year 1</i>	<i>Infected reduction %</i>	<i>Healthy reduction %</i>	<i>Infected-healthy reduction%</i>
<i>Acquaviva 1</i>	88.65	88.75	-0.1
<i>Acquaviva 2</i>	87.75	88.78	-1.03
<i>Acquaviva 3</i>	90.91	90.7	0.21
<i>Acquaviva 4</i>	92.54	83.98	8.56
<i>Acquaviva 5</i>	88.46	86.97	1.49
<i>Acquaviva 6</i>	89.25	89.9	-0.65
<i>Acquaviva 7</i>	92.03	88.54	3.49
<i>Acquaviva 8</i>	90.46	86.56	3.9
<i>Acquaviva 9</i>	86.56	90.1	-3.54
<i>Acquaviva 10</i>	88.02	88.39	-0.37
<i>Acquaviva 11</i>	87.48	90.89	-3.41
<i>Acquaviva 12</i>	93.05	91.44	1.61
<i>Rosa o Dorata Di Monteleone</i>	94.66	92.53	2.13
<i>Bianca Di Margherita</i>	89.95	88.1	1.85
<i>Pera Sanguigna Di Peschici</i>	88.82	85.99	2.83
<i>Bianca Di Castrovillari</i>	88.31	89.22	-0.91
<i>Rossa Di Margherita</i>	94.29	91.98	2.31
<i>Dorata d'Ozieri</i>	86.79	84.54	2.25
<i>Giarratana</i>	76.49	92.82	-16.33
<i>Rossa di Tropea (RC)</i>	91.3	89.94	1.36
<i>Ramata Di Montoro</i>	94.09	90.02	4.07
<i>Texas early grano 502</i>	91.71	91.88	-0.17
<i>Dorata Di Voghera</i>	89.49	90.65	-1.16
<i>Rossa Di Breme</i>	94.48	91.71	2.77
<i>Paglierina Di Sermide</i>	90.38	87.35	3.03

The analysis carried out on the bulbs of the second year also confirmed the difference in water losses in tolerant/susceptible varieties recorded previously. In fact, as can be seen from table 10, the Acquaviva 7 and the Pera Sanguigna di Peschici cultivars presented a higher reduction value than the 'Rossa di Tropea' and 'Texas early grano 502'.

Table 10. Average reduction values of infected and healthy bulbs of the second year analysed after the storage, including the percentage of water reduction comparing infected to healthy bulbs

<i>Cultivar/ecotype year 2</i>	<i>Infected reduction%</i>	<i>Healthy reduction %</i>	<i>Infected-healthy reduction %</i>
<i>Acquaviva 7</i>	91.12	90.18	1
<i>A pera sanguigna di Peschici</i>	90.32	89.66	0.65
<i>Rossa di Tropea (RC)</i>	91.73	92.09	-0.37
<i>Texas early grano 502</i>	91.09	91.15	-0.06
<i>Rossa di Tropea (VV)</i>	94.41	94.48	-0.07

Murray et al. (2016) observed that viral infection influences stomatal development in infected plants with consequent water content alteration. Results obtained supported the idea that the OYDV infection has a decisive influence on the water content of the bulbs. Moreover, data obtained suggests that OYDV infection creates favorable conditions for the development of rot (caused by post-harvest pathogens) due to the higher water content in infected tissues.

The latter feature is reported to be fundamental for a correct long-term storage and to avoid production losses in this processing phase where is reported from 30 to 50 % of the total product lost from production to retail sites (Liu, 2014).

These results indicate that OYDV infection could lead to an increase in water content in plant tissues, compromising growth and bulb formation, impacting upon product quality in particular affecting shelf life of bulbs. After the storage phase infected bulbs lost a greater amount of water. This parameter is reported to be fundamental in correct storage conditions and to prevent post harvesting pathogens infection (Petropoulos *et al.*, 2017). In fact, bulbs with low dry matter are reported to have greater susceptibility to sprouting and post-harvest diseases (Gubb and MacTanish, 2002).

2.3 Cluster analysis of onion populations by SSR

Data analysis using Genemapper v.5 allowed us to obtain the length of each amplified fragment (Table 11). The size of the fragments of each allele was similar but not identical to those previously reported (Baldwin *et al.*, 2012; Mc Callum *et al.*, 2008); the discrepancies were due to the reading of the fragments on different sequencers, but the presence of the same genotype in the different readings allowed the standardization of our data.

Table 11. Length of fragments obtained from the analysis on Genemapper v.5

ID	ACM	ACM	ACM	ACM	ACM	ACM	ACM	ACM	ACM	ACM	ACM	ACM
Acquaviva 7	83	119	208	208	271	271	91	94	116	120	243	246
Rosa o Dorata Di Monteleone	98	98	211	211	271	271	91	91	114	120	243	243
Bianca Di Margherita	102	102	208	208	278	278	92	94	112	120	239	239
Pera Sanguigna Di Peschici	102	104	202	210	277	277	92	94	104	114	240	244
Bianca Di Castrovillari	100	100	208	212	278	278	82	94	114	114	240	240
Rossa Di Margherita	84	84	211	211	277	277	94	96	104	114	240	244
Dorata d'Ozieri	84	92	200	208	277	277	91	91	114	118	244	244
Giarratana	98	104	208	208	278	278	91	94	114	120	240	242
Ramata Di Montoro	96	98	208	217	278	278	91	94	112	114	240	242
Texas early grano 502	102	103	211	217	278	278	92	96	104	114	237	240
Dorata Di Voghera	95	96	208	211	271	271	82	91	112	114	237	244
Rossa Di Brema	102	102	211	217	278	278	91	94	101	114	240	242
Paglierina Di Sermide	106	106	211	217	273	273	92	92	104	104	240	244
Rossa di Tropea (RC)	104	104	208	211	278	278	94	96	112	112	240	242
Rossa di Tropea (VV)	72	83	208	211	270	278	92	94	104	112	240	244

ID	ACM	ACM	ACM	ACM	ACM	ACM	ACM	ACM	ACM	ACM	ACM	ACM
Acquaviva 7	138	138	387	387	134	134	119	119	443	443	477	477
Rosa o Dorata Di Monteleone	218	230	126	135	169	176	240	255	225	229	130	134
Bianca Di Margherita	218	240	134	134	181	181	236	236	127	129	129	129
A Pera Sanguigna Di Peschici	218	230	136	136	177	181	240	240	126	126	129	129
Bianca Di Castrovillari	213	222	134	134	161	169	236	236	127	127	134	134
Rossa Di Margherita	250	250	130	136	181	181	227	227	127	127	126	131
Dorata d'Ozieri	300	320	121	123	176	180	226	234	126	126	124	130
Giarratana	221	230	135	135	171	181	235	235	122	126	126	131
Ramata Di Montoro	218	250	135	135	181	181	236	236	127	129	130	134
Texas early grano 502	209	217	128	135	167	176	235	235	126	127	126	132
Dorata Di Voghera	222	230	133	136	167	176	227	235	124	126	130	134
Rossa Di Brema	222	222	129	135	168	176	235	235	128	128	130	134
Paglierina Di Sermide	218	222	134	135	169	176	235	235	126	131	126	130
Rossa di Tropea (RC)	230	242	134	135	168	181	235	235	131	131	130	134
Rossa di Tropea (VV)	218	222	135	136	176	180	226	226	126	129	131	135

SSR	Size obtained	SSR	Size obtained
ACM 373	72-119	ACM 138	209-320
ACM 101	200-217	ACM 387	121-136
ACM 235	270-278	ACM 134	161-181
ACM 446	82-96	ACM 119	226-255
ACM 449	101-120	ACM 443	122-229
ACM 045	237-246	ACM 477	124-135

SSR analysis on the onion collection detected 99 alleles, reported in table 12 together with statistics and genetic summary.

Table 12. Genetic diversity parameters among Onion genotypes based on 12 SSR markers.

<i>Locus</i>	<i>Na</i>	<i>Ne</i>	<i>I</i>	<i>Ho</i>	<i>He</i>	<i>PIC</i>	<i>F</i>
<i>ACM373</i>	13	9.184	2.378	0.533	0.922	0.882	0.401
<i>ACM101</i>	7	3.409	1.455	0.667	0.731	0.659	0.057
<i>ACM235</i>	5	2.980	1.284	0.067	0.687	0.618	0.900
<i>ACM446</i>	5	3.913	1.460	0.8	0.77	0.701	-0.075
<i>ACM449</i>	7	4.245	1.620	0.8	0.791	0.731	-0.047
<i>ACM045</i>	7	4.412	1.681	0.733	0.8	0.743	0.052
<i>ACM138</i>	12	6.429	2.115	0.867	0.874	0.827	-0.026
<i>ACM387</i>	10	4.945	1.871	0.667	0.825	0.772	0.164
<i>ACM134</i>	9	5.172	1.875	0.8	0.834	0.783	0.008
<i>ACM119</i>	7	3.846	1.602	0.2	0.766	0.71	0.730
<i>ACM443</i>	9	4.592	1.802	0.533	0.809	0.756	0.318
<i>ACM477</i>	8	5.921	1.892	0.8	0.86	0.809	0.037
<i>Mean</i>	9.25	4.921	1.753	0.622	0.805	0.749	0.209

Na = No. of Different Alleles; Ne = No. of Effective Alleles; I = Shannon's Information Index; Ho = Observed Heterozygosity; He = Expected Heterozygosity; PIC= Polymorphic Information Content; F = Fixation Index

12 SSR markers amplified a total of 99 alleles (Na) with a mean of 9.25 alleles per locus. The number of alleles for each locus ranged from 5 for ACM235 and ACM446 and 13 for ACM373. The number of effective alleles (Ne) ranged from 2,980 (ACM235) to 9,184 (ACM373) with a mean of 4.91 alleles per locus. Shannon's information index (I) ranged from 1.284 (ACM235) to 2.378 (ACM373) with an average of 1.753. The observed heterozygosity (Ho) ranged from 0.2 (ACM119) to 0.867 (ACM138) with a mean of 0.662. Expected heterozygosity (He) ranged from 0.687 (ACM235) to 0.922 (ACM373) with a mean of 0.209. Polymorphic information content (PIC), ranged from 0.618 (ACM235) to 0.882 (ACM373) with a mean of 0.749. The fixation index (F) ranged from -0.026 (ACM138) to 0.900 (ACM235) with a mean of 0.805 (Table 12).

Cluster analysis based on SSR data, performed using Nei's genetic distance coefficient (Nei and Li, 1979) and the UPGMA (Unweighted Pair Group Method with Arithmetic Mean) algorithm using Mega X software, showed genetic relationships in tested onion populations (Figure 21). Principal Coordinates Analysis (PCoA) allowed to view and confirm the level of similarity between the genotypes using the GenAlex v. 6.5 (Figure 22).

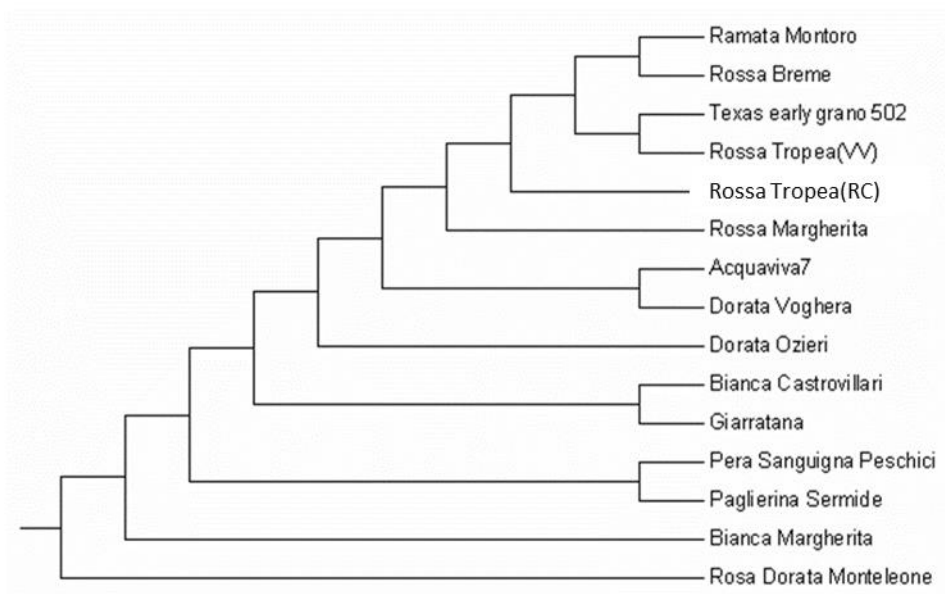


Figure 21. Genetic relationships among onion varieties

From the analysis of the Principal Coordinates Analysis it can be seen that the selected varieties tolerant 'Texas early Grano 502' and 'Rossa di Tropea' are far from those susceptible Acquaviva accession 7 and Pera Sanguigna di Peschici (Figure 22).

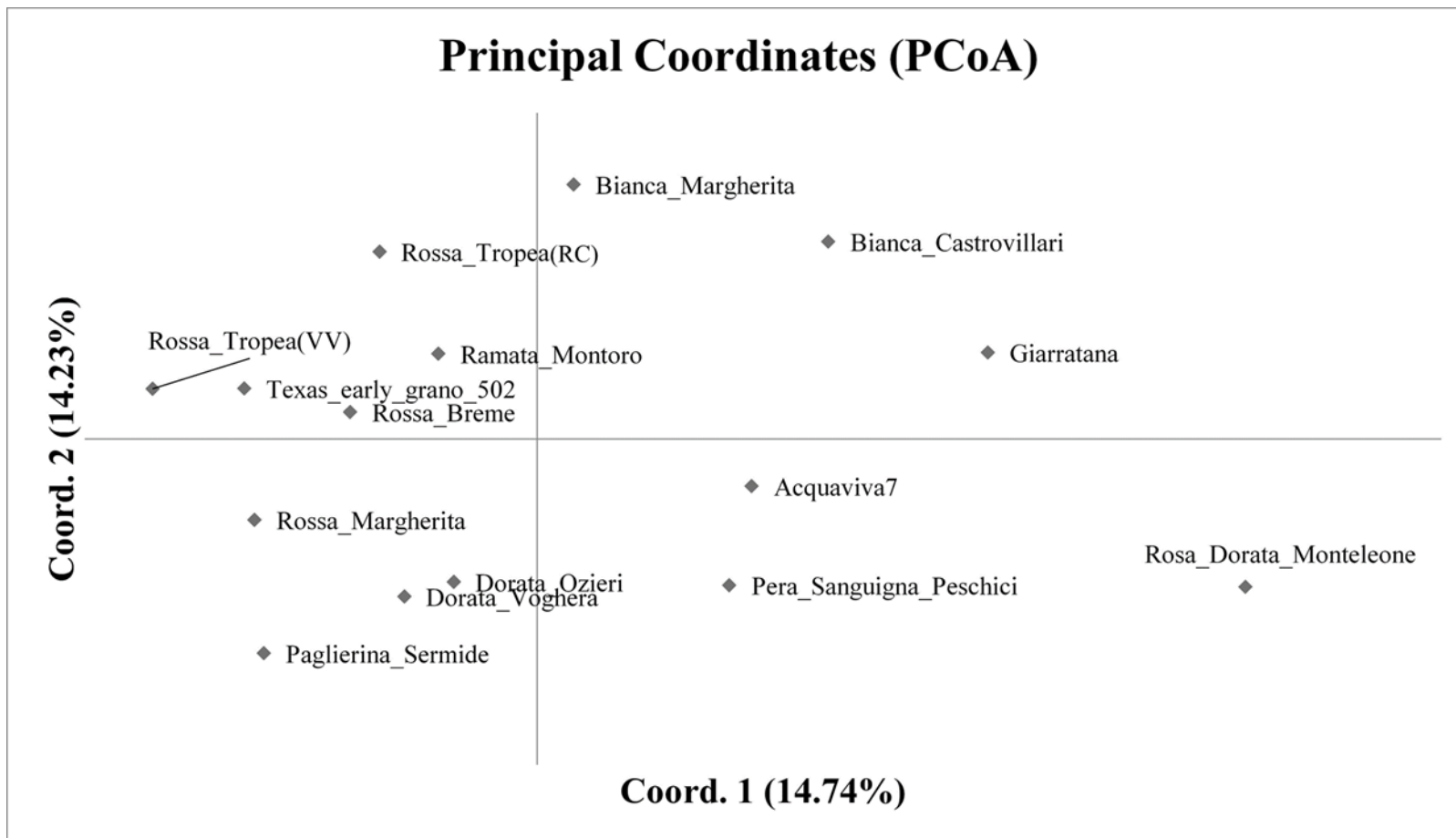


Figure 22. Principal Coordinates analysis

Chapter 2. Molecular analyses of plant responses after OYD infection

1. Materials and Methods

1.1 Gene expression analysis of the Eukaryotic translation Initiation Factors (EIF)

The EIF4 gene family has been reported to be involved in the process of infection by potyvirus (see general introduction), thus the expression levels of *eIF4E* and *eIF4G* were evaluated on the most tolerant and susceptible onion varieties. In detail, the responses to OYDV infection (see Chapter 1) were compared to the analysis of the genes expression to verify if OYVD infection caused variation on the transcript abundance.

1.1.1 Plant material

Leaf and bulb samples of healthy and OYVD-infected plants were collected from the greenhouse experimental trial carried out during the second year with ‘Rossa di Tropea’, Texas early grano’, ‘Acquaviva 7’ and ‘Pera Sanguigna di Peschici’ as described in Chapter 1.

1.1.2 Primers design and housekeeping gene detection

To find the homologous sequences of *eIF4E* and *eIF4G* genes, BLAST was used to compare the sequences of *Asparagus officinalis* (species closest to the onion among the available sequences) deposited on Genbank (<https://www.ncbi.nlm.nih.gov/genbank>) XP_020246192.1 and XP_020240923.1 respectively; based on the OTD (Onion Transcriptome Database) (<http://onion.riceblast.snu.ac.kr/download.php>). The alleged homologous sequences and the resulted isoforms were then processed by using PRIMER3 (<http://primer3.ut.ee/>) for designing the primers (Table 13). The onion Actin gene was used as reference

gene (Zhang *et al.*, 2016). The specificity of each primers was confirmed by evaluating the size of the expected PCR product.

Table 13. Primers of EIF and of housekeeping genes used in gene expression analysis

<i>Primer</i>	<i>Forward</i>	<i>Reverse</i>	<i>Ta</i> (°C)	<i>Conc.</i> (μ mol)
<i>EIF4e iso 1</i>	<i>GAGGACCCTGTTTGTGCCA</i>	<i>GTGTGCATTTTGGTCCAT</i>	59	0,5
<i>EIF4e iso 2</i>	<i>GTCACCCAAGCAATTTAATG</i>	<i>GATTTTCCTCGTGAACAGTTGAC</i>	59	0,6
<i>EIF4g iso 1</i>	<i>CCCTCAGTGTGCTTCTCC</i>	<i>TTCCATATCCACGCTGAGGC</i>	59	0,2
<i>EIF4g iso 2</i>	<i>TGGCAGGAGAGAAGGAAGGT</i>	<i>GGTCCTCGTGTCAGTCTGTT</i>	59	0,5
<i>Actin</i>	<i>CTGGGATGACATGGAGAAGATT</i>	<i>GTTAAGTGGAGCCTCCGT</i>	59	0,1

1.1.3 RNA extraction and reverse transcription

Total RNA was purified from 200 mg tissues of leaves and bulbs using the RNeasy[®] Plant Mini kit (Qiagen) RNA extraction kit. The purity and quantification of the extracted RNA was determined with Nanodrop 2000 (Thermo Scientific, Wilmington, USA) and integrity was assessed through an electrophoretic run on 1% w / v agarose gel.

The reverse transcription reaction was performed with 200 ng of RNA using Maxima First Strand cDNA Synthesis Kit for RT-qPCR, with dsDNase (Thermo Scientific[™]) in a total volume of 20 μ l. Reagents shown in Table 14 were mixed and incubated at 37 °C for 2 minutes; then, after centrifugation and cooling on ice, the reagents of Table 15 were added.

Table 14. Reagent used for the dsDNase step

Reagents	Volume μ l
RNA (200 ng)	1-12
dsDNase	1
10X dsDNase Buffer	1
H ₂ O	Up to 10
Final volume	10 ul

Table 15. Reagent used for the cDNA synthesis

Reagents	Volume μ l
5X Reaction Mix	4
Maxima Enzyme Mix	2
H ₂ O	4

The samples were finally incubated at 25 °C for 10 minutes followed by 15 minutes at 50 °C. To terminate the reaction the samples were heated at 85 °C for 5 minutes and then used for qPCR reaction.

1.1.4 Real time quantitative PCR

Gene expression was analysed using the qPCR technique, which was performed with a StepOne™ Real-Time PCR System (Applied Biosystems™) thermal cycler.

To amplify the genes, a 1:10 diluted cDNA aliquot was used in a 10 μ l reaction with 5 μ l of PowerUP SYBR Green Master Mix (applied biosystem) and 0.1-0.6 μ mol of forward and reverse primer.

The amplification reactions were carried out as follows: 50 °C for 2 minutes, followed by a phase at 95 °C for 2 minutes, and for 40 cycles: a denaturation phase for 15 seconds at 95 °C and an annealing phase / elongation for 60 seconds at 59 °C. The specificity of the amplification was assessed by melting curves for the presence of a single peak. The analysis was carried out on two biological replicates and in two technical replicates.

A relative standard curve for each gene was generated using a triple serial dilution of cDNA pools (obtained by mixing the same proportion of all cDNA samples) using StepOne software v2.3 (Applied Biosystems™). The PCR efficiency of the primer pairs has been optimized to be in the range 92-100% with R² values of 0.996. The calculation of gene expression was an approach based on the 2^{ΔCt} method (Livak and Schmittgen, 2001).

1.2 RNAseq analysis on virus-free and OYVD-infected onion bulbs

Next generation sequencing (NGS) technology provides an opportunity to characterize transcriptome wide responses to biotic and abiotic stress. An increasing number of transcriptome sequencing studies were performed to identify differential expressed genes (DEG) and regulatory control of the expression patterns correlated to the applied stress. Many studies already provided valuable information to understand the regulatory network in plants. Here, we compare the transcriptomic profiles between OYVD-infected and uninfected (control) ‘Rossa di Tropea’ onion by a RNA-seq approach.

1.2.1 Plant material

‘Rossa di Tropea’ onion (*Allium cepa* L.) bulbs, well known for its flavor and highly richness in flavonols and anthocyanins, were grown in an experimental trial at Campora (RC - Italy; 40° 18’23.076’’ N; 15°17’35.88’’ E) in January 2019, using ‘Rossa di Tropea’ virus-free onion seeds. Bulbs were farmed in a proof-insect greenhouse under controlled and standard conditions (soil, temperature, photoperiod and light intensity), providing thorough pest and fertilizer management. A randomized block design was utilized, and 180 plants were split in six parcels (30 plants for each one). Artificial infection was carried out on 3 parcels, randomly chosen, in two month-old onion seedlings (March 2019) by mechanical inoculation using the potyvirus onion yellow dwarf virus (OYDV), which infects various plants of the *Allium* genus. Since the virus infection induce a dormancy alteration with a premature sprouting and bulbs rooting, with a rapid decay during storage, infected samples were used as filter to highlight the key mechanisms involved in dormancy modulation and release. Bulbs from mature plants of both uninfected and OYDV-infected plants were collected just after harvest, at three different stages: endo-dormancy (T_{ED}; May 2018); eco-dormancy (T_{EC}; July 2019) and internal sprouting (T_{IS}; September 2019) (Figure 23), checking key morphological traits (e.g. external sprouting and rooting) during times and between conditions (uninfected vs infected samples).

1.2.2 OYDV infection evaluation using DAS-ELISA and Real Time RT-PCR

To verify the inoculation efficacy, in addition to visual inspection for symptoms development, one month after inoculation both uninfected and OYDV-inoculated plants were assayed by a specific OYDV serological assay (ELISA) (BIOREBA, Switzerland), following manufacturer's instructions. The analyses were performed in duplicate including negative and positive controls provided by the kit. ELISA reactions were measured by spectrophotometer Multiscan FC (Thermo Scientific, Carlsbad, CA) at 450 nm. Samples showing an optical density twice than negative control were considered positive. The inoculated plants resulted negative though ELISA test were further verified by Real-Time quantitative PCR (qPCR) assay (Tiberini *et al.*, 2019). The assays were performed in triplicate, including negative (uninfected plants and water), and positive (OYDV-infected plants by ELISA) controls, respectively.

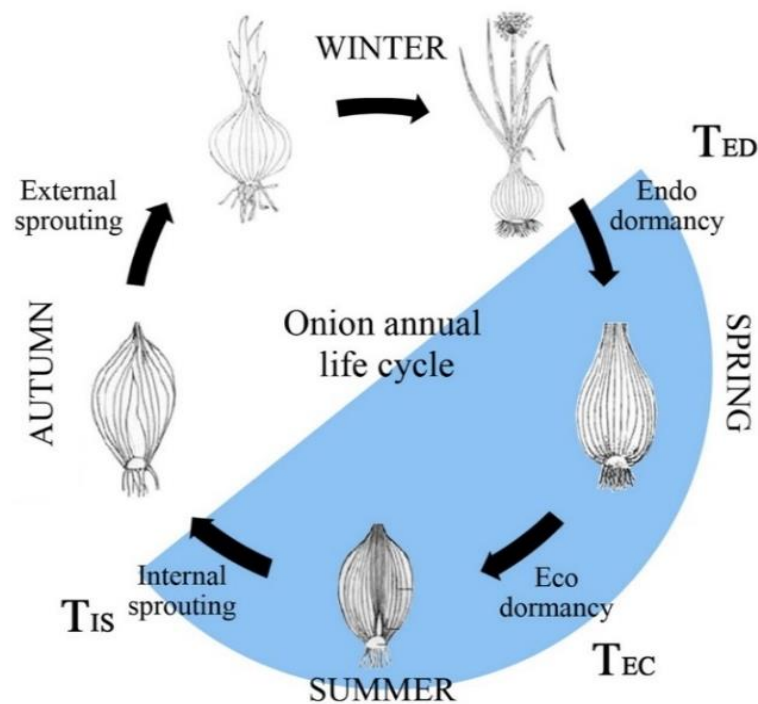


Figure 23. Onion annual life cycle (modify by Sharma *et al.*, 2016). The phase between endo-dormancy (T_{ED}), eco-dormancy (T_{EC}), and internal sprouting (T_{IS}) (the three time points investigated) was highlighted.

1.2.3 RNA isolation and sequencing

RNA-seq data sequences were obtained from virus-free and OYVD-infected samples (three biological replicates for each time points and infection condition). Collected material was frozen immediately in liquid nitrogen and stored at -80 °C until use. Total RNA was isolated using a NucleoSpin RNA Plant (Macherey-Nagel GmbH & Co. KG, 52355 Düren, Germany) and treated with RNase-free DNase. RNA quality (RNA Integrity Number - RIN - > 8.0) was evaluated using an Agilent Bioanalyzer RNA nanochip (Agilent, Wilmington, DE). Sequencing libraries were prepared using a TruSeq RNA Sample Preparation Kit v2 (Illumina, San Diego, CA, USA), according to the manufacturer's instructions. Quality and insert size distribution were assessed using an Agilent Bioanalyzer DNA 1000 chip. Sequencing library was quantified using qPCR, pooled in equimolar concentration and analyzed on an Illumina NextSeq500 generating 2x150nt paired-end (PE) reads. Sequences generated were deposited in the NCBI (National Center for Biotechnology Information).

1.2.4 De novo transcriptome assembly and annotation

Raw reads from each sample were quality assessed using the FastQC tool v0.11.8 (<https://www.bioinformatics.babraham.uk/projects/fastqc>). Adapters were removal and the quality trimming were performed using the Trimmomatic software v0.38 (Bolger *et al.*, 2014). Reads were filtered by length and only those longer than 36 base pairs were selected. The filtered reads were pooled into a single dataset and de novo transcriptome assembled through Trinity software v2.8.4 (Haas *et al.*, 2013). Cd-hit (v4.7) tool (Fu *et al.*, 2012) was then used to reduce the number of transcripts and to collapse highly similar sequences, with default parameters. The assembly completeness was evaluated with BUSCO v2/v3, using the web service gVolante (<https://gvolante.riken.jp/>), and the online tool Mercator (Lohse *et al.*, 2014) was used for functional annotation.

1.2.5 Differential gene expression analysis and co-network analysis

To identify the Differentially Expressed Genes (DEGs) ($P_{adj} < 0.05$) highlighting the pathways involved in modulation of dormancy in onion bulbs, all sampling times (TED, TEC and TIS) were compared using both uninfected and OYDV-infected plants. Transcript quantification was performed using Salmon (Patro *et al.*, 2017), while differential gene expression analysis and Principal Component Analysis (PCA) were carried out by Deseq2 (<http://www.bioconductor.org/packages/release/bioc/html/DESeq2.html>). To visualize DEGs among times in both conditions (uninfected and OYDV-infected bulbs) and assigning to specific metabolic pathways, MapMan tool (<http://gabi.rzpd.de/projects/MapMan/>) was utilized. Venn Diagrams were drawn by the R package VennDiagram (<https://cran.r-project.org/web/packages/VennDiagram/index.html>), while GO enrichment analysis was carried out with the topGO (<http://bioconductor.org/packages/release/bioc/html/topGO.html>) package.

To predict and translate the putative ORFs for each transcript, NCBI's ORFfinder (<https://www.ncbi.nlm.nih.gov/orffinder/>) was used. To search the ORFs dataset with the Pfam profile of *WRKY* protein family (PF03106), HMMER hmmscan v3.2.1 (<http://hmmer.org/>) was used. After selecting the best scoring isoform from hmmscan results, sequences were filtered for complete *WRKY* domain presence and for sequence length (>30 AA) with a custom bash script. Transcripts were then annotated with a blastp v2.7.1+ (https://kbase.us/applist/apps/kb_blast/BLASTp_Search) search against the NCBI's nr database and aligned with Clustal Omega tool (<http://www.clustal.org/omega/>). The *WRKY* identified were validated by mapping their sequences on the draft of assembled genome (data not published). Differentially expressed *AcWRKYs* were extracted for each sampling time and in both conditions, in order to identify genes belonging to *WRKY* family missed by the Mercator annotation.

Real-Time quantitative PCR (qPCR) was used to validate the differentially expressed *AcWRKYs* isolated in the comparisons, and putatively involved in dormancy modulation. The *AcWRKY* sequences, previously validated on the draft onion genome (data not published), were used for designing primer pairs for each

candidate TF by using Primer 3.0 software (<http://primer3.ut.ee/>). Reverse transcription was carried out from 200 ng of total RNA extracted by uninfected and OYDV-infected bulbs at T_{ED}, T_{EC} and T_{IS}, using iScript Reverse Transcription Supermix (Bio-Rad, USA), according to manufacturer's instructions. qPCR was performed using 1.5 µL cDNA diluted 1:10, 0.3 µM forward and reverse primers and 5 µL of iQ SYBR Green Supermix (Bio-Rad, USA) in 10 µL final volume, with the follow thermal program: initial activation at 95 °C for 3 min, 40 cycles at 95 °C for 15 s and annealing temperature (60 °C) for 1 min. This procedure was followed by melting curve analysis from 95 °C for 10 s, 65 °C for 5 s, to 95 °C for 5 s. Actin gene was used as reference (Khosa *et al.*, 2016). Each treatment was performed on three biological and two technical replicates. The expected fragment amplification was verified on agarose gel 1.5% w/v electrophoresis and melting curve analysis; PCR efficiency of each primer pairs was optimized, using a range from 92 to 100% as cut-off. The relative expression ratio of each gene was calculated using the 2^{-ΔCT} method (Livak and Schmittgen, 2001). Pearson correlation analysis between RNA-Seq and qPCR results was carried out.

A co-expression network analysis was performed with Comparative Co-Expression Network Construction and Visualization tool (CoExpNetViz; Tzfadia *et al.*, 2015). Normalized expression data were used to calculate the Pearson correlation coefficient using the 1st and 99th percentiles of the correlation distribution as thresholds. Differential expressed *AcWRKYs* isolated during sampling times and between conditions were used as baits. The resulting network was then analyzed and visualized through Cytoscape (Shannon *et al.*, 2003).

2 Results and discussion

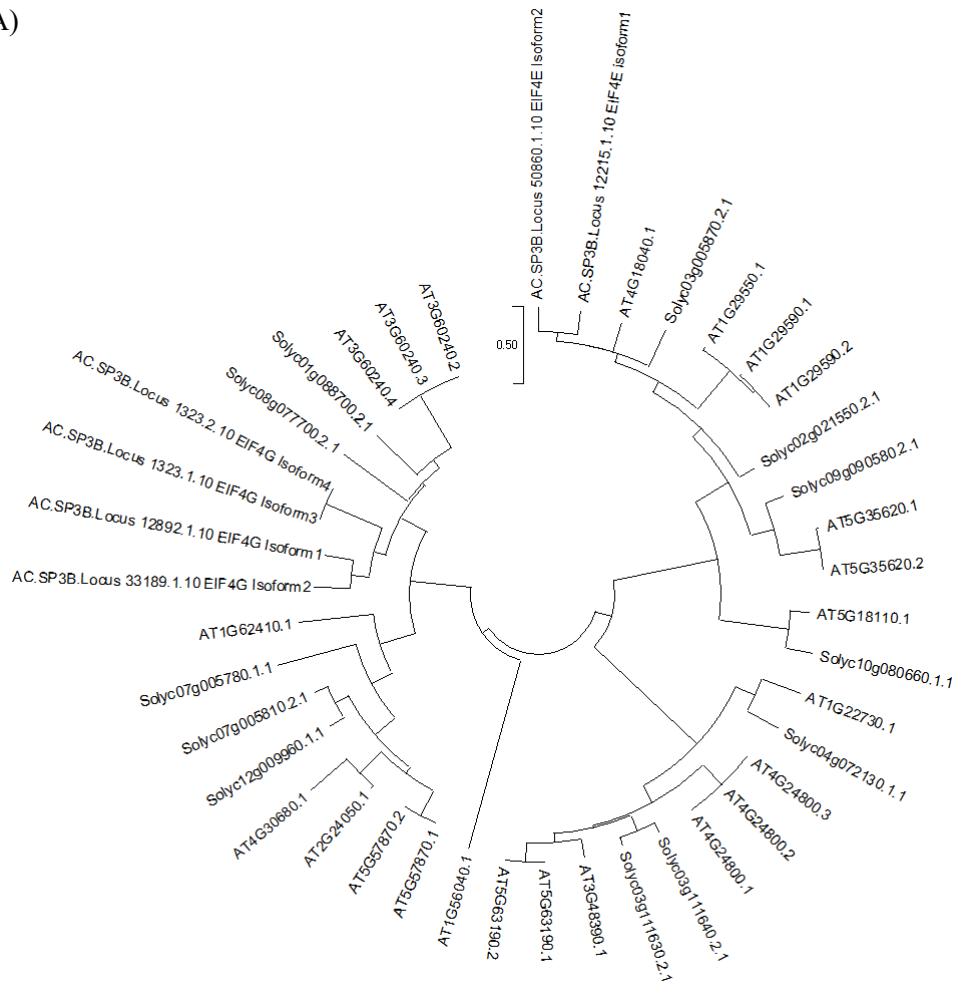
2.1 Gene expression analysis of the Eukaryotic translation Initiation Factors (EIF)

2.1.1 Differential expression of EIF gene family in OYVD infected onion

A phylogenetic tree defines the historical and evolutionary path of biological entities according to a divergent evolution model. For this purpose, we considered forty-one (41) peptide sequences from *Arabidopsis*, tomato and onion, selected from public databases and traceable as *eIF4* genes. Afterwards, they were aligned for constructing a phylogenetic tree useful to identify the possible clade consisting of sequences target (onion, *Allium cepa*) and reference sequences such as *Arabidopsis* and tomato already characterized and studied previously (Figure 24A). In figure 24B, the relationships among four *eIF4G* isoforms from onion, three sequences from *Arabidopsis* (AT3G60240) and two from tomato (*Solyc01g088700.2.1* and *Solyc08g077700.2.1*) are shown. The two *eIF4E* isoforms from onion clustered with *eIF4E* from *Arabidopsis* and tomato, *AT4G18040.1* and *Solyc03g005870.2.1*, respectively.

The sequences grouped in the same clade were used for highlighting the conserved domains, typical of the superfamily eukaryotic translation initiation factor *eIF4E* family protein and MIF4G and MA3 domain-containing protein for *eIF4G*, (Toribio et al., 2019) (Figure 24B).

A)



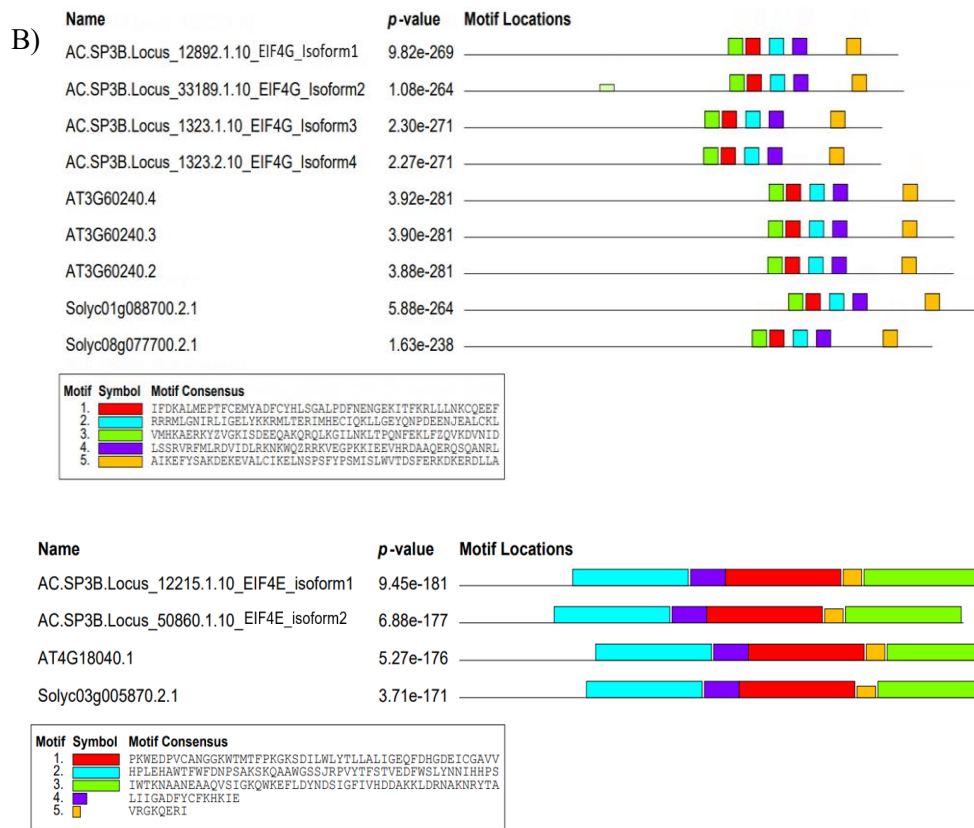


Figure 24. A) Sequences of forty-one (41) peptide sequences from *Arabidopsis*, tomato and onion, selected from public databases and traceable as *eIF4* genes were aligned using ClustalW and the phylogenetic tree constructed using the Neighbor-Joining method. **B)** To discover the conserved motifs MEME online tool v5.0.5 was utilized with four *eIF4G* isoforms from onion, three sequences from *Arabidopsis* (AT3G60240) and two from tomato (*Solyc01g088700.2.1* and *Solyc08g077700.2.1*). The two *eIF4E* isoforms from onion clustered with *eIF4E* from *Arabidopsis* and tomato, *AT4G18040.1* and *Solyc03g005870.2.1*

Previously, several studies reported that viruses belonging to the genus *Potyvirus* utilize the EIF complex for their replication process in many species (Charron *et al.*, 2008; Mazier *et al.*, 2011). However, starting from the gene expression levels relative to the four putative isoforms selected for this study, significant differences in transcript abundance were not detectable comparing the four varieties (two sensitive and two tolerant to OYVD-infection) in leaf tissue (Figure 25), in addition EIF4G isoforms 3 and 4 were excluded because of the very limited levels of expression.

EIF4 isoform and relative expression in leaf

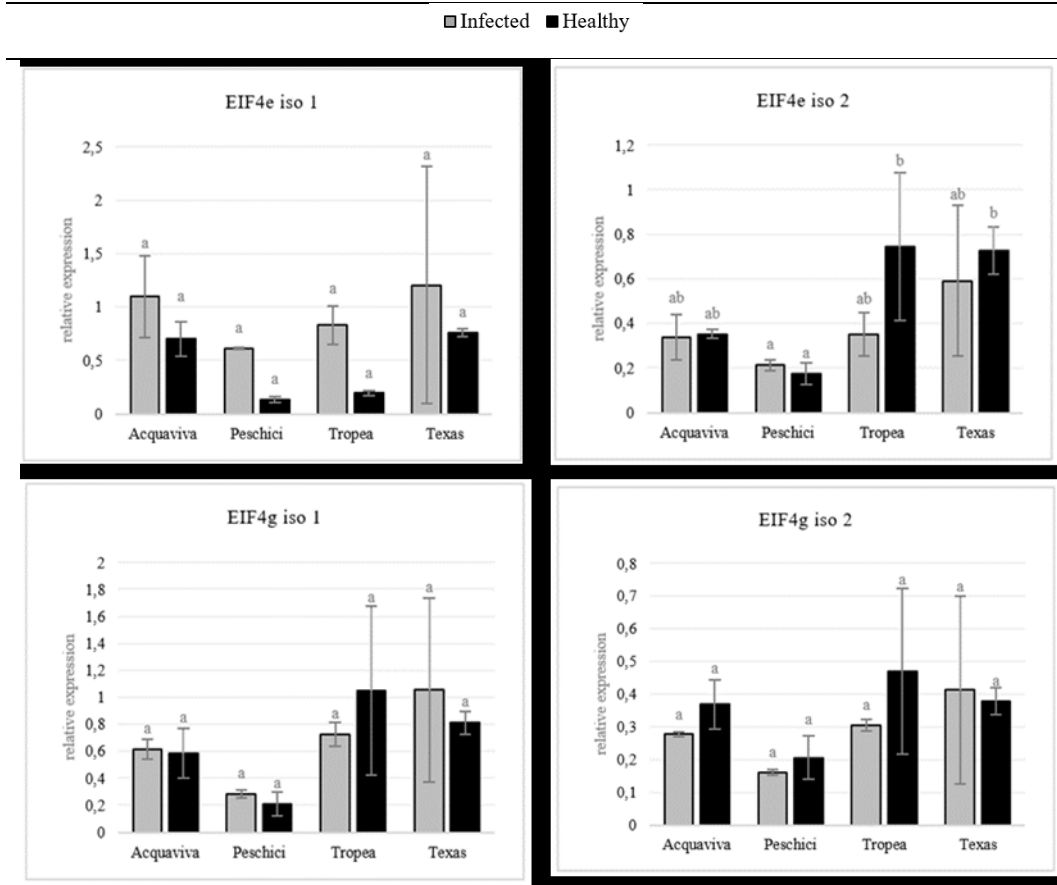


Figure 25. Gene expression analysis of EIF4E e EIF4G isoforms in the leaves (expressed as $2^{\Delta\Delta Ct}$ method by Livak and Schmittgen, 2001) compared to the Actin as reference gene.

The scenario appeared different on the bulbs; indeed, we observed a significant different expression, for *eIF4E* isoform 2 in the cultivar Peschici and Tropea between “OYVD-infected” bulbs compared to the virus-free control. The *eIF4G* isoform 1 showed higher but not significant expression levels in “Tropea control” compared to “Tropea OYVD-infected” as well as in all the other varieties; regardless the virus infection, no differences were highlighted among genotypes. Finally, the *eIF4G* isoform 2 showed higher and significant different levels of expression in “Tropea OYVD-infected” while “Acquaviva OYVD-infected” exhibited intermediate expression levels not significant different from both the others (Figure 26).

EIF4 isoform and relative expression in bulb

■ Infected ■ Healthy

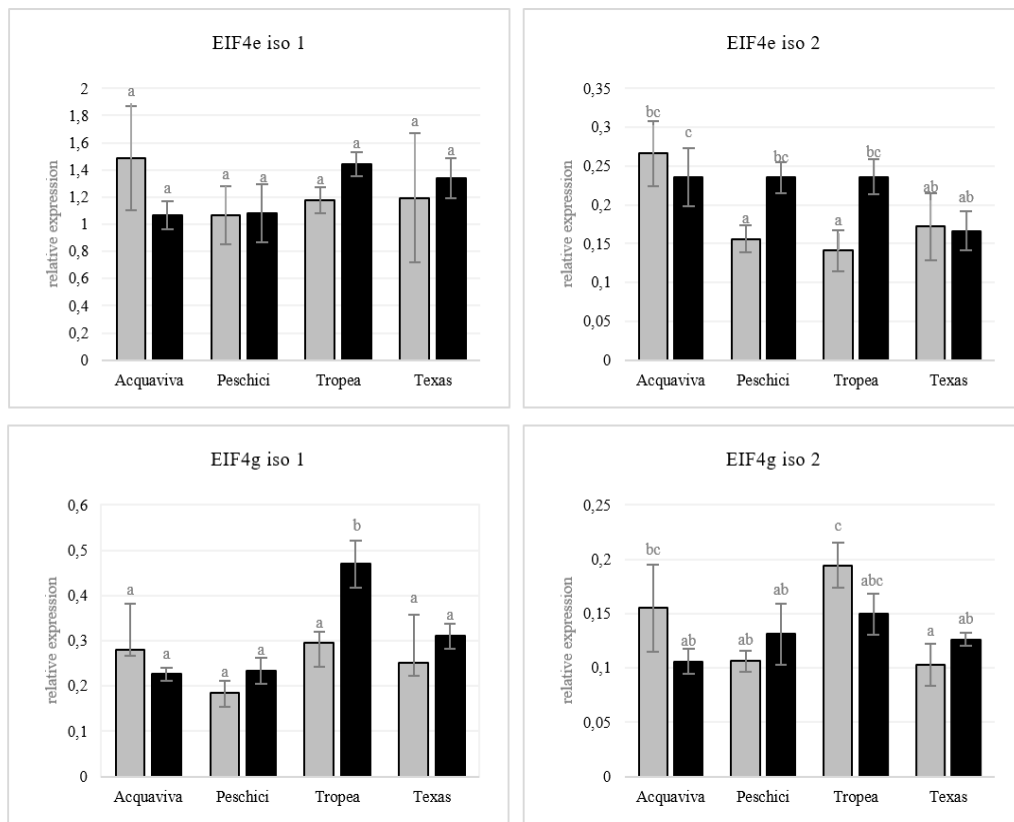


Figure 26. Gene expression analysis of EIF4E e EIF4G isoforms in the onion bulbs (expressed as $2^{-\Delta Ct}$ method by Livak and Schmittgen, 2001) compared to the Actin as reference gene.

The lack of evidence that the virus replication process is based on these genes could be explained by the recent discover of other EIF genes isoforms that the virus may use for this purpose (Keima *et al.*, 2017), these last genes was not analysed due to the lack of knowledge of the onion genome.

2.2 RNAseq analysis on virus-free and OYVD-infected onion bulbs

2.2.1 *De novo* assembly and annotation of onion bulb transcriptome

Inoculation efficiency was assessed by both ELISA and qPCR methods. ELISA assay showed a strong and clean reaction in positive controls and on 87% of inoculated plants; no signal was detected in both negative controls and uninfected samples, with values of 230 nm absorbance close to zero. Inoculated plants without signal in ELISA reaction were also investigated by qPCR. Positive controls showed a Ct values ranging from 16 to 18, while inoculated bulb samples had values included from 18 to 21 (data not shown), expression profiles comparable to results obtained in previous studies using OYDV infected samples (Tiberini *et al.*, 2019). Uninfected plants and water (negative control) did not show amplification, confirming both the healthiness of samples that have not been infected and the specificity of the assay.

Four hundred ninety-two (492) million paired-end reads were generated using the Illumina NextSeq500 platform from *A. cepa* with 150 bp length. After filtering, two hundred ninety-nine (299) million paired-end reads was retained for Trinity assembling with a read length ranging from 36 to 150 bp. The assembly showed a high number contigs (581,029) that were collapsed based on sequence similarity with the cd-hit tool for a final counting of 479,145 transcripts and 316,298 genes (sequence identity threshold = 0.9), with N50 of 1,615 and an average sequence length of 494 (Table 16). Finally, the complete core genes detected were 87.71% (91.88% complete + partial), by using BUSCO for the completeness assembly assessment.

Table 16. Overview of sequencing output and assembly of *A. cepa* bulb transcriptome.

Items	Statistics
Number of contigs	581,029
Number of sequences after cd-hit tool	479,145
Total length (nt) of transcripts	440,954,936
Total number of genes	316,298
Longest sequence (nt)	15,759
Mean sequence length (nt)	920
Median sequence length (nt)	494
N50 sequence length (nt)	1,615
GC-content (%)	36.72
BUSCO Complete	87.71%
BUSCO Complete + Partial	91.88%
BUSCO Missing	8.12%

2.2.2 Transcript abundance estimation and differentially expressed genes (DEGs)

Trimmed reads were used for transcripts expression quantification at T_{ED} (endodormancy), T_{EC} (eco-dormancy), and T_{IS} (internal sprouting) (Figure 23), respectively in both uninfected and OYDV-infected bulbs. Overall, in both conditions DEGs were mainly isolated at T_{IS}/T_{ED} and T_{IS}/T_{EC} comparison, while T_{EC}/T_{ED} yielded the lower one. All three comparisons showed a significantly higher number of up and downregulated genes in uninfected plants with respect to OYDV samples (Figure 27). Indeed, in total, 5,390 DEGs were found in the uninfected samples during the dormancy transition process (Table 17). Among these, 1,253 were found in the T_{EC}/T_{ED} comparison, while 1,859 and 2,278 were isolated from T_{IS}/T_{EC} and T_{IS}/T_{ED} comparison, respectively. By contrast, only 1,322 DEGs were found during the time course in the inoculated samples, with 304, 401 and 617 DEGs T_{EC}/T_{ED}, T_{IS}/T_{ED} and T_{IS}/T_{EC}, respectively (Table 17). PCA analysis shows a clear clustering of uninfected and infected samples (Figure 27D). Interestingly, uninfected bulbs display a way higher separation between the three sampling times in comparison to OYDV-infected bulbs. The separation became much more pronounced at T_{IS}. This observation is supported by the numbers of DEGs being highest when contrasting uninfected samples with infected plants at any other time

point investigated (Table 17). These findings highlight the interfering action of the virus during physiological dormancy process.

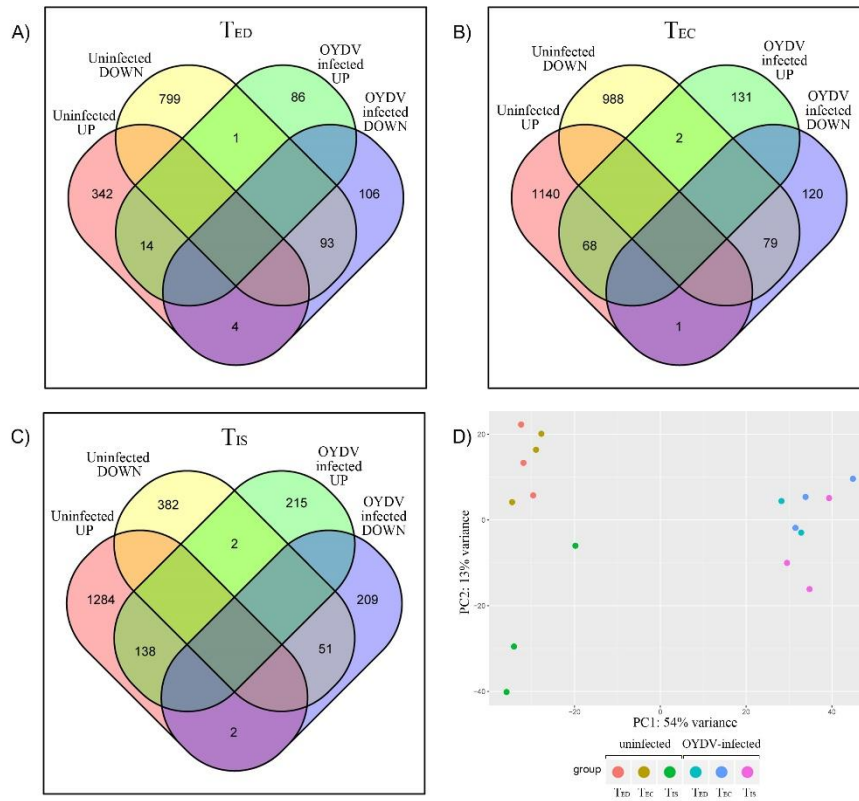


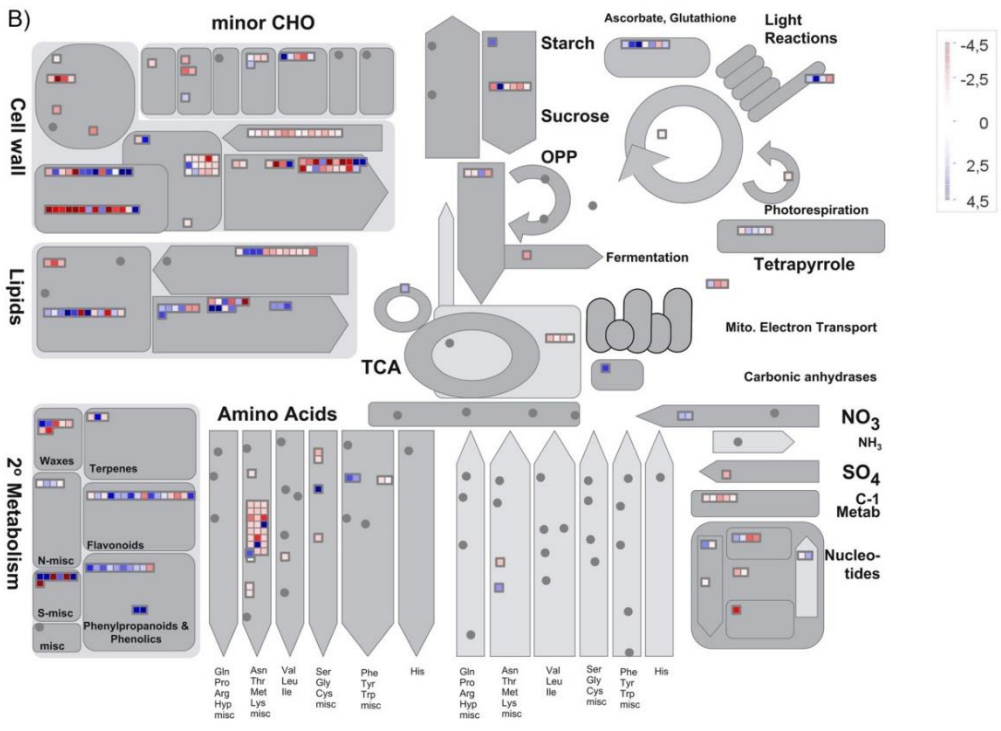
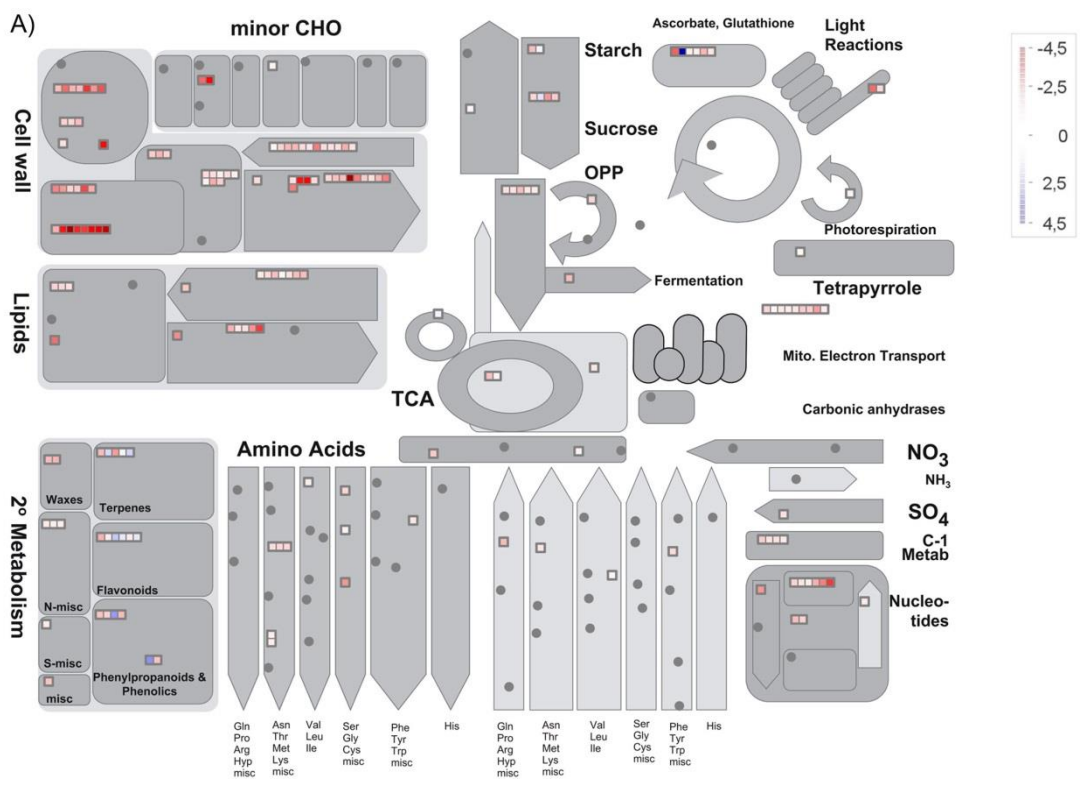
Figure 27. Transcriptome relationships among 3 time points during onion bulb dormancy of uninfected and OYDV-infected plants. VENN diagrams of transcriptome profiles at TED (A), TEC (B), and TIS (C). PCA (D) developed using five hundred most variable genes

Table 17. Summary of DEGs ($P_{adj} < 0.05$) extracted between uninfected and OYDV infected samples at TEC/TED, TIS/TED, and TIS/TEC comparisons.

Sample	Comparison	Number of DEGs	Log2 fold change > 1	Log2 fold change < -1
Uninfected	T _{EC} /T _{ED}	1,253	325	796
	T _{IS} /T _{ED}	2,278	1,129	861
	T _{IS} /T _{EC}	1,859	1,326	362
	<i>Total</i>	<i>5,390</i>	<i>2,780</i>	<i>2,019</i>
OYDV-infected	T _{EC} /T _{ED}	304	100	189
	T _{IS} /T _{ED}	401	191	184
	T _{IS} /T _{EC}	617	319	248
	<i>Total</i>	<i>1,322</i>	<i>610</i>	<i>621</i>

2.2.3 OYDV infection alters the onion bulb dormancy

MapMan BINs analysis was carried out to highlight main metabolic pathways and functional groups regulating bulb dormancy in both endo-/eco-dormancy transition and in the eco-dormancy/internal sprouting switch, as well as transcripts involved in the dormancy break. In uninfected samples, as previously reported, there were generally more DEGs than infected bulbs, with an almost constant number between the three times analyzed in the latter group (Table 17). Furthermore, in uninfected samples the number of upregulated genes was highest in the eco-dormancy (T_{EC}) / internal sprouting (T_{IS}) transition, while downregulated genes decrease at the same switch. In the T_{EC}/T_{ED} comparison seven hundred ninety-six (796) genes was found downregulated (Table 17), and many of which was involved in cell wall modification (65), proteolysis (52), and hormone signaling (30). By contrast, at both T_{IS}/T_{ED} and T_{IS}/T_{EC} comparisons upregulated genes was higher (1,129 and 1,326, respectively) than downregulated transcripts. Cell wall modification, proteolysis, hormone signaling, transcription factors, protein degradation, receptor like kinase, as well as nitrate transport and amino acid biosynthesis, were the main upregulated categories at T_{IS} in uninfected bulbs (Figure 28), underlining the enhancing of key processes for the subsequent phases, such as remobilization and control of reserve compounds, after dormancy breakdown. Indeed, a high number of protein degradation enzymes, mainly E3 ligases, involved in the regulation of proteins level related to seed germination (Oracz and Stawska, 2016) were found upregulated at T_{IS} (Figure 28). Additionally, many transcripts related to ethylene signal transduction, auxin-responsive family (such as SAUR-like protein) and several TFs belonging to WRKY, MYB, and MAPKs families were significantly higher at T_{IS} than T_{ED} in uninfected bulbs. Particularly, four *MAPKs*, *MPK3*, *MPK6*, *MPK11*, and *MMK2*, known to be involved in ethylene production, ABA signaling, seed development and response to cold, respectively (Jagodzik *et al.*, 2018), were upregulated. Three genes related to gibberellin (GA) synthesis, *GAI*, *KAO2* and *G3OX1*, were also upregulated at T_{IS} , in agreement with previous studies underlining their activity during dormancy release (Zheng *et al.*, 2018).



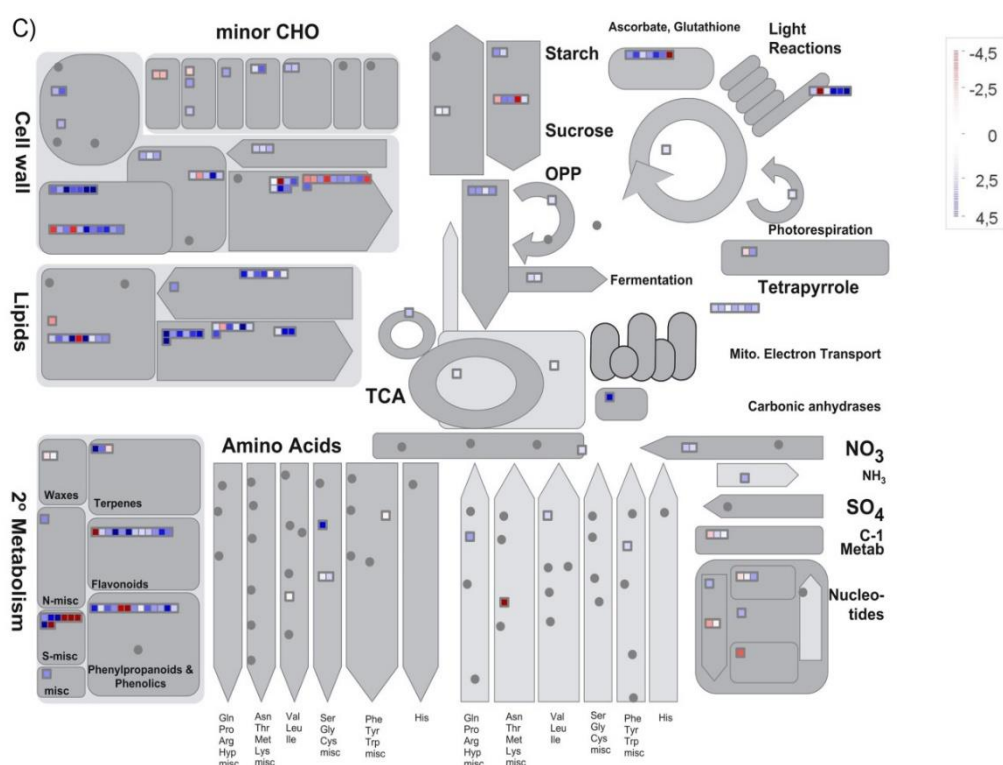


Figure 28. Overview expression level changes of genes associated to primary and secondary metabolism pathways in uninfected bulbs during dormancy, following the Mercator annotation. **A)** T_{EC}/T_{ED} , **B)** T_{IS}/T_{ED} , and **C)** T_{IS}/T_{EC} comparisons. Transcription levels with a value $\log_2 FC > 1$ for pairwise comparisons are displayed in coloured squares. The blue and red indicate up- and down-regulated genes, respectively. The scale showing the expression level is displayed in the pictures that have been exported from MapMan and their quality was further improved accordingly

Furthermore, GO terms enrichment analysis was performed for upregulated genes at each sampling time (T_{ED} , T_{EC} , and T_{IS}) in uninfected samples (Figure 29). Significantly enriched GO terms are strictly in agreement with MapMan BINs analysis. GO terms like “cell wall organization” and “cell wall biogenesis” were found in upregulated genes at T_{ED} , together with “actin filament bundle assembly”, “carbohydrate metabolic process” and “regulation of jasmonic acid mediated signaling pathway” in the Biological Process (BP) category. In upregulated genes at T_{IC} , “response to jasmonic acid”, “response to cold”, “signal transduction”, “xenobiotic transport”, and “response to chitin” categories were identified in the BP. T_{ED} and T_{IS} shared GO terms linked to biotic and abiotic stress response, like “response to wounding”, “defense response” and “response to chitin” (Figure 29). BP GO terms of upregulated genes at T_{EC} showed a very different pattern with

respect to both T_{ED} and T_{IS}, showing the “intracellular sterol transport”, “embryo development ending in seed dormancy” and “response to hydrogen peroxide” as the main GO categories found. Nevertheless, the two terms “cellulose catabolic process” and “phragmoplast assembly”, isolated at T_{EC}, indicated that cell wall modification and cell division processes, started in the endo-dormancy phase, are still active during eco-dormancy. In the Molecular Function (MF) category the only common GO term enriched both at T_{ED} and T_{EC} was “calcium ion binding”. Three different “CoA ligase activity” related terms were found at T_{ED}, while “cellulase activity” was the most enriched term at T_{EC} together with “pectate lyase”, “UDP-galactosyltransferase activity” and “sterol binding”. By contrast at T_{IS} the most enriched term was “DNA-binding transcription factor activity” together with “carbohydrate binding”, “polysaccharide binding”, “calmodulin binding” and “xyloglucan:xyloglucosyl transferase activity”. Finally, in the Cellular Component (CC) category the two-time points T_{ED} and T_{IS} shared several terms like “plant-type cell wall”, “extracellular region”, “apoplast” and “anchored component of plasma membrane”. At T_{EC} “chromocenter”, “chloroplast nucleoid” and “chloroplast photosystem II” were the top three enriched terms and no common terms was found between T_{IS} and T_{ED} (Figure 29).



Figure 29. GO terms enrichment analysis carried out for upregulated genes at different sampling times (T_{ED} , T_{EC} , and T_{IS}) in uninfected bulbs

Transcriptome profiles of uninfected and OYDV-infected plants during the time course were compared (Figure 30) to easily display the molecular changes in onion bulbs during dormancy process and to select the key factors driving the dormancy release. OYDV-infected plants showed a low and fixed number of DEGs during the time course (Table 17). Starting from this evidence, as expected many pathways related to key physiological processes, as cell wall modification, hormone signaling, transcription factors and receptor like kinase, showed significant differences between the two conditions (Figure 30; Figure 31).

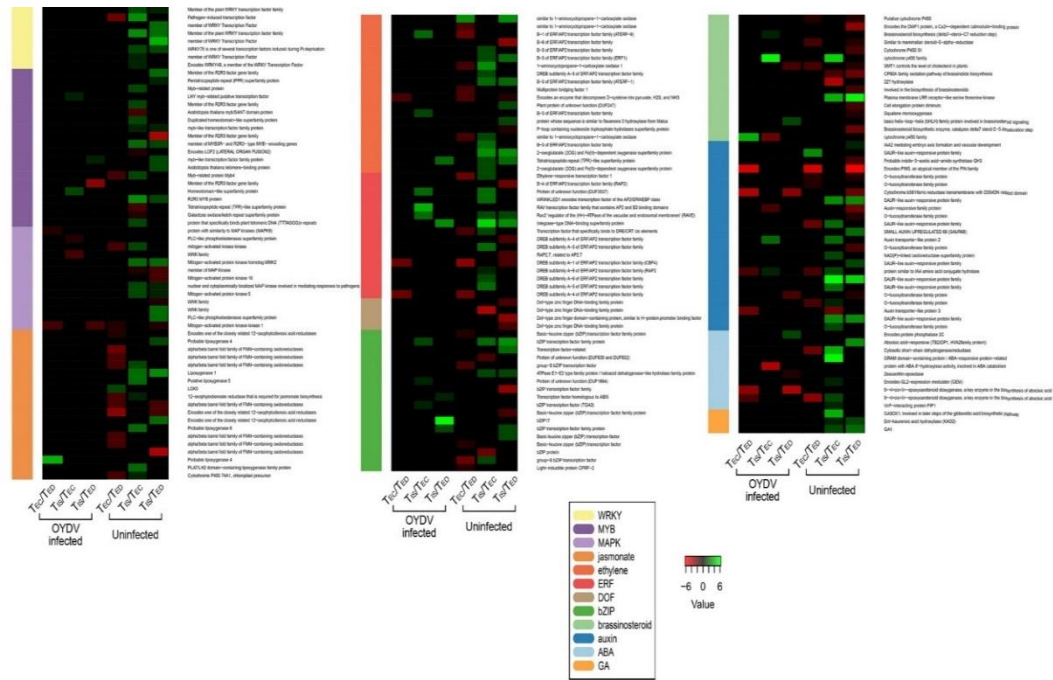


Figure 30. Heatmap developed using DEGs isolated in uninfected bulbs in the three comparisons T_{EC}/T_{ED} , T_{IS}/T_{ED} , and T_{IS}/T_{EC} . Log₂ FC for uninfected (U) and OYDV-infected (I) conditions were displayed.

In the ABA-dependent signaling pathway regulation genes for ABA levels in plants, such as *NCED3* and *CYP707A1*, the ABI5 leucine zipper transcriptional factor, *FIP1*, *AHG3* and *GEM* were differentially expressed between conditions. In particular, *NCED3*, and *CYP707A*, two key genes regulating the ABA levels, were downregulated (\log_2 FC = -3.231; \log_2 FC = -4.459) in OYDV-infected bulbs at T_{EC} and T_{IS} , respectively. By contrast, *GEM*, expressed throughout many stages of vegetative and reproductive development, and considered as a positive effector of germination, was upregulated (\log_2 FC = 6.035) in uninfected bulbs at T_{IS} , as well as the polyadenylation factor *FIP1* (\log_2 FC = 1.206), usually expressed in root and shoot meristems during cell division, and *AHG3* (\log_2 FC = 3.207) involved in seed dormancy release. In agreement, during the internal sprouting phase (T_{IS}), *ABI5* was down (\log_2 FC = -3.053) and upregulated (\log_2 FC = 1.243) respectively in uninfected bulbs and OYDV-infected samples. More interestingly, several genes encoding for SAUR-like auxin-responsive family protein resulted upregulated only in uninfected plants at T_{IS} , while a transcript encoding putative auxin transporter (*NRT1.1*), as well as *ILL6*, an amid hydrolase involved in the IAA biosynthesis,

were both downregulated ($\log_2 \text{FC} = -2.3715$ and -1.5127 , respectively) in latent bulbs (T_{EC}) in uninfected samples. Congruent to other auxin related-genes, *IAA4*, a short-lived TF, working as repressors of early auxin response genes at low auxin concentrations, and the auxin efflux carrier *PIN7* were upregulated at T_{EC} ($\log_2 \text{FC} = 1.3091$) and T_{IS} ($\log_2 \text{FC} = 4.0866$), respectively in uninfected condition (Figure 31).

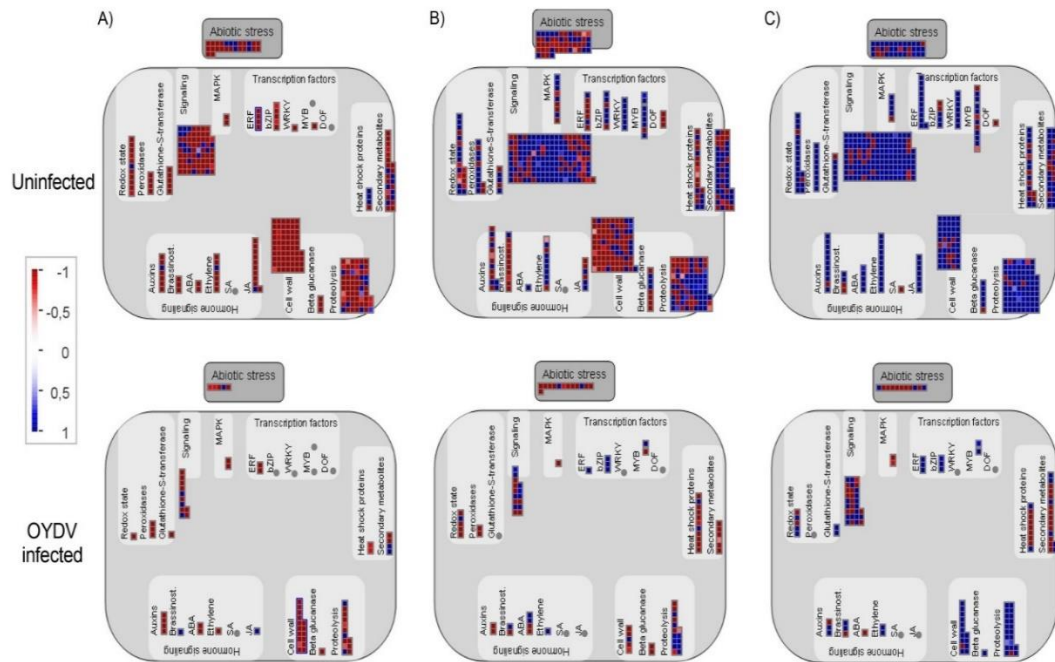


Figure 31. Overview expression level changes of genes associated to hormone signaling, and some key metabolism pathways involved in dormancy process between uninfected and OYDV infected, following the Mercator annotation. **A)** T_{EC}/T_{ED} , **B)** T_{IS}/T_{ED} , and **C)** T_{IS}/T_{EC} comparisons. Transcription levels with a value $\log_2 \text{FC} \geq 1$ for pairwise comparisons are displayed in colored squares. The blue and red indicate up- and down-regulated genes, respectively. The scale showing the expression level, is displayed in the pictures that have been exported from MapMan and their quality was further improved accordingly.

Except a known LRR-RLK (LRR receptor-like serine threonine kinase) member (*SERK1*), the other isolated transcripts related to brassinosteroid (BR) was downregulated in uninfected samples in all comparisons. By contrast, *BESI-INTERACTING MYC-LIKE1* (*BIMI*), involved in BR mediated signaling in plants, was upregulated ($\log_2 \text{FC} = 1.511$) in OYVD-infected plants at T_{IS} . Finally, the 1-aminocyclopropane-1-carboxylate oxidase (*ACO5*), involved in the ethylene (ETH)

metabolism, and several genes belonging to lipoxygenase family (*LOX1*, *LOX4*, *LOX5*), related to Jasmonic Acid (JA) biosynthesis, were up regulated only in uninfected plants at T_{IS} (Figure 31) Three gibberellin-related genes, *KAO2*, *GA3OX1* and *GAI* were also upregulated in uninfected samples at T_{IS}, while *ATH1* that encodes a transcription factor involved in gibberellin biosynthesis was downregulated (log₂ FC = -1.424) at T_{EC} in the same samples. Congruent to this trend, NAC1 transcription factor, linked to gibberellin-mediated endosperm expansion, was over expressed (log₂ FC = 2.080) at T_{IS} in uninfected bulbs.

Furthermore, beyond the large gene families in which several members presented strong different responses to the virus infection during sampling times, the MAP-Kinases signaling cascades (MAPKs), and several TFs displayed different profiles in all comparisons. Remarkably, using the MapMan's annotation, eight genes belonging to *WRKY* family, an essential class of transcriptional regulators involved in many biological processes, were found differentially expressed only in uninfected bulbs, and resulted upregulated at T_{IS} (Figure 31). Because of their importance in modulating of several key mechanisms, to further test the assumptions highlighted from the pathway and GO enrichment analysis during the time course and between conditions, DE transcripts mapping to specific pathways related to *WRKYs*, that potentially may be involved in dormancy and dormancy release, were explored in the next paragraph.

2.2.4 Transcription factors differentially expressed during dormancy

To validate the members of *WRKY* family previously isolated, NCBI's ORFfinder was used to predict the Open Reading Frames (ORFs) for each transcript with 10 million ORFs predicted for the whole transcriptome. HMMER hmmscan was used with the Pfam HMM profile of the *WRKY* gene family to identify proteins among the predicted ORFs. The final set of *AcWRKY* was obtained by selecting the best isoform for each transcript based on the hmmscan score and after filtering for a complete *WRKY* domain presence. Fifty-three *AcWRKY* were selected and termed *AcWRKY* from 1 to 53 (Table 18). Among them, four sequences (*AcWRKY24*, *AcWRKY35*, *AcWRKY43*, and *AcWRKY51*) were excluded for the following analysis due to their short amino acid length. Therefore, the final set of *AcWRKY*

counts 49 transcripts, annotated through blastp search against the nr database and to the Mercator annotation. *AcWRKY* transcripts were clustered into the three known main groups using an in-house bash script and based on the previous WRKY gene family classification (Eulgem *et al.*, 2000). 11 out of 49 *AcWRKYs*, showing two WRKY domains, were assigned to Group I; 24 to Group II (C2H2 domain) and 13 to Group III (C2HC domain) (Table 18). Finally, fifteen *AcWRKY* transcripts did not group in any of the three expected groups, due to slightly different zinc-finger-like motifs or WRKY domains (Table 18).

Table 18. List of *A. cepa* WRKY genes (*AcWRKYs*) extracted, showing a complete WRKY domain.

Gene ID	Transcript ID	Start	End	nt (length)	AA (length)	Group
<i>AcWRKY1</i>	TRINITY_DN15477_c0_g1_i5	1549	782	768	255	Ile
<i>AcWRKY2</i>	TRINITY_DN24552_c0_g2_i5	1303	437	867	288	III
<i>AcWRKY3</i>	TRINITY_DN22804_c0_g1_i2	969	1433	465	154	Ile
<i>AcWRKY4</i>	TRINITY_DN5822_c0_g1_i2	929	123	807	268	III
<i>AcWRKY5</i>	TRINITY_DN15430_c0_g1_i10	308	12	297	98	IIf
<i>AcWRKY6</i>	TRINITY_DN28163_c2_g1_i15	1026	2090	1065	354	I
<i>AcWRKY7</i>	TRINITY_DN17049_c0_g1_i2	381	1220	840	279	III
<i>AcWRKY8</i>	TRINITY_DN222825_c0_g1_i1	54	425	372	124	Ile
<i>AcWRKY9</i>	TRINITY_DN33211_c0_g1_i2	503	1276	774	257	III
<i>AcWRKY10</i>	TRINITY_DN61020_c0_g1_i2	764	123	642	213	Ile
<i>AcWRKY11</i>	TRINITY_DN170973_c0_g1_i1	934	2	933	311	IIf
<i>AcWRKY12</i>	TRINITY_DN1383_c0_g1_i1	825	283	543	180	Ile
<i>AcWRKY13</i>	TRINITY_DN45888_c1_g1_i5	83	1354	1272	423	IIf
<i>AcWRKY14</i>	TRINITY_DN14003_c0_g2_i1	447	34	414	137	I
<i>AcWRKY15</i>	TRINITY_DN1573_c8_g1_i1	167	322	156	51	III
<i>AcWRKY16</i>	TRINITY_DN53363_c0_g1_i2	35	499	465	154	X
<i>AcWRKY17</i>	TRINITY_DN6283_c1_g1_i10	1565	198	1368	455	I
<i>AcWRKY18</i>	TRINITY_DN9124_c1_g1_i7	545	955	411	137	III
<i>AcWRKY19</i>	TRINITY_DN1537_c0_g3_i7	2356	602	1755	584	I
<i>AcWRKY20</i>	TRINITY_DN1730_c0_g1_i2	1100	2263	1164	387	I
<i>AcWRKY21</i>	TRINITY_DN10137_c1_g1_i4	2464	3249	786	261	IIf
<i>AcWRKY22</i>	TRINITY_DN35443_c0_g1_i4	1372	1524	153	50	Ile
<i>AcWRKY23</i>	TRINITY_DN44968_c0_g1_i2	1217	243	975	324	I
<i>AcWRKY24</i>	TRINITY_DN18212_c0_g1_i1	601	512	90	29	-

<i>AcWRKY25</i>	TRINITY_DN256199_c0_g1_i1	350	189	162	53	Ile
<i>AcWRKY26</i>	TRINITY_DN8131_c0_g1_i8	72	329	258	85	Ilc
<i>AcWRKY27</i>	TRINITY_DN28479_c0_g1_i3	333	1364	1032	343	IId
<i>AcWRKY28</i>	TRINITY_DN42557_c0_g1_i1	484	1056	573	190	Ile
<i>AcWRKY29</i>	TRINITY_DN6105_c0_g1_i2	435	1091	657	218	I
<i>AcWRKY30</i>	TRINITY_DN32880_c0_g1_i4	376	1101	726	241	Ile
<i>AcWRKY31</i>	TRINITY_DN1023_c2_g1_i3	1545	790	756	251	III
<i>AcWRKY32</i>	TRINITY_DN15141_c0_g1_i1	579	1661	1083	360	IIb
<i>AcWRKY33</i>	TRINITY_DN28418_c0_g1_i11	631	1035	405	134	III
<i>AcWRKY34</i>	TRINITY_DN40008_c0_g1_i1	829	173	657	218	Ilc
<i>AcWRKY35</i>	TRINITY_DN8388_c0_g1_i9	1479	1387	93	30	-
<i>AcWRKY36</i>	TRINITY_DN92506_c0_g1_i2	1815	97	1719	572	I
<i>AcWRKY37</i>	TRINITY_DN24099_c0_g1_i5	2186	1596	591	196	III
<i>AcWRKY38</i>	TRINITY_DN14175_c0_g2_i3	696	2000	1305	434	I
<i>AcWRKY39</i>	TRINITY_DN71397_c0_g1_i2	304	990	687	228	Ile
<i>AcWRKY40</i>	TRINITY_DN20923_c0_g1_i1	394	104	291	96	III
<i>AcWRKY41</i>	TRINITY_DN15245_c0_g1_i4	388	1485	1098	365	Ile
<i>AcWRKY42</i>	TRINITY_DN2402_c0_g1_i4	1067	501	567	188	III
<i>AcWRKY43</i>	TRINITY_DN72539_c0_g1_i1	282	362	81	27	-
<i>AcWRKY44</i>	TRINITY_DN231786_c0_g1_i1	387	34	354	117	Ilc
<i>AcWRKY45</i>	TRINITY_DN6098_c0_g1_i6	999	115	885	294	IIb
<i>AcWRKY46</i>	TRINITY_DN13617_c0_g1_i3	1122	511	612	203	III
<i>AcWRKY47</i>	TRINITY_DN62468_c0_g1_i1	10	255	246	81	IIb
<i>AcWRKY48</i>	TRINITY_DN49432_c0_g1_i2	541	1380	840	279	IIa
<i>AcWRKY49</i>	TRINITY_DN13634_c0_g1_i3	463	1437	975	324	IId
<i>AcWRKY50</i>	TRINITY_DN2971_c5_g2_i2	2043	406	1638	545	I
<i>AcWRKY51</i>	TRINITY_DN24099_c0_g3_i1	92	0	93	30	-
<i>AcWRKY52</i>	TRINITY_DN6283_c0_g1_i1	633	2072	1440	479	I
<i>AcWRKY53</i>	TRINITY_DN24099_c0_g2_i1	16	162	147	48	III

After validation, among DEGs identified in the differential expression analysis we found fourteen *AcWRKY* upregulated (*AcWRKY1*, 2, 3, 9, 12, 17, 18, 21, 26, 30, 32, 37, 46, and 52) in uninfected samples, overlapping to the MapMan annotation; by contrast *AcWRKYs* did not result differentially expressed in OYDV-infected bulbs in all comparisons (Table 19). Interestingly, three (*AcWRKY2*, *AcWRKY30*, and *AcWRKY32*) out of 14 WRKY genes differentially expressed showed also a significantly higher expression ($p < 0.05$) in uninfected compared to the OYDV-

infected plants at T_{IS}, during dormancy release (Figure 32A, B). Whereas *AcWRKY18*, *21*, and *37* were significantly downregulated between conditions at T_{EC}.

Table 19. Summary of *AcWRKYs* detected in both uninfected and OYDV-infected bulbs in each comparison.

Condition	TEC/TED	TIS/TED	TIS/TEC
Uninfected	<i>WRKY18, 21 37</i>	<i>WRKY2, 9, 12, 17, 30, 32, 46, 52</i>	<i>WRKY1, 2, 3, 9, 12, 17, 18, 21, 26, 37, 46, 52</i>
OYDV-infected	-	-	-

Transcriptomic profiles of all differentially expressed *AcWRKYs*, isolated through RNA-seq analysis, were validated by qPCR. WRKY gene expression trend in qPCR was in accordance to transcriptome expression patterns (Figure 32). To verify the reliability and reproducibility a Pearson correlation analysis between RNA-seq and qPCR results was carried out. The correlation coefficient was 0.88 (R), which was significant at the $p < 0.001$ level (Figure 33). Quantitative PCR confirmed the expression values showed by RNA-Seq analysis for *AcWRKY2*, *AcWRKY30*, and *AcWRKY32* at T_{IS} and, interestingly, also *AcWRKY52* was significantly upregulated in uninfected samples (Figure 32C).

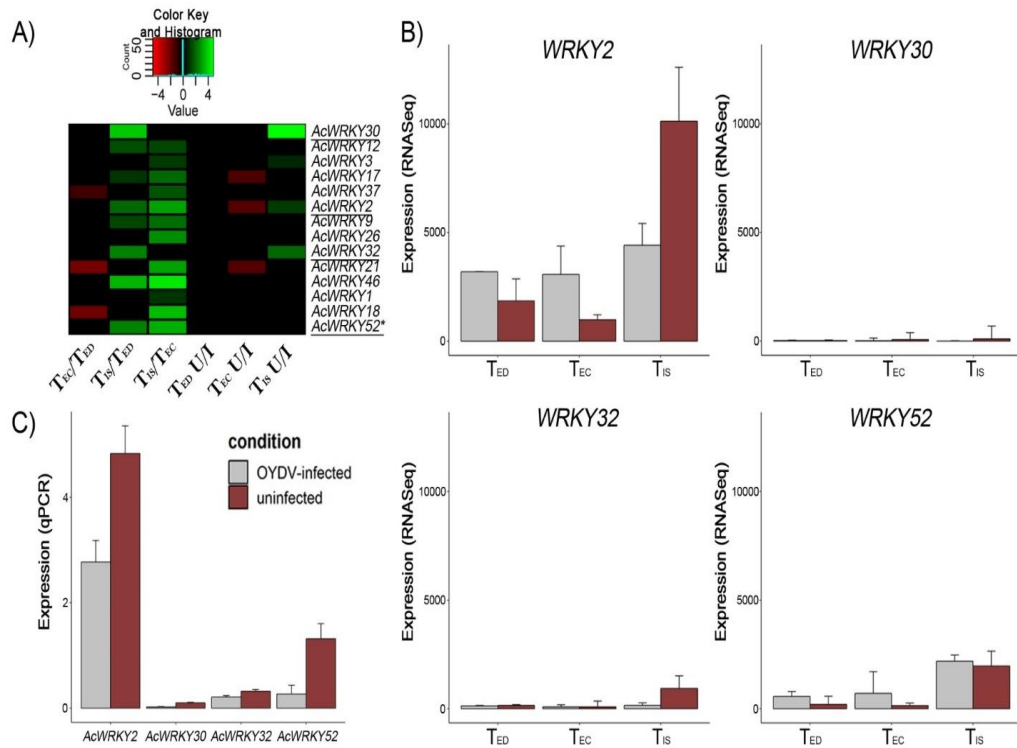


Figure 32. Expression levels of AcWRKY genes isolated during dormancy phases (endo-dormancy, eco-dormancy and internal sprouting). **A)** Heatmap developed using log₂ Fold-Change (by Deseq2) values of *AcWRKYs* for T_{EC}/T_{ED}, T_{IS}/T_{ED}, and T_{IS}/T_{EC} comparisons. Genes differentially expressed between uninfected (U) and OYDV-infected (I) bulbs at each time (T_{ED}, T_{EC}, and T_{IS}) was also visualized; *AcWRKYs* showing significant differences (p<0.05) by RNASeq and qPCR between the two conditions during dormancy release (T_{IS}) were underlined. **B)** RNA-Seq counts normalized of *AcWRKY2*, 30, 32, and 52 at each sampling time, detected from uninfected (red) and OYDV-infected (gray) samples. **C)** qPCR analysis of *AcWRKY2*, 30, 32, and 52 during internal-sprouting phase (T_{IS}) for uninfected (red) and OYDV-infected (gray) bulbs.

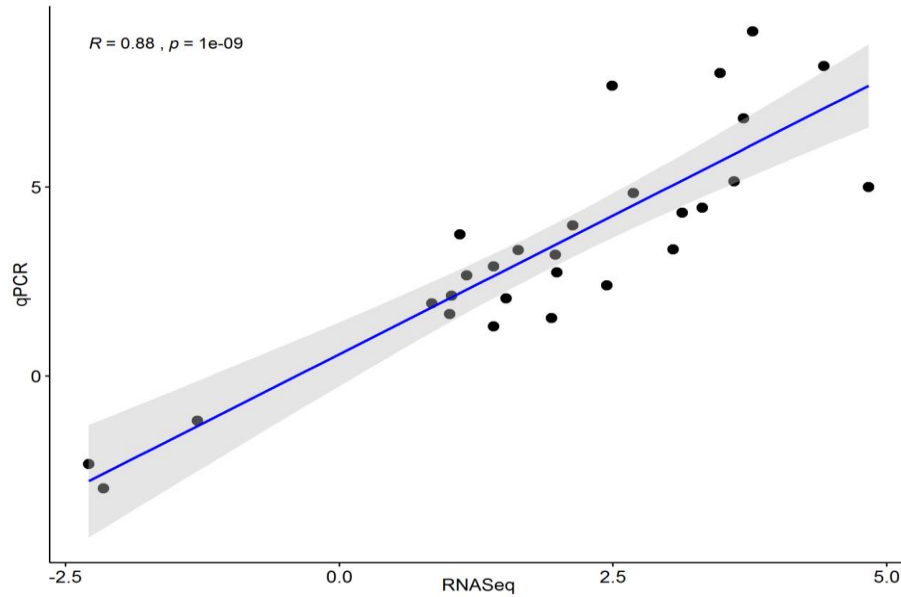


Figure 33. Correlation analysis between RNA-Seq and qPCR data for *AcWRKYs* differentially expressed in each comparison. The same RNAs from NGS experiment were utilized for validation. The Pearson Correlation Coefficient ($R = 0.88$) and the p-value ($p = 1e-09$) were reported.

2.2.5 Gene co-expression network analysis

A co-expression network analysis was carried out to gain insight on the *AcWRKYs* role in dormancy break, selecting up regulated TF at T_{IS} in the uninfected/OYDV infected bulbs comparison (*AcWRKY2*, 30, 32, and 52; Figure 32). We observed three hundred-eight (308) genes co-expressed with the four *AcWRKYs* used as baits for the CoExpNetViz tool (Figure 34). Nearly 44% (134) was correlated to *AcWRKY32*, followed by *AcWRKY2* (69; 22%), *AcWRKY52* (33; 11%) and *AcWRKY30* (8; 3%). Additionally, other 64 genes were shared by the pair *AcWRKY2-52*, with 34 (11%) and 30 (9%) positively and negatively co-expressed, respectively (Figure 34). In agreement to MapMan and GO enrichment analyses, several genes encoding MAP kinases, ethylene-, brassinosteroid-, ABA-, jasmonic acid and auxin-related proteins, together with TFs and cell cycle regulation proteins were isolated.

In detail, the main auxin-carriers, *PIN7* and *Nrt1.1*, together with another high affinity nitrate transporter (*Nrt2.5*), were found co-expressed with *AcWRKY32*. Another auxin related gene, *SAUR50*, was found co-expressed with the sub-network *AcWRKY2-52*, while *LOX1*, expressed both during germination and biotic stresses

in *Arabidopsis* (Melan *et al.*, 1994), and the auxin response factor *ARF2A* were found correlated with *AcWRKY32*.

In addition to auxin linked genes, *SERK1*, Phospholipase D PLD alpha 1, and serine/threonine protein kinase ARK3 belonged to the *AcWRKY32* sub-network. Furthermore, transcripts involved in calcium signaling, like the plasma membrane calcium pump ACA9, calcium influx regulator *GLR2.8* and calmodulin binding proteins (*CML27*), inositol polyphosphate 5-phosphatase (*5PT*), driving the pollen dormancy (Wang *et al.*, 2012), and genes related to cell wall development and biosynthesis (*WALK20*, *WAV3*, *MWL-1*) were also co-expressed with *AcWRKY32*. Three important ABA signaling related genes were extracted from networking analysis and were co-expressed with *AcWRKY32* (*PYL6*, *HVA22*) and *AcWRKY52* (*SnRK2.3*), while three other calcium-dependent protein kinases, *CDPK7*, 28 and 32, were linked to *AcWRKY32*, 52, and 2, respectively.

The ERF104 protein was found co-expressed with *AcWRKY52*, while two MYB TFs were linked to *AcWRKY30*, and 52. SRG1 gene belonging to 2-oxoglutarate (2OG)/Fe(II)-dependent oxygenase superfamily was found in the sub-network of *AcWRKY52*, while the protein kinase APK2b, involved in ABA signaling during seed germination (Nakashima *et al.*, 2009) was found co-expressed with *AcWRKY2*.

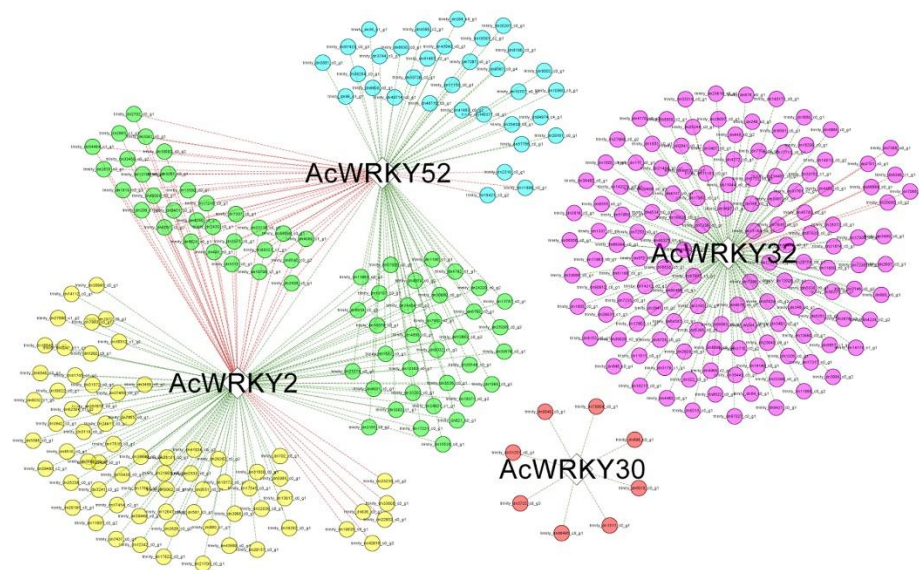


Figure 34. Co-expression network analyses of four AcWRKY up regulated at T_{1S} in the uninfected/OYDV infected bulbs comparison (*AcWRKY2*, 30, 32, and 52). The network was obtained with Comparative Co-Expression Network Construction and Visualization tool and visualized by Cytoscape. Green and red lines denote positive correlation and negative correlation, respectively.

2.2.6 Conclusion

In the present study, we described the atlas of differences in genes transcription triggered by OYVD infection in onion bulb. For the first time, the role of genes belonging to the *WRKY* family in *A. cepa*, were underlined. Furthermore, using the OYDV-infected samples as filter, we highlighted the key pathways and metabolomics changes during dormancy in onion bulbs. Interestingly, infected samples showed only few differentially expressed genes related to dormancy during storage. This is probably the cause of the worst shelf life and the premature sprouting of infected bulbs that are unable to enter on time in their physiological dormancy phase. Finally, transcriptomic profiles and co-expression analysis allowed to identify a WRKY-TF (*AcWRKY32*) potentially driving the dormancy release in onion bulbs.

Chapter 3 Study on molecular plant-pathogen interactions: host factors involved in the cell-cell movement of potyviruses?

1. Material and methods

1.1 Split Ubiquitin Yeast Two Hybrid System (DUAL membrane system)

The SUY2H approach is used for the identification of membrane-related proteins interactions that cannot be identified using a classical Y2H system (Stagljar *et al.*, 1998). The SUY2H is based on ubiquitin complementation. Ubiquitin can be split into two parts, N-terminal ubiquitin (Nub) and C-terminal ubiquitin (Cub), which are able to re-associate *in vivo* to form active ubiquitin. The bait protein is fused to the Cub moiety linked to a chimeric transcription factor (LexA-VP16), while potential membranous or cytosolic protein interactor, called the « prey », is fused to the N-terminal (Nub) ubiquitin moiety (Figure 35). When Bait and Prey interact, the ubiquitin is reformed and recognized by the yeast Deubiquitinating protease (DUB) which releases the LexA-VP16 transcription factor. The LexA-VP16 transcription factor is then translocated into the nucleus where it recruits the RNA polymerase II and induces the expression of reporter genes (*ADE2*, *HIS3*, which are auxotrophic growth markers for adenine and histidine) and *LacZ* (the colorimetric reporter gene) (Figure 35). The bait and prey plasmids contain the auxotrophic growth markers *LEU* and *TRP* respectively (leucine and tryptophane), that allow to select co-transformed yeasts on minimal growth medium deprived of the two amino acids (SD-leu-trp) (SD-LT). When interaction occurs, the transformed yeasts will grow on the selective media SD-leu-trp-his (SD-LTH) and SD-leu-trp-his-ade (SD-LTHA), due to induction of the reporter genes. The more the medium is deficient in amino acids, the stronger is the selection stringency.

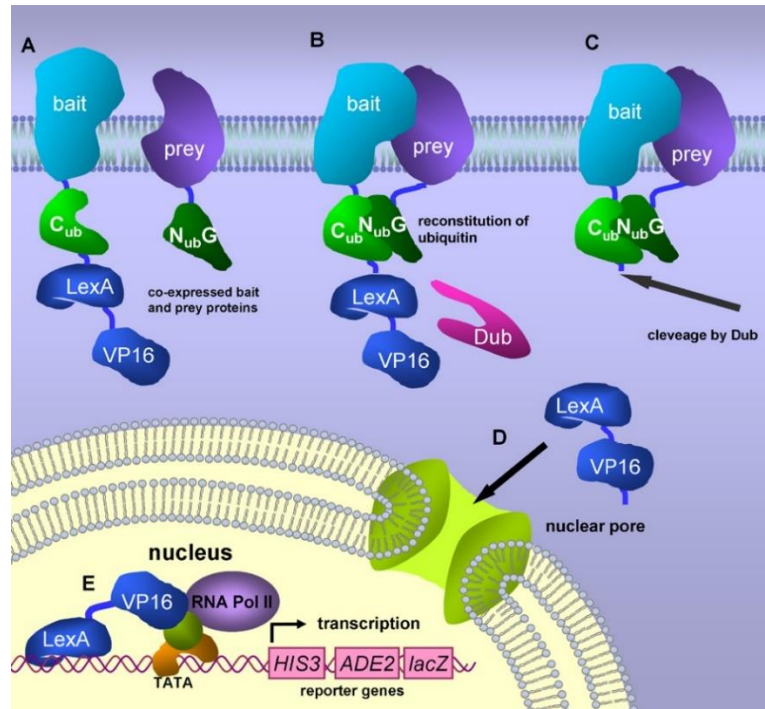


Figure 35. Schematic representation of the SUY2H system (Ivanusic *et al.*, 2015)

The WMV-6K2 bait and the sixteen melon preys CmXX (*Cucumis melo* proteins) listed in Table 20 were previously cloned and supplied by INRAE-Avignon: WMV-6K2 was cloned in pBT3-N vector, and the preys were cloned in pPR3-N vector. The positive control of the experiment was based on the already shown interaction between AtHVA22a prey and TuMV-6K2 bait. The negative control was performed with AtCER1 that does not interact with any of the CmXX preys but does interact with AtCytB5b [Luc Sofer, personal communication and Bernard *et al.* (2012)]. The THY.AP4 strain of *Saccharomyces cerevisiae* was used (genotype *lexA-lacZ lexA-HIS3 lexA-ADE2 ura3 leu2 trp1*) for protein interactions analysis in SUY2H. This strain is auxotrophic for Leucine and Tryptophan and carries *ADE2* and *HIS3* growth reporter genes for interaction.

Table 20. List of the sixteen candidate interactors of WMV-6K2 (For confidentiality the exact names are not given)

CmProtein prey	
CmXX4	CmXX36
CmXX2.1	CmXX25
CmXX2.2	CmXX37.1
CmXX2.3	CmXX37.2
CmXX32.1	CmXX28
CmXX32.2	CmXX23.1
CmXX32.3	CmXX23.2
CmXX24	CmXX4mut

Split ubiquitin assay was performed in the frame of three independent experiments using the DUAL membrane system (Dualsystems Biotech AG). *Saccharomyces cerevisiae* THY.AP4 cells were co-transformed and grown according to Dualsystems Biotech AG protocols, using 500 ng of bait plasmid (pBT3N-WMW-6K2) and 500 ng of prey plasmid (pPR3-N-CmXX) with 100 µg of ssDNA carrier (Invitrogen). The co-transformed yeasts were spread on SD-LT plates and incubated for 5 days at 37 °C.

Six independent colonies per plate were resuspended into 50 µl H₂O and 5 µl were spread on the selective media SD-LTH and SD-LTHA plates.

To increase the stringency of the selective medium, 1mM 3-aminotriazole (3-AT) was added to SD-LTH and SD-LTHA plates. The 3AT is a competitive inhibitor of *HIS3* gene product. Therefore, the presence of 3AT will allow to select yeast clones with a high level of expression of *HIS3* which depends on the strength of the interaction between the bait and the prey. The growth of the yeast colonies on the selective media was monitored 5 days later and an image of the plate was scanned.

1.2 Cloning of AtXX4, the *Arabidopsis orthologous* gene of *CmXX4* into entry and destination vectors using Gateway® technology

The Gateway® cloning technology is a universal cloning method based on the site-specific recombination properties of bacteriophage lambda (Landy, 1989). One of the main advantages of the GATEWAY® Cloning Technology is that once you have made an Entry Clone, the gene of interest can then be easily subcloned into a wide variety of Destination Vectors using the LR Reaction, principle that is explained on Figure 36.

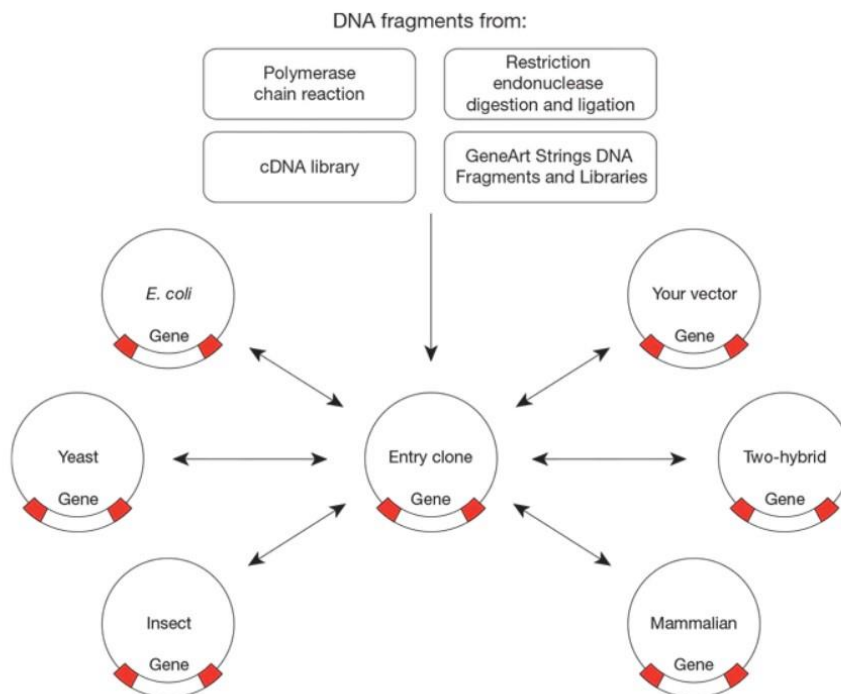


Figure 36. Schematic representation of Gateway® technology. Once a gene is cloned into an Entry clone it can then be moved into different Destination vectors through in vitro recombination reactions (ThermoFisher)

1.2.1 PCR amplification of *AtXX4* cDNA

Nicotiana benthamiana and *Arabidopsis thaliana* (At-Col0) plants were cultivated in controlled conditions in the greenhouse at the INRAE with a 10 h of daylight and temperature of 24 °C.

Total RNAs were previously extracted from *Arabidopsis thaliana* by Roxane Lion in the Bordeaux-Virology team, using the NucleoSpin® RNA plant kit (Macherey-Nagel) and cDNA synthesized. A PCR reaction was performed to amplify the *AtXX4* gene with the primers pair F (CACCATGGCTGCGGTTCCGCCTG) and R (ACCTTCTTCTCCAAACTCCTG), using a thermocycler Eppendorf™ Mastercycler™ pro PCR System, and the Phusion™ High-Fidelity DNA Polymerase (Thermo Scientific™).

Table 21 and 22 show the amplification reaction mix composition and the PCR cycles conditions respectively.

Table 21. Composition of the reaction mix used for *AtXX4* PCR amplification

Reagents	Volume µl
cDNA	1
5x GC Taq buffer	4
Taq Phusion (2U/µl)	0.25
Primer F/R (5 µM)	1/1
dNTPs (10mM)	0.25
H ₂ O	12,5
Final volume	20

Table 22. PCR reaction steps for *AtXX4* PCR amplification

Step	Temperature	Time	Cycle number
Initialiation	98 °C	30 s	1
Denaturation	98 °C	5 s	48
Annealing	62 °C	20 s	
Elongation	72 °C	1.30 min	
Final elongation	72 °C	5 min	1
Hold	14 °C	∞	

The presence and the size of PCR amplification products (amplicons) were verified after migration on agarose gel 1,5% after loading of 5 ul of PCR reaction and 1ul of 6x loading buffer. The 1Kb ladder (Invitrogen) was used to estimate the size of the bands.

1.2.2 Cloning of *AtXX4* into the pENTRTM/D-TOPO[®] vector

The pENTRTM Directional TOPO[®] Cloning Kit (Invitrogen) was used following the guidelines provided by the manufacturer, to clone the PCR product *AtXX4* into of the pENTRTM/D-TOPO[®] vector to generate an entry clone (Figure 37 and Table 23).

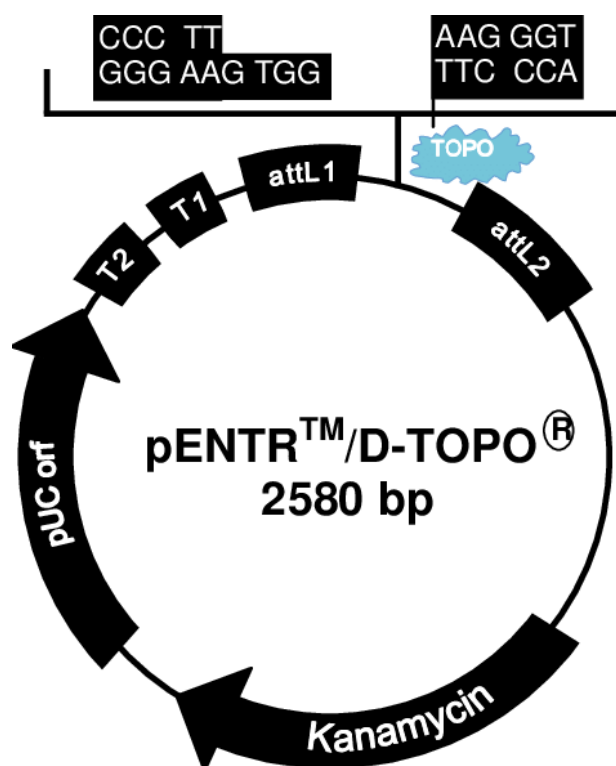


Figure 37. Vector pENTRTM/SD/D-TOPO[®] (Invitrogen) used to clone *AtXX4* gene

To clone the PCR product into the pENTRTM/D-TOPO[®] the following reaction was done and incubated overnight at 4 °C (Table 23).

Table 23. Reaction mix used for pENTRTM/D-TOPO[®] cloning

Reagents	Volume μ l
PCR products	3
TE 1X buffer	2
TOPO [®] vector (20g/ μ L)	1
Final volume	6 ul

DH10B *E. coli* competent cells (ThermoScientific™) were transformed by electroporation in a pre-cooled 0,1cm Electroporation cuvette, we added 1,5 µl of TOPO® Cloning reaction, 40 µl of *E. coli* DH10B competent cells and 60 µl of Glycerol 10%. The cuvette containing the cell suspension was then placed into the Gene Pulser® II (Biorad™) to perform electroporation (1.8kV, 25 µF capacitance and 200 Ω resistance). Then, 200 µl of room temperature S.O.C. medium was added to the electropored bacteria in the cuvette, and the solution was transferred into a 1,5 ml Eppendorf tube and incubated at 37 °C for 45 minutes.

The transformed competent cells were spread on selective LB agar medium plate (containing 50 µg/ml Kanamycin) and incubated at 37 °C for 24 hours.

1.2.3 Rapid PCR-based colony screening for cloned inserts

Following transformation of the TOPO cloning reaction into competent *E. coli* cells, the successful subclones were identified by a PCR-based method for direct screening of transformants. For this purpose, 94 transformed colonies were directly tooth-picked into 10 µl of PCR reaction mix that includes the pair of universal primers flanking the cloning site [M13F (GTAAAACGACGGCCAG) and M13R (CAGGAAACAGCTATGAC)] and the *Taq* DNA Polymerase ThermoPol® (Biolabs™) (Tables 24 and 25).

Table 24. PCR reaction mix used for colonies screening

Reagents	Volume µl
Colonic+ H ₂ O	8.35
Primer F/R (5 µM)	0.05/0.05
10X ThermoPol Reaction Buffer	1
BSA (1mg/ml)	0.1
dNTPs (10mM)	0.1
Taq DNA Polymerase (5U/µL)	0.1
Final volume	10 ul

Table 25. PCR reaction steps for colonies screening

Step	Temperature	Time	Cycle number
Initiation	94 °C	3 min	1
Denaturation	92 °C	30 s	36
Annealing	62 °C	30 s	
Elongation	72 °C	1.30 min	
Final elongation	72 °C	5 min	1
Hold	14 °C	∞	1

1.2.4 Plasmid extraction from positive bacteria colonies and sequencing of the cDNA insert

The bacteria colonies from which a PCR product of the correct size was amplified were resuspended in 5mL of LB medium with 10µL of Kanamycin (50 µg/ml) and placed in an incubator at 37 °C at 200 rpm overnight. Colonies cultures were centrifuged at 7500 rpm for 1 min and after discarding the supernatant, the bacteria pellets were used for plasmid extraction and purification using the kit NucleoSpin® Plasmid EasyPure (Macherey-Nagel).

The purified DNA was quantified with the Spectrophotometer Epoch (Biotek®), and an aliquot of 80 ng/ul was sent to the Genewiz® company (Leipzig, Germany) for sequencing to confirm the nucleotide sequence and the cloning orientation, using the universal M13F and M13R primers cited before.

1.2.5 Subcloning the AtXX4 gene from the Entry clone into a Destination Vector for expression of fluorescent-tag-fusion protein

LR recombination from entry clone to destination vector allowed the cloning of AtXX4 gene in different expression vectors as described in Figure 38, according to Gateway® LR Clonase® II Enzyme Mix (Invitrogen®) protocol (Table 26).

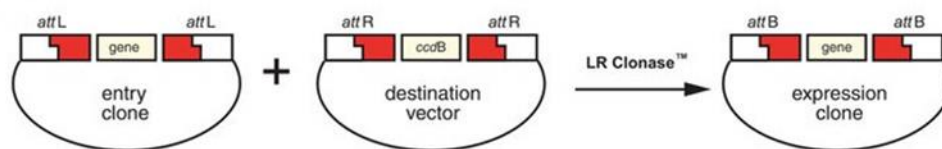


Figure 38. Schematic view of the LR recombination: The gene of interest in the entry clone is flanked by the two attL sites that recombine with the attR sites of the destination vector in presence of LR clonase mix, leading to an expression clone (Gateway technology manual)

Table 26. Reaction mix used for LR recombination in a destination vector

Reagents	Volume µl
Entry clone (300ng/µL)	3,8
Destination vector (150ng/µL)	0,5
LR clonase	2
TE 1X buffer	1,7
Final volume	8 ul

The reaction mix was incubated in a thermocycler at 25 °C for 4 hours with a final step at 65 °C for 20 minutes, followed by an electroporation of DH10B *E. coli* competent cells (Thermo Scientific™) as described before and spreading on LB agar medium plate with 100 µg/ml spectinomycin and incubation at 37 °C overnight. A rapid PCR-based colony screening was performed to identify the recombinant colonies as described before using the attB primers pairs described Figure 5. Two positive colonies were chosen, the plasmid extracted and sequenced to control that fusion of AtXX4 with the expected tag is correct. The different destination vectors and constructs obtained are schematically represented in Figure 39.

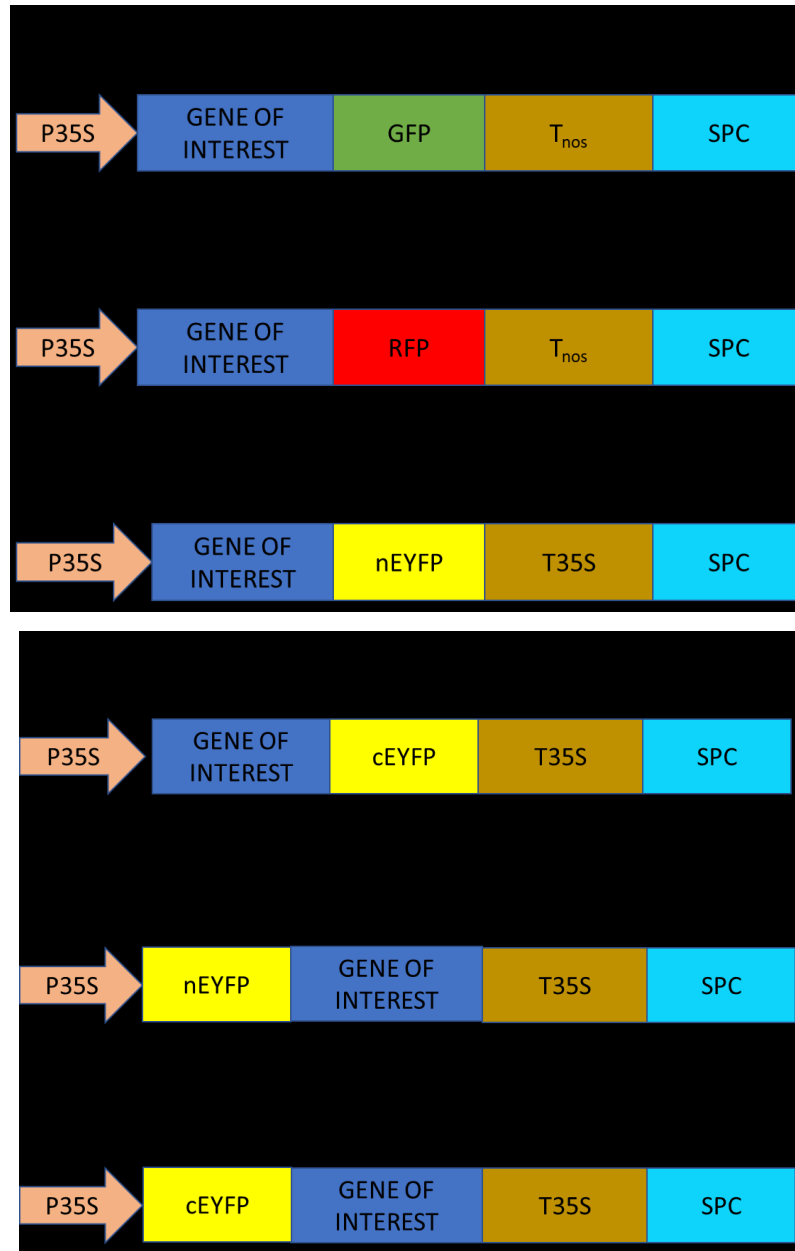


Figure 39. Gateway binary vectors used in this study. The pGW705 and pGW754 vectors allow the expression of C-terminal fusion with GFP- and RFP-at the C-ter of the protein of interest. The Psite vectors are used for BiFC experiments: the protein of interest is fused either at its N-ter (serie “N1”) or at its C-ter (serie C1) to the N-ter part (nEYFP) or C-ter part (cEYFP) of the YFP. SPC: spectinomycin resistance gene. P35S and T35S: transcription promoter and transcription termination derived from CaMV. Tnos: poly-adenylation signal of the nopaline synthase gene.

1.3 Use of *Agrobacterium tumefaciens* for transient expression of proteins and virus inoculation in *N. benthamiana*

The technique of agroinfiltration has been widely used in *Nicotiana benthamiana* for the rapid detection of gene expression of fluorescent fusion proteins, protein-protein interactions analysis, protein subcellular localization and also virus inoculation. For this purpose, *N. benthamiana* leaves are infiltrated with recombinant agrobacteria transformed with a binary vector that harbors the gene of interest cloned into the T-DNA between the left and right borders.

1.3.1. Viral and other molecular constructs cloned into binary vectors

The TuMV-6K2-mCherry construct was kindly supplied by J. F Laliberté (Jiang *et al.*, 2015). The full-length infectious cDNA TuMV-UK1 is cloned into an agrobacterium binary vector under the control of a 35S transcription promoter and 35S terminator. In this construct, the genome of TuMV is engineered to ectopically express the mCherry fluorescent protein fused at the C-terminus of the 6K2 (Figure 40A). This allows to visualize the TuMV-produced 6K2:mCherry vesicles labelling the VRC in infected cells (Figure 40B).

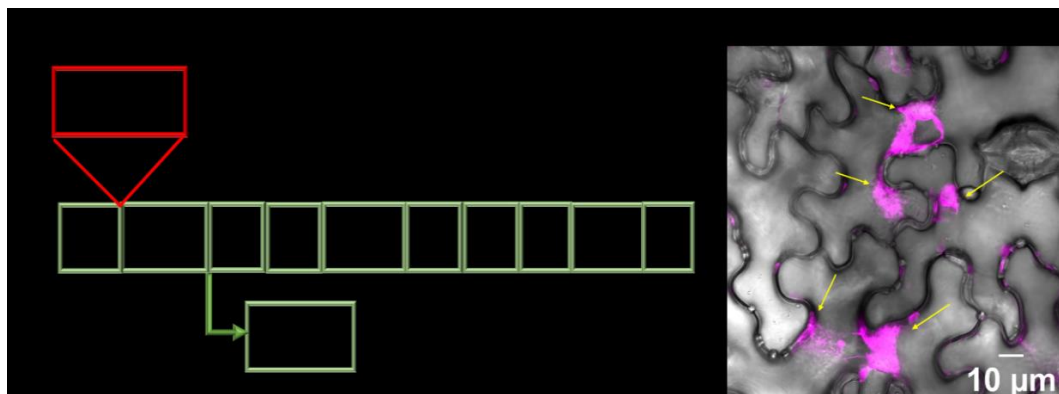


Figure 40. **A)** Schematic representation of recombinant TuMV expressing 6K2-mCherry. **B)** During TuMV-6K2-mcherry replication, the virus induces the formation of viral replication complexes (VRC) that are labelled by the 6K2-mcherry and indicated by yellow arrows

For transient expression of fluorescent fusion proteins, the P19 construct corresponds to the cDNA of the RNA silencing suppressor encoded by TBSV: the co-expression of this P19 silencing suppressor with the protein of interest, enhances its expression (Voinnet *et al.*, 2003).

In this work, all the binary vectors constructs (including the fluorescent fusion-AtXX4 constructs obtained in § 1.2.5 and shown in Figure 39 were transformed into the agrobacterium strain C58C1.

The transformed agrobacteria were spread on selective LB agar medium plate and incubated at 28 °C for 48 hours. As agrobacterium strain C58C1's chromosome carries resistance to Rifampicin, the Ti-plasmid resistance to Gentamycin and our expression vectors resistance to Spectinomycin, we prepared LB agar medium with Rifampicin (40 µg /mL), Gentamycin (20 µg/mL) and Spectinomycin (100 µg/mL).

1.3.2. Preparation of Agrobacterium cultures for infiltration

Agrobacteria transformed with the binary plasmids were grown until reaching an optical density at 600 nm (OD_{600nm}) of 0.8 to 1 measured with a spectrophotometer DU[®]-64 (Beckman). Then the culture was diluted to obtain a final OD_{600nm} of 0.5. Each agrobacterium culture transformed with an expression vector was grown separately and then depending on the experiment, mixed with another one. The agrobacteria mixes were centrifuged at 4700 rpm for 10 minutes, the supernatant was discarded, and the bacteria pellet was resuspended in 5mL of sterile H₂O containing 50µL of MES (1M) and 7.5µL of acetosyringone (100mM).

The agroinfiltration of the agrobacteria was performed using a 1ml syringe on the second and third leaves of 3-4 weeks old *N. Benthamiana* plants: the open end of the syringe was placed against the bottom of the leaf, and gentle pressure was applied while pressing down on the syringe.

1.3.3 Confocal microscopy analysis

Bimolecular fluorescence Complementation (BiFC) technique, based on the reconstitution of a fluorescent YFP protein separated into N-terminal and C-terminal parts (nEYFP and cEYFP), linked respectively to the proteins whose interaction, was tested. If interaction occurs, the two YFP parts join together reconstituting the protein and resulting in fluorescence emission (Figure 41).

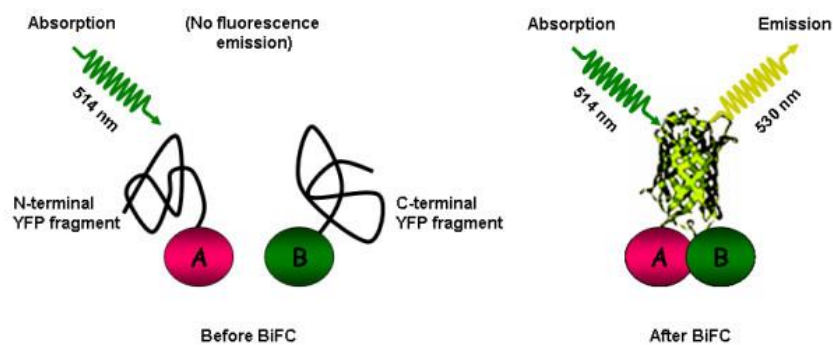


Figure 41. Principle of the BiFC assay. Proteins A and B are fused to N- and C-terminal fragments of YFP, respectively. In the absence of an interaction between A and B, the fluorophore remains non-functional. With interaction between A and B, a functional fluorophore is reconstituted which exhibits emission of fluorescence upon excitation with an appropriate wavelength. (Bhat *et al.*, 2006).

The observations of AtXX4 interaction with TuMV-6K2 (BiFC) in healthy and TuMV-6K2mcherry infected plants and subcellular localization of AtXX4-RFP and -GFP fusions, were made 3-4 days post agro-infiltration using a confocal microscope Zeiss Axio Imager.Z2 Airscan LMS880 under 10X and 63X objectives. The 488-nm Laser Argon was used to detect YFP (maximal excitation wavelength at 514 nm and emission wavelength at 530 nm) and GFP (excitation wavelength at 488 nm and emission wavelength at 507 nm). The 514-nm Laser Argon was used to detect RFP (excitation wavelength at 555 nm and emission wavelength at 584 nm). The DPSS 561-nm laser was used to detect mCherry (excitation wavelength at 585 nm and emission wavelength at 611 nm).

The Lambda-mode was used to control the spectral signature of the fluorescent-signal in confocal experiments.

Images were processed using the ImageJ software (<https://imagej.nih.gov/ij/index.html>).

2. Results and Discussion

2.1 Four out of sixteen CmXXX candidates interact with WMV-6K2 in Yeast

In order to check whether the CmXXX proteins listed in Table 20 interact with the WMV-6K2 as a bait, a SuY2H was performed as described in § 1.1 (Material and Methods) in 3 independent experiments.

The aim of this approach is to screen which melon ESCRT-related proteins with the potyviral bait WMV-6K2

The level of interaction for each combination (CmXX + WMV-6K2) was evaluated after plating six independent colonies on the selective medium SD-LTHA and after 5 days of incubation at 28 °C. When 4 to 6 colonies (65%-100 %) grew well on SD-LTHA plate, it was concluded that there was a strong interaction. When 3 colonies (50%) grew it was considered to be a medium interaction, and no interaction when 0 to 2 colonies only grew.

Figure 42 illustrates the results obtained for each of the 16 CmXXX / WMV-6K2 combinations tested in one experiment. For the interactions involving CmXX4, CmXX2.1 CmXX 24 and CmXX28, at least 4 colonies grew well (boxed in green), suggesting a strong level of interaction. A medium level of interaction was observed for CmXX2.2, CmXX 2.3 and CmXX25 (boxed in yellow) where 3 colonies grew, while in the remaining samples (boxed in red) only 2 or even less colonies grew, indicating that there is no interaction between the protein and the WMV-6K2.

A strong interaction was also observed for the positive control combination AtHVA22a / TuMV-6K2 (boxed in green). AtCER1 was used as negative control: no interaction with any of the CmXXX proteins occurred, confirming the validity of the system. It was also previously checked that AtCER1 interacts with AtCytB5b (data not shown) showing that the lack of interactions with CmXXX proteins is not due to a lack of expression in yeast of the negative control AtCER1.

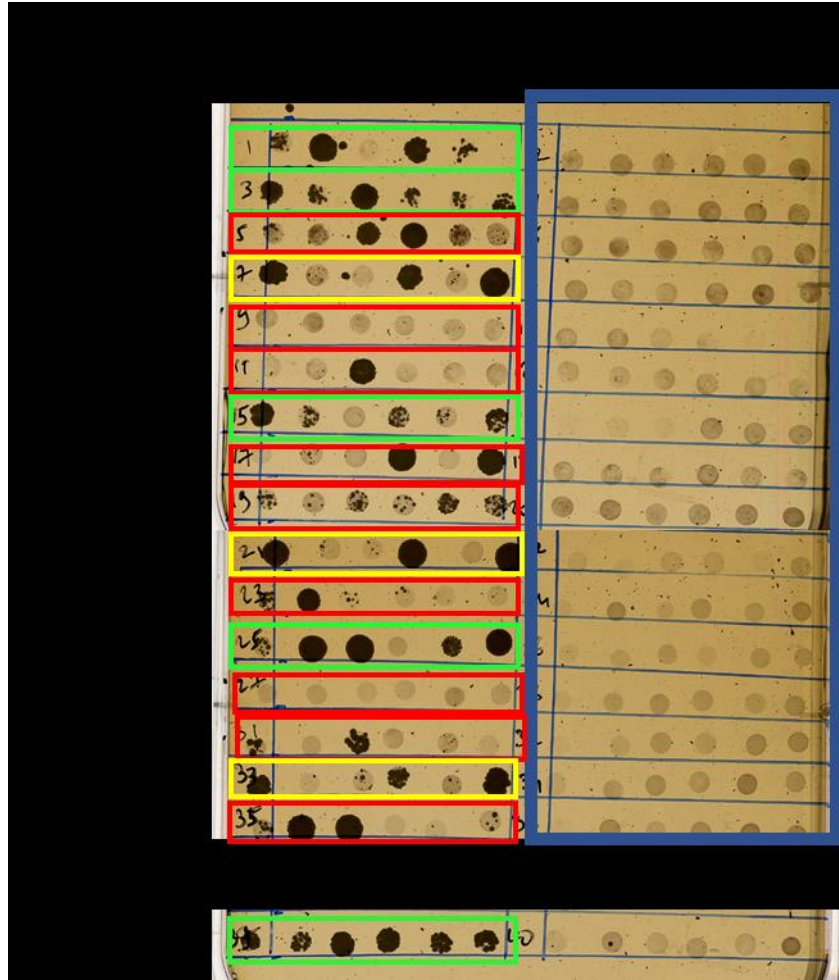


Figure 42. Analysis of interactions between WMV-6K2 and CmXX proteins by SuY2H assay. Six independent yeast colonies co-transformed with CmXX (prey) and WMV-6K2 (bait) were grown on SD-LTHA medium. Colonies boxed in green, yellow and red correspond to strong, medium and lack of interaction respectively. AtCER1 (boxed in blue) is the negative control used as a bait (no colonies grew). AtHVA22a / TuMV-6K2 interaction (boxed in green) is the internal positive control of the experiment (6/6 colonies grew). This figure is representative of the three independent experiments that were performed.

Table 27 summarizes the results obtained in the three independent experiments. It can be clearly noted that the four proteins CmXX4, CmXX2.1 CmXX 24 and CmXX28 presented a strong interaction with the WMV-6K2, while the proteins CmXX2.2, CmXX 2.3 and CmXX25 interacted moderately

Table 27. Synthesis of the results of three independent experiments performed for each combination

Prey (pPR3N)	Bait (pBT3-N)
	WMV-6K2
CmXX4	strong interaction
CmXX2.1	strong interaction
CmXX24	strong interaction
CmXX28	strong interaction
CmXX2.2	medium interaction
CmXX2.3	medium interaction
CmXX25	medium interaction
CmXX32.1	no interaction
CmXX32.2	no interaction
CmXX32.3	no interaction
CmXX36	no interaction
CmXX37.1	no interaction
CmXX37.2	no interaction
CmXX23.1	no interaction
CmXX23.2	no interaction
CmXX4mut	no interaction
	<i>TuMV-6K2</i>
HVA22a	strong interaction

Attention was further focused on one of the CmXX candidates for functional assays. The CmXX4 protein was chosen for reasons that cannot explained here because of confidentiality. As the pathosystem studied in the virology group in Bordeaux is TuMV / *Arabidopsis thaliana*, the orthologous gene of *CmXX4* was cloned in *Arabidopsis*, called *AtXX4*, and performed the functional assays described below.

2.2 Confirmation of the interaction between AtXX4 and TuMV-6K2 *in planta* using BiFC

2.2.1 *AtXX4* and *TuMV-6K2* interact in healthy plants

As a strong interaction was observed in yeast between CmXX4 and WMW-6K2, we aimed at checking whether an interaction between the orthologous protein AtXX4 with TuMV-6K2 occurred *in planta*. BiFC experiments were conducted in healthy and TuMV-6K2mCherry infected plants.

As described in § 1.3 (Material and Methods) we used *Agrobacterium tumefaciens* for transient expression of proteins and virus inoculation. Table 28 summarizes all the combinations of agrobacteria that were agroinfiltrated on 3-4 weeks old *Nicotiana benthamiana* plants in the frame of at least three independent experiments.

Table 28. Summary of the combinations used to check AtXX4/TuMV-6K2 interaction in healthy plants using BiFC. Positive and negative control combinations are also indicated.

P19 + nY-AtXX4 + cY-6K2
P19 + cY-AtXX4 + nY-6K2
P19 + cY-AtXX4 + nY-AtDIR (negative control for AtXX4)
P19 + cY-6K2 + nY-AtDIR (positive control for 6K2 and AtDIR)

For the first combination nY-AtXX4 with cY-6K2 (Table 28), no fluorescence signal was recovered suggesting that those fusion proteins cannot interact (data not shown). But as shown on Figure 43, a YFP signal is recovered when the fusion proteins cY-AtXX4 and nY-6K2 are co-expressed (Figures 43B and 43F). This signal corresponds to 0.5-1 µm dots indicated by arrowheads (Figure 43B) that can cluster (Figure 43F). Some of those spots indicated by yellow arrows seem to be close to some chloroplasts (Figures 43D and 43H). To confirm that the YFP signal observed in Figures 43B and 43F is a real YFP-reconstituted signal and not an artefact, a spectral analysis was performed for each of the dots indicated by colored arrowheads. The maximum emission peak of the fluorescence observed at 530 nm for all the fluorescent dots is typical of the YFP confirming that a real YFP signal is observed (Figures 43S1 and 43S2).

Even though we did not check whether AtXX4 interacts with TuMV-6K2 in yeast in SuY2H (which is already planned) we clearly showed an interaction between those proteins *in planta* by BiFC.

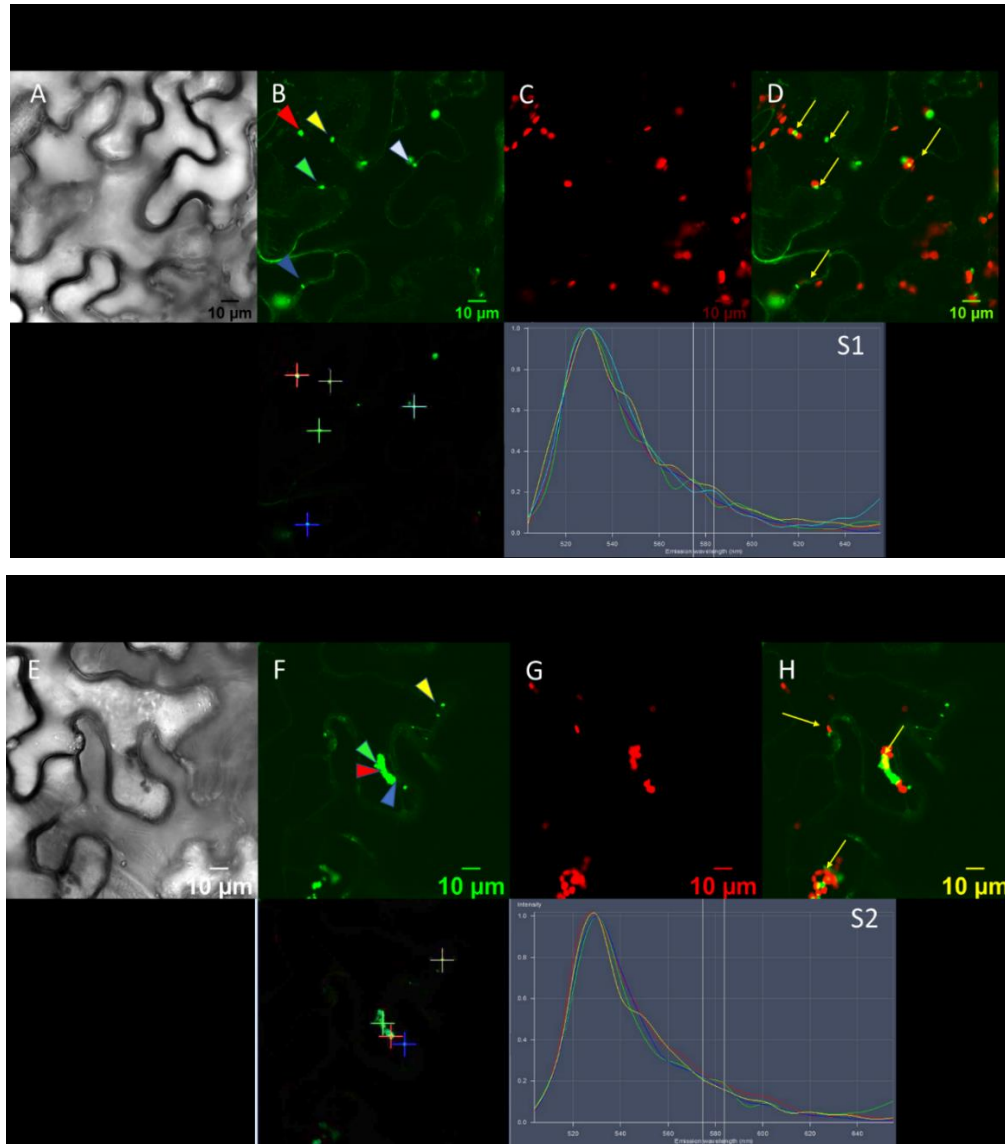


Figure 43. AtXX4 and TuMV-6K2 interact in *N. benthamiana*. BiFC assay was performed to check the interaction between AtXX4 and TuMV-6K2. Confocal imaging was performed at 72 h post agroinoculation (hpi). TuMV-6K2 and AtXX4 were fused to the N (nY-6K2) and C-terminal (cY-AtXX4) fragments of yellow fluorescent protein (YFP) respectively. **A)** “Trans”: image obtained in transmitted light **B)** reconstitution of a YFP fluorescence signal **C)** “Chloroplast”: fluorescence emitted by chlorophyll **D)** “merged”: superimposition of images acquired in panels B and C. Arrows indicate the YFP dots observed associated with chloroplasts. Arrowheads indicate which dots were chosen in panel B and F to perform the spectral analysis shown in S1 and S2. The peaks at 530nm are typical of the YFP maximum emission signal confirming that the YFP observed in B and F is a real signal due to the interaction between AtXX4 and TuMV-6K2. Scale bar 10μm.

As BiFC can lead to false positive signals, we also performed a negative control (Table 28) using the combination cY-AtXX4 + nY-AtDIR which is a protein localized in the extracellular space that should not interact with AtXX4 (Figure 44). This negative control was chosen on the basis of previous tests carried out by L. Sofer in the Virology team in Bordeaux (personal communication). Although a very faint “pseudo fluorescent” signal is observed in Figure 44B, the analysis of the spectrum reveals multiple aspecific signals (Figure 44S1) and confirms that it is an artefact contrarily to what was observed in Figures 43S1 and 43S2. To check that this lack of interaction is not due to a lack of expression of nY-AtDIR, we performed the combination cY-6K2 with nY-AtDIR as we already know that those proteins interact (Luc Sofer’s personal communication). A positive interaction is observed (Figures 44H and 44S2) showing that nY-AtDIR is well expressed. Altogether those results suggest that AtXX4 and TuMV-6K2 interact *in planta*.

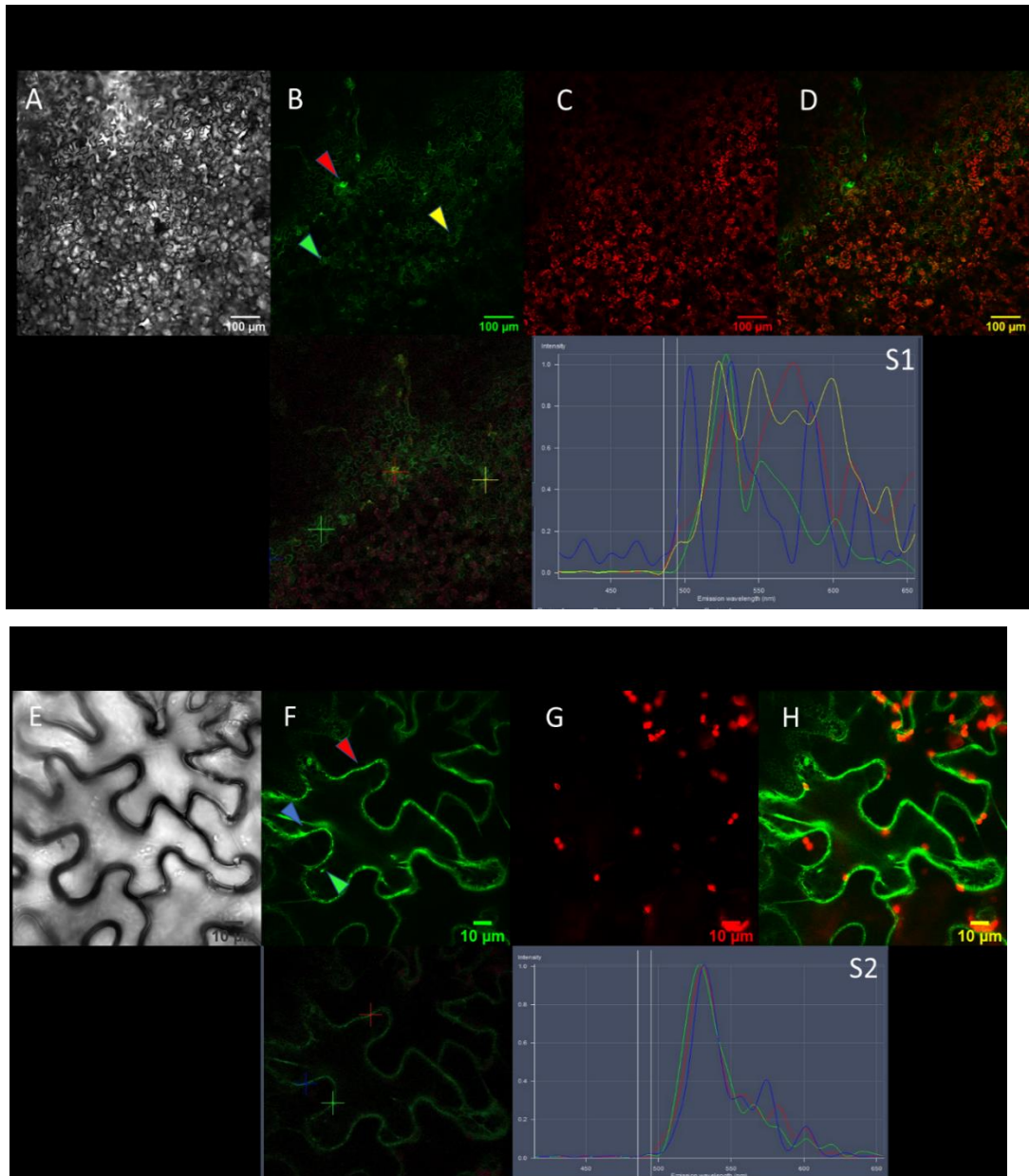


Figure 44. Negative and positive controls of the BiFC experiment. AtDIR fused to the N terminal fragment of YFP (nY-AtDIR) was used as either a negative control for AtXX4 (A-D, S1) or a positive control for TuMV-6K2 (E-H, S2). Confocal imaging was performed at 72 h post agroinoculation (hpi). Arrowheads indicate which dots were chosen in panel B and F to perform the spectral analysis. Peaks at 530nm are obtained for TuMV-6K2/AtDIR confirming the interaction (S2) and aspecific peaks for AtXX4/AtDIR (S1) confirming a lack of interaction. A/E) “Trans”: image obtained in transmitted light B/F) reconstitution of YFP fluorescence C/G) “Chloroplast”: fluorescence emitted by chlorophyll D/H) “merged”: superimposition of images acquired in panels B and C. Scale bars: 100µm (A-D, S1); 10µm (E-H, S2).

2.2.2 *AtXX4* /*TuMV-6K2* interaction occurs at the level of the viral replication complex in infected cells

In order to check whether the interaction between *AtXX4* and *TuMV-6K2* differs or not during viral infection when all the viral proteins are expressed, BIFC assays were conducted during *TuMV-6k2mcherry* infection (§ 1.3.1 Material and Methods). For this purpose, P19 + cY-*AtXX4* + nY-6K2 + *TuMV-6K2mcherry* constructs were co-infiltrated. Figure 45 shows that a YFP signal was reconstituted (Figure 45B and 45S) which largely colocalizes at the level of the viral replication complexes (VRC) labelled by the 6K2-mcherry and indicated by yellow arrows (Figure 45D and 45E).

This interaction seems to occur at the level of the viral replication complex during *TuMV* infection. This result is in good agreement with the previous papers of Jiang *et al.* 2006, Cabanillas *et al.* 2018 and Movahed *et al.* 2019 who showed a role of ESCRT-related proteins in *TuMV* cycle

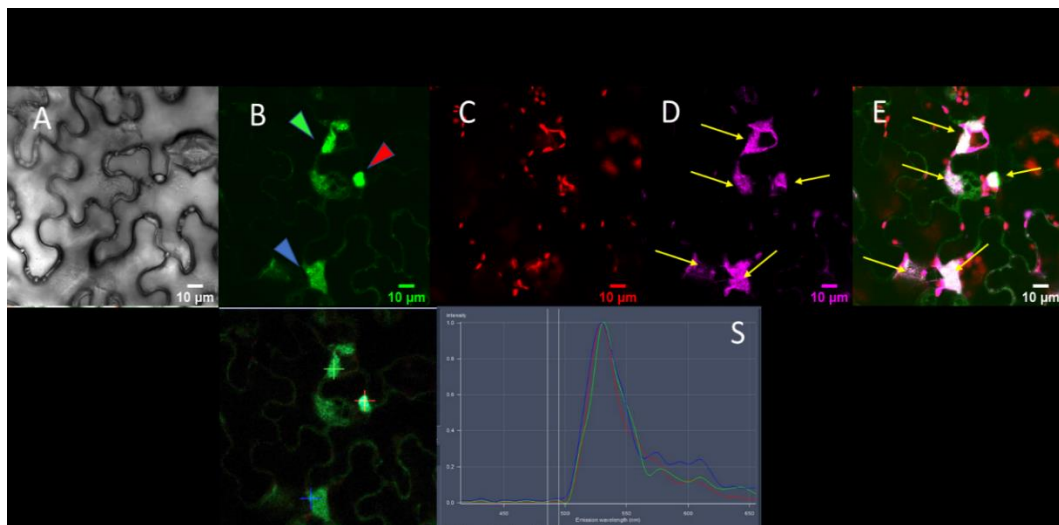


Figure 45. *AtXX4* and *TuMV-6K2* interact at the level of the Viral replication complexes (VRCs) during *TuMV* infection. cY-*AtXX4* and nY-6K2 were co-expressed with the viral construct *TuMV-6K2mcherry* using agroinoculation. Confocal imaging was performed 72 hpi. **A)** “Trans”: image obtained in transmitted light **B)** YFP fluorescence **C)** “Chloroplast”: fluorescence emitted by chlorophyll **D)** mcherry fluorescence emitted by the 6K2-mcherry fusion protein expressed during *TuMV-6K2-mcherry* infection **E)** “merged”: superimposition of images acquired in panels B, C and D. Arrows in panels D and E indicate the VRC (viral replication complexes). The arrowheads in B indicate which dots were chosen for the spectral analysis shown in panel S: the maximum peaks at 530nm are typical of YFP emission confirming the interaction between *AtXX4* and *TuMV-6K2*. Scale bar: 10µm.

To confirm that this colocalization is not an artefact due to an interference with the mCherry fluorophore fused to the 6K2, the combination P19 + cY-AtXX4 + nY-6K2 + RFP (a modified mCherry protein with the same spectral properties) was used as the non-infected negative control.

Figure 46B confirms the AtXX4 / TuMV-6K2 interaction, as a YFP signal is observed, similar to what observed in Figure 43B in healthy plants. The RFP protein shows an expected nucleocytoplasmic localization indicated by arrows in Figure 46D. Contrarily to what can be observed in Figure 45E, the reconstituted YFP signal does not colocalize with the RFP one, showing a condition similar to healthy plants confirming that the interaction is not altered by the co-expression of RFP (Figure 46).

Altogether those results confirmed that during viral infection AtXX4 and TuMV-6K2 interact potentially at the level of the VRCs.

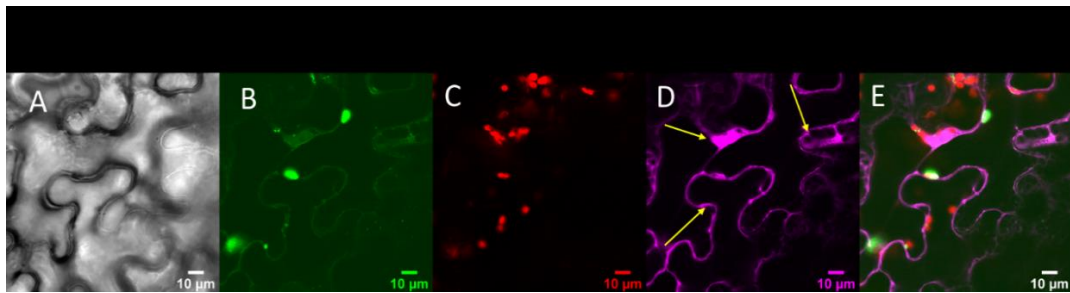


Figure 46. The fluorophore RFP doesn't interfere with the interaction observed between AtXX4 and TuMV-6K2 in BiFC. TuMV-6K2 and AtXX4 were fused to the N (nY-6K2) and C-terminal (cY-AtXX4) fragments of yellow fluorescent protein (YFP) respectively. Confocal imaging was performed 72 hpi **A**) "Trans": image obtained in transmitted light **B**) "YFP fluorescence **C**) "Chloroplast": fluorescence emitted by chlorophyll **D**): fluorescence emitted by the RFP **E**) "merged": superimposition of images acquired in panels B, C and D. Arrows in panel D indicate the nucleocytoplasmic localization of RFP signal. Scale bar: 10μm.

2.3 Observation of AtXX4 self-interaction *in planta* by BiFC

As it is described in the literature that XX4 proteins can make dimers, the combination P19 + cY-AtXX4 + nY-AtXX4 was agroinfiltrated in healthy plants. Figure 47B and 47D show that a YFP signal is recovered suggesting that AtXX4 self-interacts as indicated by yellow arrows (Figure 47).

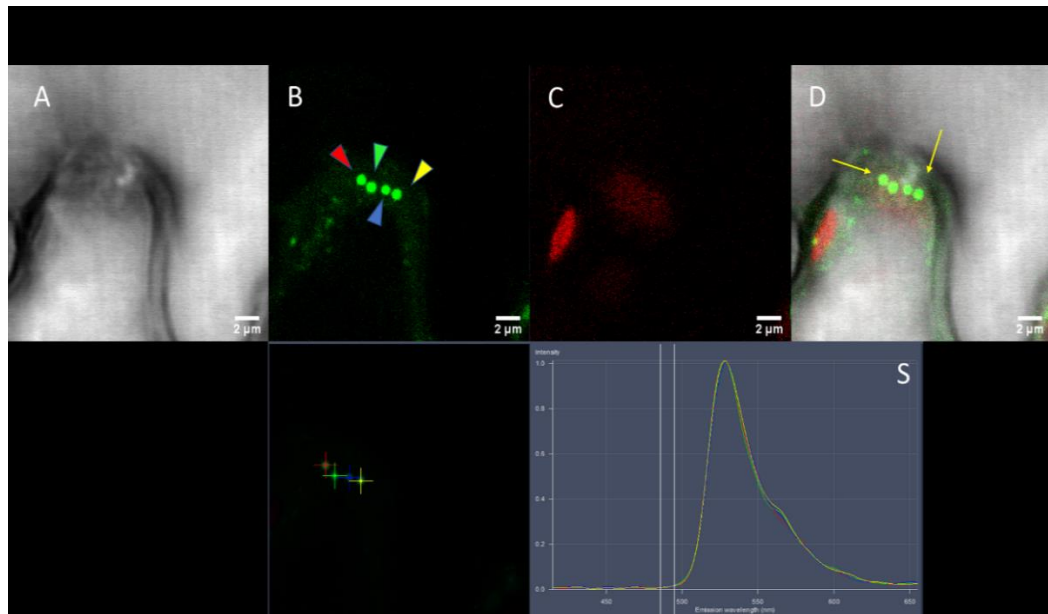


Figure 47. AtXX4 self-interacts in healthy condition. BiFC assay was performed to check the self-interaction of AtXX4. Confocal imaging was performed at 72 h post agroinoculation (hpi). AtXX4 was fused to the N (nY-AtXX4) and C-terminal (cY-AtXX4) fragments of yellow fluorescent protein (YFP). **A** “Trans”: image obtained in transmitted light **B** YFP fluorescence reconstituted **C** “Chloroplast”: fluorescence emitted by chlorophyll **D** “merged”: superimposition of images acquired in panels B and C. Arrows indicate the self-interaction of AtXX4. Arrowheads indicate which dots were chosen in panel B to perform the spectral analysis shown in S. The peaks at 530nm are typical of the YFP maximum emission signal confirming that the YFP observed in B is not an artefact signal. Scale bar 2 μ m.

This self-interaction was also checked in infected plants using the combination P19 + cY-AtXX4 + nY-AtXX4 + TuMV-6K2mcherry. Figure 48 shows a partial relocation of the AtXX4 protein to the VRCs indicated by arrows (Figures 48B and 48F).

Altogether those results confirm that AtXX4 can self-interact and that potential multimers can be recruited by the 6K2 at the level of VRCs during viral infection.

This characteristic has been observed in other studies for the orthologous protein in yeast (cannot be cited because confidentiality) where it has been associated with an inactivation state. Our BiFC analysis seems to confirm that AtXX4 is able to self-interact and during TuMV infection it's partially relocated at the level of VRC

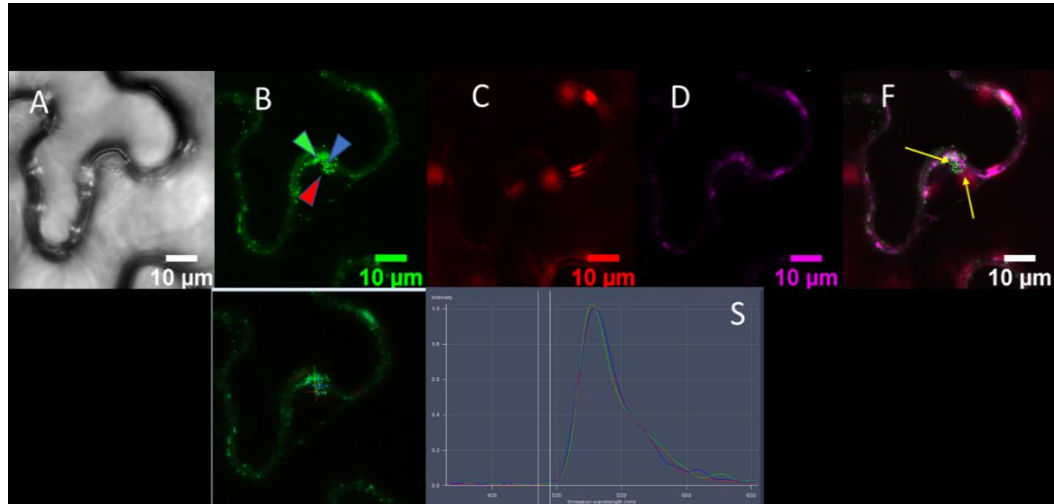


Figure 48. Self-interacting AtXX4 shows a partial relocation during TuMV infection to the VRCs. BiFC assay was performed to check the self-interaction of AtXX4 during TuMV infection. Confocal imaging was performed at 72 h post agroinoculation (hpi). AtXX4 was fused to the N (nY-AtXX4) and C-terminal (cY-AtXX4) fragments of yellow fluorescent protein (YFP). **A)** “Trans”: image obtained in transmitted light **B)** YFP fluorescence **C)** “Chloroplast”: fluorescence emitted by chlorophyll **D)** fluorescence emitted by the 6K2-mcherry expressed during TuMV-6K2-mcherry infection **E)** “merged”: superimposition of images acquired in panels B, C and D. The yellow arrows in F indicate a colocalization of AtXX4 with the VRC. Arrowheads in B indicate which dots were chosen to perform the spectral analysis shown in S. The peaks at 530nm are typical of the YFP maximum emission signal confirming that the YFP observed in B is a real signal. Scale bar 10μm.

2.4 Subcellular localization of AtXX4 in healthy and infected plants

By the use of fluorophore fusion proteins AtXX4-GFP and AtXX4-RFP the subcellular localization of AtXX4 was assessed. In particular, both AtXX4-GFP and AtXX4-RFP were transiently expressed in *N. benthamiana* plants to check their subcellular localization in either healthy (Figure 49) or TuMV-6K2mcherry-infected plants (Figure 50). Figures 49B and 49F show that both fusion proteins are located in the cytoplasm and in the nucleus as indicated in B and F by red arrows. Surprisingly, the observed localization (nucleocytoplasmic) in healthy conditions was never observed during the self-interaction assays, and such a localization was never described for the orthologous protein in yeast.

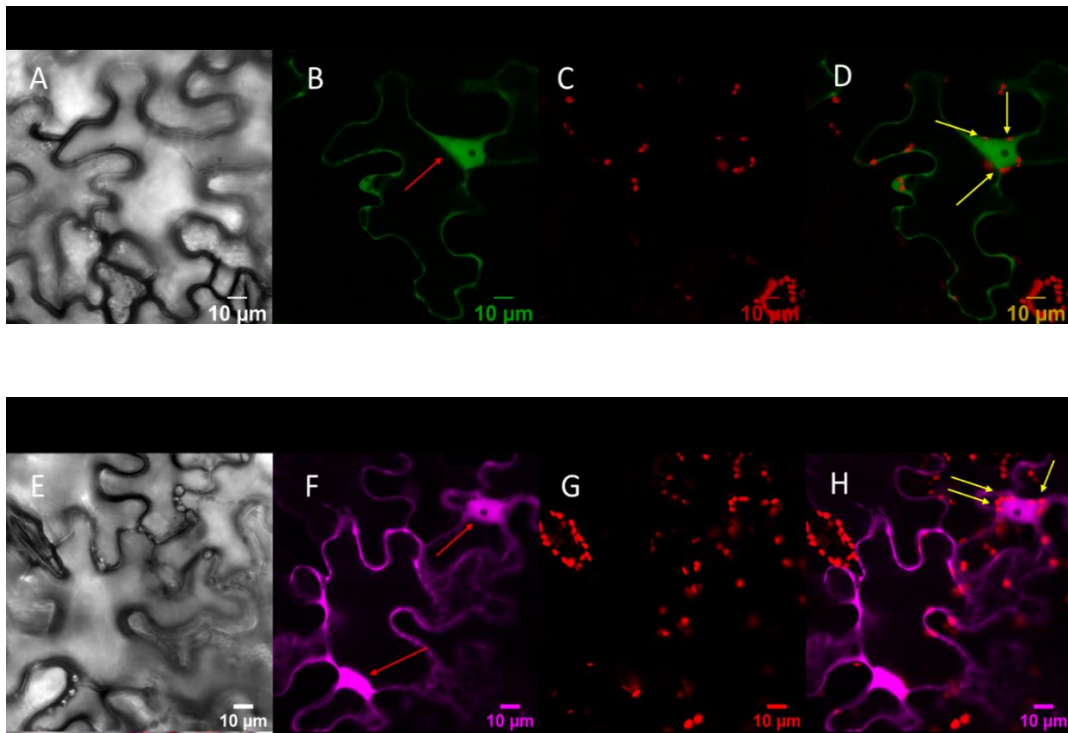


Figure 49. Subcellular localization of AtXX4-GFP and ATXX4-RFP fusion proteins in healthy plants. (A-D) and RFP (E-H) fusion proteins. Confocal imaging was performed at 72 h post agroinfiltration of AtXX4-GFP (A-D) or AtXX4-RFP (E-H) fusion proteins. A/E) “Trans”: image obtained in transmitted light B/F) GFP and RFP fluorescence signals respectively C/G) “Chloroplast”: fluorescence emitted by chlorophyll D/H) “merged”: superimposition of images acquired in panels B and C or F and H. Red arrows in panels B and F indicate the nucleus surrounded by chloroplasts indicated by yellow arrows in panels D and H. Scale bar 10 μ m.

During TuMV-6K2-mcherry infection, AtXX4-GFP fusion protein was not relocated at the level of the VRC (Figure 50E), contrarily to what was observed in BiFC in infected condition. We suppose that the AtXX4-GFP and RFP fusion proteins might not be able to interact with the 6K2 or self-interact because the tag is fused at the C-terminal

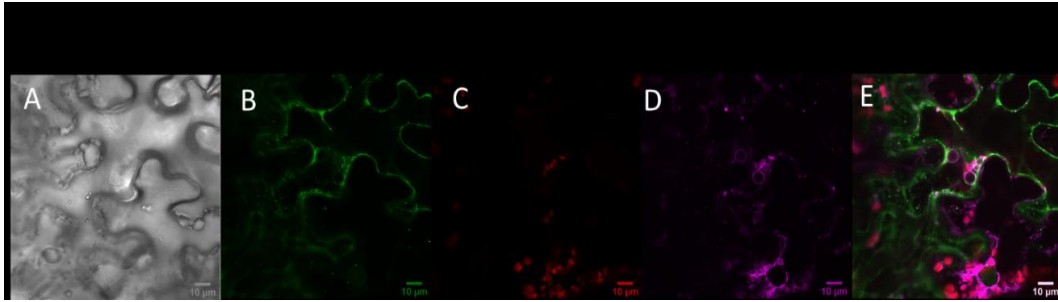


Figure 50. Subcellular localization of AtXX4-GFP fusion protein during TuMV infection. Confocal imaging was performed at 72 h post agroinfiltration of AtXX4-GFP fusion protein together with the viral construct TuMV-6K2mcherry. **A)** “Trans”: image obtained in transmitted light **B)** GFP fluorescence emitted by the AtXX4-GFP fusion protein **C)** “Chloroplast”: fluorescence emitted by chlorophyll **D)** fluorescence emitted by the 6K2-mcherry expressed during TuMV-6K2mcherry infection **E)** “merged”: superimposition of images acquired in panels B, C and D. Scale bar 10 μ m.

Whether the AtXX4-GFP and AtXX4-RFP fusion proteins are still able to interact with 6K2 remain to be tested. Indeed, in our BiFC assays, the fusions made were at the N-ter of AtXX4 instead of the C-ter. GFP-AtXX4 and RFP-AtXX4 are being cloned in the laboratory. Further, analysis should be done to observe what could occur with N-terminal fusion by BiFC assay.

General Conclusions and Future Perspectives

The research activities included in this PhD thesis were aimed to better investigate the plant responses to virus infection; in particular, the choice for our project was a virus belonging to the *potyvirus* genus and more in detail the onion-OYDV (onion yellow dwarf virus) patho-system. To achieve the main aims of the research different and independent approaches were followed starting from the agronomic and bio-morphological approach to evaluate the onion tolerance/resistance to virus, passing through to a wider approach as RNASeq and finally the determination of the key factors determining the virus movement in the plants.

The final aim was to increase knowledge about plant responses to determine putative OYVD-tolerant traits that could be in the future applied as means to control this plant virus in onion.

The activities were focused on several local Italian onion varieties which genetic distances were determined by molecular analysis using 12 SSR previously isolated and reported for onion (Baldwin *et al.*, 2012; Mc Callum *et al.*, 2008). Starting from a common experimental trial setting up, all the analyses were planned and performed as independent approaches. As stated above, OYDV represent one of the most limiting biotic stress for onion, not only for its primary effect on plant development but, as also suggested by our results, as crucial factor for establishing secondary and post-harvest pathogens in OYVD-infected onion bulbs.

The OYVD effects determined by using a visive approach together bio-morphologic traits analysis allowed us to select two varieties that could considered tolerant/resistant. A commercial variety, Texas early grano 502, confirmed its behaviour previously reported; a second variety/population represents one of the most economically important Italian landraces, 'Rossa di Tropea'. These tolerant varieties showed a better physiological response to virus, with a reduced symptomatology and impact on plant development, as plant height and number of leaves. Nevertheless, considering the evaluation of water balance and losses from the bulbs, the tolerant bulbs showed reduced water losses in comparison to the susceptible ones, and in general, the infected bulbs lost more water than their healthy control. Combining bio-morphological features, and fresh to dry weight

ratio data it could be assumed that OYDV infection induced a water accumulation in bulb and leaves tissues. Therefore, although the infected bulb tissues could accumulate water, in first attempt suggesting the production of bigger and heavier bulbs, after long-term storage conditions could be evident that this initial weight and size increasing were generally due to less dry matter and more compact bulbs. Indeed, these parameters, together with water content and losses balance, showed an influence upon long-term storage and product quality. These cellular changes affecting bulb quality represent, in addition, a risk factor for the establishment of secondary pathogens infections, leading to post-harvest losses. The long-term storage is essential for onion crop in covering market demands throughout the year. The increased knowledge on the virus-infection effects on overall plant physiology and development but also on marketable product with their organoleptic property could resulted pivotal for an accurate crop management from the field to post-harvest storage, in view of the increasing awareness of final consumers in terms of healthy food.

In the two pairs of varieties more susceptible and resistant to OYDV, the eukaryotic translation initiation factor (EIF) family genes expression level were investigated, as key factors for several potyvirus replication. Surprisingly, the data did not evidence a crucial role of these factors in OYVD-replication, suggesting the use of an alternative preferred pathway for this potyvirus. In future perspective, more studies should be performed to determine how the virus replicates in plant cells and to identify the factors involved among the plant biosynthetic machinery.

More interest findings were achieved by the RNASeq analysis approach. Indeed, it could be possible to highlight a wide range of DEGs induced by OYDV. This approach allowed us to investigate the role of genes belonging to the *WRKY* transcription factor (TF) family in onion, with more new insights on their classification. Furthermore, using the OYDV-infected samples as filter, we highlighted the key pathways and metabolomics changes during dormancy in onion bulbs. Interestingly, infected samples showed only few DEGs related to dormancy during storage. This is probably the cause of the worst shelf life and the premature sprouting of infected bulbs that are unable to enter on time in the physiological dormancy. Finally, transcriptomic profiles and co-expression analysis allowed us

to identify a WRKY-TF (*AcWRKY32*) that putatively driven the dormancy release in onion bulbs.

These results could be easily overlapped and could justify what observed in bio-morphological comparison assay. The OYDV is able to alter *in toto* the physiology of plants, in particular in the bulb. The cellular metabolism in infected bulbs is nonstop triggered by the virus presence, not allowing the entering in dormancy. The increased metabolism rate caused a bigger respiratory rate as well as water accumulation and therefore losses. The metabolism rate so altered along with the primary effect of virus on membrane status could contrast the accumulation of complex metabolites in favor to the simple forms (Taglienti *et al.*, 2020a, 2020b). The increased water content with consequent less dry matter, the alteration of membranes states and the increased metabolism rate in onion bulbs could explain the higher rate of secondary pathogens established in infected bulbs in comparison to healthier control.

Furthermore, the screening of melon ESCRT related proteins and the potyviral bait WMV 6K2, and the derived assay on *Arabidopsis* vs TuMV, developed at the INRAE Centre of Bordeaux, allowed us to confirm an effective involvement of the ESCRT AtXX4 protein in the replication and movement processes of TuMV. These results lay the scientific background to transfer a similar approach to onion-OYDV system, to determine if AtXX4 could have also a similar biological role. Overall, the results in the frame of the internship at INRAE allowed us to elucidate the mechanism and pathway triggered by a potyvirus in plant movement. The acquirement of a more complete view of the components involved in virus replication and the translocation processes within the plant, could allow us to identify the key factors useful for conferring virus tolerance to the host-plant.

Our results greatly improved the knowledge about OYDV infection pathway; confirming that virus tolerance could be retrieved within the landraces biodiversity. The OYDV infection was confirmed to represent a primary factor for the establishment of secondary pathogens in onion bulbs; the role of OYDV in dormancy breaking in infected bulb was identified throughout the characterization of WRKY TF gene family in onion; shed light to a better understanding of the pathway involved in the OYDV translocation along the plant.

Acknowledgements

This research was carried out in the frame of the project: *Study on Interaction between Onion yellow dwarf virus and nutraceutical compounds of 'Rossa di Tropea' Onion* (SI.ORTO), funded by the Italian Ministry of Education, University and Research – MIUR in a wide initiative called *Scientific Independence of young Researcher – SIR* (SIR-MIUR grant – SIORTO-RBSI149LD5) in which Dr. Antonio Tiberini was the Principal Investigator (PI) at the Mediterranean University of Reggio Calabria (UNIRC).

The third part of research “*Study on molecular plant-pathogen interactions: host factors involved in the cell-cell movement of potyviruses?*” was accomplished in France, at the National Research Institute for Agriculture, Food and Environment (INRAE) in the Centre de Nouvelle Aquitaine Bordeaux. Dr. Sylvie German-Retana directed the activity in the frame of a collaboration between INRAE-Bordeaux and INRAE-Avignon together with a private company (Gautier Semences, France), with a financial support from the funded project PotyMove (ANR-16-CE20-0008-01) coordinated by Dr. Sylvie German-Retana.

I would like to thank those who guided and advised me during the development of this research:

For chapter 1 and 2 from UNIRC: Prof. Francesco Sunseri, Prof. Giuliana Renata Albanese, Dr. Antonio Tiberini, Dr. Antonio Lupini, Dr. Antonio Mauceri.

For chapter 2 I also like to thank Dr. Francesco Mercati from the Institute of Bioscience and Bioresources of the Council National of Research (CNR-IBBR), Palermo and Dr. Guglielmo Puccio from the Dipartimento di Scienze Agrarie, Alimentari e Forestali, Università degli Studi di Palermo.

For chapter 3 from INRAE Bordeaux UMR BFP 1332, Virology Team: Dr. Sylvie German-Retana, Luc Sofer (technician), Mingshuo Xue (PhD student), and from INRAE-Avignon, GAFL: Dr. Catherine Dogimont, Aimeric Agaoua (PhD student).

Reference

Abd El-Wahab A.S. (2009)b Aphid-transmission efficiency of two main viruses on garlic in Egypt, Onion Yellow Dwarf Virus (OYDV-G) and Leek Yellow Stripe Virus (LYSV-G). *Academic Journal of Entomology* 2 (1), 40-42.

Abd El-Wahab A.S., Elnagar. S., and El-Sheikh M.A.K. (2009)a Incidence of aphid-borne Onion yellow dwarf virus (OYDV) in *alliaceae* crops and associated weeds in Egypt. *4th Conference on Recent Technologies in Agriculture* 21-33.

Abdel-Maksoud G., Abdel-Rahman E. (2011) “A review on the materials used during the mummification process in ancient Egypt”. *Mediterranean Archaeology and Archaeometry*. 11 (2): 129–150.

Agati G. (1952) Indagini ed osservazioni sulla biologia florale della cipolla. *Rivista di ortoflorofrutticoltura italiana* Vol. 36, No. 3/4, pp. 67-77.

Agosteo G.E., Magnano di San Lio G. (2005) Le malattie fungine e batteriche della cipolla. *Informatore fitopatologico* 10/2005, 8-19.

Andret-Link P., and Fuchs M. (2005) Transmission specificity of plant viruses by vectors. *Journal of Plant Pathology*, 87 (3), 153-165.

Ansari N.A. (2007) Onion Cultivation and Production in Iran. *Middle Eastern and Russian Journal of Plant Science and Biotechnology* 1 (2): 26–38.

APG III., (2009) An update of the Angiosperm Phylogeny Group classification for the orders and families of flowering plants: *APG III. Botanical Journal of the Linnean Society* 161: 105–121.

Astley, D., Innes, N.L. and Van der Meer, Q.P. (1982) Genetic Resources of *Allium* species, *IBPGR secretariat, Rome, Italy* p.38.

Ayme V., Petit-Pierre J., Souche S., Palloix A., Moury B. (2007) Molecular dissection of the potato virus Y VPg virulence factor reveals complex adaptations to the pvr2 resistance allelic series in pepper. *Journal of General Virology*. 88, 1594–1601.

Ayme V., Souche S., Caranta C., Jacquemond M., Chadoeuf J., Palloix A., Moury B. (2006) Different mutations in the genome-linked protein VPg of potato virus Y confer virulence on the pvr2(3) resistance in pepper. *Molecular Plant Microbe Interactions* 19(5):557-63.

Baldoni R., Giardini L. (2007) Coltivazioni erbacee, *Pàtron*.

Baldwin S., Pither-Joyce M., Wright K., Chen L., McCallum J. (2012) Development of robust genomic simple sequence repeat markers for estimation of genetic diversity within and among bulb onion (*Allium cepa* L.) populations. *Molecular Breeding* 30:1401–1411

Banfi E., Galasso G., Soldano A. (2011) Notes on systematics and taxonomy for the Italian vascular flora. 2. *Natural History Sciences* 152 (2): 85–106.

Barajas D., Jiang Y., Nagy P.D. (2019) A Unique Role for the Host ESCRT Proteins in Replication of Tomato bushy stunt virus. *PLoS Pathogens* 5(12).

Barg E., Lesemann D.E., Vetten H.J., and Schojfelder M. (1995) Differentiation of potyviruses infecting cultivated *Allium* species. *Proceedings of the 8th Conference on Virus Disease of Vegetables*, Prague July 9-15, 29-31.

Bernard A., Domergue F., Pascal S., Jetter R., Renne C., Faure J.D., Haslam R.P., Napier J.A., Lessire R., Joubès J. (2012) Reconstitution of plant alkane biosynthesis in yeast demonstrates that Arabidopsis ECERIFERUM1 and ECERIFERUM3 are core components of a very-long-chain alkane synthesis complex. *Plant Cell* 24(7):3106-18.

- Bhat R.A., Lahaye T., Panstruga R. (2006) The visible touch: in planta visualization of protein-protein interactions by fluorophore-based methods. *Plant Methods* 2(1):12.
- Boateng C.O., and Schwartz H.F. (2013) Temporal and Localized Distribution of *Iris Yellow Spot Virus* within Tissues of Infected Onion Plants. *Southwestern Entomologist* 38(2):183-200.
- Bolger A.M., Lohse M., Usadel B. (2014) Trimmomatic: a flexible trimmer for Illumina sequence data. *Bioinformatics* 30:2114–2120.
- Brewster J.L. (2008) *Onion and Other Vegetable Alliums, 2nd edition*. Cab International, Wallingford, UK.
- Browning K.S. (1996) The plant translational apparatus. *Plant Molecular Biology* 32:107-144.
- Bulajić, A., Djekić, I., Jović, J., Krnjajić, S., Vučurović, A., and Krstić, B., (2009) Incidence and distribution of *Iris yellow spot virus* on onion in Serbia. *Plant Disease* 93:976-982.
- Cabanillas D.G., Jiang J., Movahed N., Germain H., Yamaji Y., Zheng H., Laliberté J.F. (2018) Turnip Mosaic Virus Uses the SNARE Protein VTI11 in an Unconventional Route for Replication Vesicle Trafficking. *Plant Cell*;30(10):2594-2615.
- Calvo M., Martinez-Turino S., Garcia J.A. (2014). Resistance to Plum pox virus Strain C in *Arabidopsis thaliana* and *Chenopodium foetidum* involves genome-linked viral protein and other viral determinants and might depend on compatibility with host translation initiation factors. *Molecular Plant Microbe Interaction* 27:1291–1301.

Cavatorta J., Perez K.W., Gray S.M., Van Eck J., Yeam I., Jahn M. (2011) Engineering virus resistance using a modified potato gene. *Plant Biotechnology Journal* 9, 1014–1021.

Celli M.G., Torrico A.K., Kiehr M., and Conci V.C. (2013) Striking differences in the biological and molecular properties of onion and garlic isolates of Onion yellow dwarf virus. *Archives of Virology* 158 (6), 1377-1382.

Charron C., Nicolai M., Gallois J.L., Robaglia C., Moury B., Palloix A., Caranta C. (2008) Natural variation and functional analyses provide evidence for co-evolution between plant eIF4E and potyviral VPg. *Plant Journal*, 54, 56–68.

Chen M., Tan Q., Sun M., Li D., Fu X., Chen X., Xiao W., Li L., Gao D. (2016) Genome-wide identification of WRKY family genes in peach and analysis of WRKY expression during bud dormancy. *Molecular Genetics and Genomics* 291:1319–1332.

Cheng Y., Jalalahammed G., Yu J., Yao Z., Ruan M., Ye Q., Li Z., Wang R., Feng K., Zhou G. (2016) Putative WRKYs associated with regulation of fruit ripening revealed by detailed expression analysis of the WRKY gene family in pepper. *Scientific Reports*. 7:43498.

Choi, Hyeok J., Oh, Byoung U. (2011) “A partial revision of *Allium* (Amaryllidaceae) in Korea and north-eastern China”. *Botanical Journal of the Linnean Society* 167 (2): 153–211.

Chope G.A., Cools K., Terry L.A., Hammond J.P., Thompson A.J. (2012) Association of gene expression data with dormancy and sprout suppression in onion bulbs using a newly developed onion microarray. In *VI International Symposium on Edible Alliaceae* 969, 169-174.

Chope G.A., Terry L.A., White P.J. (2006) Effect of controlled atmosphere storage on abscisic acid concentration and other biochemical attributes of onion bulbs. *Postharvest Biology and Technology*, 39, 233–246.

Chung B.Y.W., Miller W.A., Atkins J.F., and Firth A.E. (2008) An overlapping essential gene in the *Potyviridae*. *Proceedings of the National Academy of Sciences of the USA*, 105, 5897–5902.

Clark M.F., Adams A.N. (1977) Characteristics of the microplate method of enzyme-linked immunosorbent assay for the detection of plant viruses. *Journal of General Virology*, 34(3):475-83.

Conci V., Nome S.F., and Milne R.G. (1992) Filamentous viruses of garlic in Argentina. *Plant Disease*, Vol. 76, No.6, 594-596.

Cools K., Chope G.A., Hammond J.P., Thompson A.J., Terry L.A. (2011) Ethylene and 1-methylcyclopropene differentially regulate gene expression during onion sprout suppression. *Plant Physiology*, 156, 1639–1652.

Cortês I., Livieratos I.C., Derks A., Peters D., and Kormelink R. (1998) Molecular and serological characterization of *Iris yellow spot virus*, a new and distinct tospovirus species. *Phytopathology*, 88, 1276-1282.

Cotton S, Grangeon R, Thivierge K, Mathieu I, Ide C, Wei T, Wang A, Laliberté J.F. (2009) Turnip mosaic virus RNA replication complex vesicles are mobile, align with microfilaments, and are each derived from a single viral genome. *Journal of Virology*, 83: 10460–10471.

Cui Y., Shen J., Gao C., Zhuang X., Wang J., Jiang L. (2016) Biogenesis of plant prevacuolar multivesicular bodies. *Molecular Plant*, 9, 774–786.

Cumo C. (2015) Onion. In: Foods that Changed History: How Foods Shaped Civilization from the Ancient World to the Present. *ABC-CLIO Press*. pp. 248–50.

Dafni A., Cohen D., Noy-Meir I. (1981) Life-cycle variation in geophytes. *Annals of the Missouri Botanical Garden* 68(4):652.

Davidson T.M.W. (1958) Dormancy in the potato tuber and the effects of storage conditions on initial sprouting and on subsequent sprout growth. *American Potato Journal*, 35, 451–65.

Davis F., Terry L.A., Chope G.A., Faul C.F.L. (2007). Effect of extraction procedure on measured sugar concentrations in onion (*Allium cepa* L.) bulbs. *Journal of Agricultural Food Chemistry*, 55, 4299–4306.

de Sarker D., Johnson M.A.T., Reynolds A., Brandham P.E. (1997) Cytology of the highly polyploid disjunct species, *Allium dregeanum* (*Alliaceae*), and of some Eurasian relatives. *Botanical Journal of the Linnean Society* 124, 361–373.

De Wilde-Duyfjes B.E.E. (1976) A revision of the genus *Allium* L. (*Liliaceae*) in Africa. *Belmontia* 7:75–78.

Deniz İ.G., Genç İ., Sari D. (2015) Morphological and molecular data reveal a new species of *Allium* (*Amaryllidaceae*) from SW Anatolia, Turkey. *Phytotaxa* 212 (4): 283–292.

Ding Z.J., Yan J.Y., Li G.X., Wu Z.C., Zhang S.Q., Zheng S.J. (2014) WRKY 41 controls Arabidopsis seed dormancy via direct regulation of ABI3 transcript levels not downstream of ABA. *Plant Journal*, 79:810–823.

Don G. (1832) A monograph of the genus *Allium*. *Memoirs of the Wernerian Natural History Society* 6: 1–102.

Dovas C.I and Volvas C. (2003) Viruses infecting *Allium* Spp. in Southern Italy. *Plant Pathology* 85 (2), 135.

Duan H., Richael C., Rommens C.M. (2012) Overexpression of the wild potato eIF4E-1 variant Eva1 elicits Potato virus Y resistance in plants silenced for native eIF4E-1. *Transgenic Research*, 21, 929–938.

Duprat A., Caranta C., Revers F., Menand B., Browning K.S., Robaglia C. (2002) The Arabidopsis eukaryotic initiation factor (iso)4E is dispensable for plant growth but required for susceptibility to potyviruses. *Plant Journal*, 32:927-934.

Elnagar S., El-Sheikh M.A.K., Abd El-Wahab A.S. (2011) Effect of Natural infection with Onion yellow dwarf virus (OYDV) on yield of onion and garlic crops in Egypt. *Journal of Life Science* 5, 634-638.

Estes, J.W. (2000) “Staple Foods: Domesticated Plants and Animals: Onion.”. The Cambridge World History of Food. Ed. Kenneth F. Kiple and Kriemhild coneo Omelas: Cambridge University Press.

Estevan J., Marena A., Callot C., Lacombe S., Moretti A., Caranta C., Gallois J.L. (2014) Specific requirement for translation initiation factor 4E or its isoform drives plant host susceptibility to Tobacco etch virus. *BMC Plant Biology* 14(1):67.

Eulgem T., Rushton P.J., Robatzek S., Somssich I.E. (2000) The WRKY superfamily of plant transcription factors. *Trends in Plant Science* 5,199–206.

Faggioli F., Loretto S., Tomassoli L. (2012) Importanza della diagnosi su seme di pomodoro per l'identificazione di alcuni agenti infettivi “Seed-borne”. *Petria – Workshop Ancona “Difesa ortive da seme”*.

Fraser R.S.S. (1990) The genetics of resistance to plant viruses. *Annual Review of Phytopathology*, 28, 179– 200.

Friesen N., Fritsch R.M.; Blattner F.R. (2006) Phylogeny and new intrageneric classification of *Allium* (Alliaceae) based on nuclear ribosomal DNA ITS sequences. *Aliso*. 22: 372–395.

Friesen N., Pollner S., Bachmann K. and Blattner F.R. (1999) RAPDs and non-coding chloroplast DNA reveal a single origin of the cultivated *Allium fistulosum* from *A. altaicum* (Alliaceae). *American Journal of Botany* 86, 554–562.

Fritsch R.M., Blattner F.R., Gurushidze M. (2010) “New classification of *Allium* L. subg. *Melanocrommyum* (Webb & Berthel) Rouy (Alliaceae) based on molecular and morphological characters”. *Phyton*. 49: 145–220.

Fritsch R.M., Friesen N. (2002) Evolution, Domestication and Taxonomy. In *Allium Crop Science: Recent Advances*. Wallingford, UK: *CABI Publishing* 5–30.

Fu L, Niu B, Zhu Z, Wu S, Li W (2012) Cd-hit: accelerated for clustering the next-generation sequencing data. *Bioinformatics*, 28(23):3150–3152

Gallie D.R. (1996) Translational control of cellular and viral mRNAs. *Plant Molecular Biology*, 32:145-158.

Gallois J.L., Charron C., Sanchez F., Pagny G., Houvenaghel M.C., Moretti A., Ponz F., Revers F., Caranta C., German-Retana S. (2010) Single amino acid changes in the turnip mosaic virus viral genome-linked protein (VPg) confer virulence towards *Arabidopsis thaliana* mutants knocked out for eukaryotic initiation factors eIFISO4E and eIFISO4G. *Journal of General Virology*, 91, 288–293.

Gao Z., Johansen E., Eyers S., Thomas C.L., Noel Ellis T.H., Maule A.J. (2004) The potyvirus recessive resistance gene, *sbm1*, identifies a novel role for translation initiation factor eIF4E in cell-to-cell trafficking. *Plant Journal*, 40, 376–385.

Gent D.H., du Toit L, Fichtner S.F., Krishna Mohan S, Pappu H.R., Schwartz H.F. (2006) *Iris yellow spot virus*: An emerging threat to onion bulb and seed production. *Plant Disease* 90:1468-1479.

Gibbs A., and Ohshima K. (2010) Potyviruses and the digital revolution. *Annual Review of Phytopathology* 48, 205-223.

Gibbs A.J., Ohshima K., Phillips M.J. and Gibbs M.J. (2008) The prehistory of potyviruses: their initial radiation during the dawn of agriculture. *PLOS ONE* 3.

Giner A., Pascual L., Bourgeois M., Gyetvai G., Rios P., Picó B., Troadec C., Bendahmane A., Garcia-Mas J., Martín-Hernández A.M. (2017) A mutation in the melon Vacuolar Protein Sorting 41 prevents systemic infection of Cucumber mosaic virus. *Scientific Reports volume* 7, 10471.

Gingras A.C., Raught B., Sonenberg N. (1999) eIF4 initiation factors: effectors of mRNA recruitment to ribosomes and regulators of translation. *Annual Review of Biochemistry*. 68:913-963.

Giunchedi L., Conti M., Gallitelli D., Martelli G.P. (2007) *Elementi di Virologia Vegetale, Piccin*.

Grangeon R, Jiang J, Wan J, Agbeci M, Zheng H, Laliberté J.F. (2013) 6K2-induced vesicles can move cell to cell during turnip mosaic virus infection. *Frontiers Microbiology*, 4: 351.

Gray S.M., Banerjee N. (1999) Mechanisms of arthropod transmission of plant and animal viruses. *Microbiology and Molecular Biology Reviews*, 63, pp. 128-148.

Gubb I.R.; MacTavish, H.S. (2002) Onion pre- and post-harvest considerations. *In Allium Crop Sciences: Recent Advances; Rabinowitch, H.D., Currah, L., Eds.; CAB Int.: Wallingford, UK: pp 233–266.*

Guo C., Guo R., Xu X., Gao M., Li X., Song J., Zheng Y., Wang X. (2014) Evolution and expression analysis of the grape (*Vitis vinifera* L.) WRKY gene family. *Journal of Experimental Botany*, 1513–28.

Gurushidze M., Mashayekhi S., Blattner F., Friesen N., Fritsch R.M. (2007) Phylogenetic relationships of wild and cultivated species of *Allium* section *Cepa* inferred by nuclear rDNA ITS sequence analysis. *Plant Systematics and Evolution* (269), 259-269.

Haas B.J., Papanicolaou A., Yassour M., Grabherr M., Blood P.D., Bowden J., Couger M.B., Eccles D., Li B., Lieber M., Macmanes M.D., Ott M., Orvis J., Pochet N., Strozzi F., Weeks N., Westerman R., William T., Dewey C.N., Henschel R., Leduc R.D., Friedman N., Regev A. (2013) De novo transcript sequence reconstruction from RNA-seq using the Trinity platform for reference generation and analysis. *Nature Protocols* 1494-512

Hanelt P. (1985) Zur Taxonomie, Chorologie und Ökologie der Wildarten von *Allium* L. sect. *Cepa* (Mill.) Prokh. *Flora* 176, 99–116.

Hanelt P. (1990) Taxonomy, evolution and history. In: Rabinowitch, H. D. and Brewster (eds) *Onion and Allied Crops*, Vol. 1. *CRC Press, Boca Raton, Florida*, 1-26.

Hanelt P.; Hammer K.; Knüpfker H. (1992) The genus *Allium*: taxonomic problems and genetic resources. Proceedings of an international symposium held at Gatersleben, Germany, 11–13 June 1991. Gatersleben, Germany: *Institut für Pflanzengenetik und Kulturpflanzenforschung*.

Hanssen I.M., Mumford R., Blystad D.R., Cortez I., Hasiów-Jaroszewska B., Hristova D., Pagà I., Pereira A.M., Peters J., Pospieszny H., Ravnica M., Stijger I., Tomassoli L., Varveri C., Van der Vlugt R., and Nielsen S.L. (2010) Seed

transmission of *Pepino mosaic virus* in tomato. *European Journal of Plant Pathology* 126, 145-152.

Heinlein, M. (2015) Plasmodesmata: channels for viruses on the move. *Methods in Molecular Biology*. 1217:25-52.

Henne, W.M., Buchkovich N.J., Emr S.D. (2011) The ESCRT Pathway. *Developmental Cell*, 21, 77–91.

Hoa N.V., Ahlawat Y.S., and Pant R.P. (2003) Partial characterization of Onion yellow dwarf virus from onion in India. *Indian Phytopathology* 56 (3), 276-282.

Huang R.F., Xu J.M., Yu H. (1995) A study on karyotypes and their evolutionary trends in *Allium* Sect. Bromatorrhiza Ekberg (Liliaceae) *Cathaya* 7:133–145.

Hull R. (2002) Matthew's Plant Virology. *Academic Press New York*.

Idris E.E., Elsheikh E.A.E., EL Hassan S.M. (1997) A Note on the Response of Three Onion (*Allium cepa* L.) Cultivars to Infection with VAM-fungi and Onion Yellow Dwarf Virus (OYDV). U.K. *J. Agric. Sci.* 5(2): 158-161.

Ivanusic D., Heinisch J.J., Eschricht M., Laube U. and Denner, J. (2015) Improved split-ubiquitin screening technique to identify surface membrane protein-protein interactions. *Biotechniques* 59(2):63-73.

Jagodzik P., Tajdel-Zielinska M., Ciesla A., Marczak M. Ludwikow A. (2018) Mitogen-Activated Protein Kinase Cascades in Plant Hormone Signaling. *Frontiers Plant Science*, 9:1387.

Jiang Y, Serviène E, Gal J, Panavas T, Nagy PD (2006) Identification of essential host factors affecting tombusvirus RNA replication based on the yeast Tet promoters Hughes Collection. *Journal of Virology*, 80: 7394–7404.

Jiang, J., Patarroyo, C., Garcia Cabanillas, D., Zheng, H. and Laliberté, J.F. (2015) The Vesicle-Forming 6K2 Protein of Turnip Mosaic Virus Interacts with the COPII Coatomer Sec24a for Viral Systemic Infection. *Journal of Virology*, 89, 6695–710.

Jones H.A., Mann L.K. (1963) Onions and Their Allies: Botany, Cultivation and Utilization. *Leonard Hill, London and Interscience, New York*, 285.

Kamelin R.V. (1973) Florogeneticheskij analiz estestvennoj flory gornoj Srednej Azii. *Nauka, Leningrad, Russia*. 354 p.

Kamenetsky R., Rabinoswitch H.D. (2006) The genus *Allium*: A developmental and horticultural analysis. *Horticultural Reviews*, 32: 329-337.

Kang B.C., Yeam I., Li H., Perez K.W., Jahn M.M. (2007) Ectopic expression of a recessive resistance gene generates dominant potyvirus resistance in plants. *Plant Biotechnology Journal*. 4, 526–536.

Katis N.I., Maliogka V.I., and Dovas C.I. (2012) Viruses of the genus *Allium* in the Mediterranean Region. In: Lecoq H., Loebenstein G., (eds) *Viruses and Virus Diseases of Vegetables in the Mediterranean Basin*. Academic Press, San Diego, CA, USA, 163–208.

Katis N.I., Maliogka V.I., Dovas C.I. (2012) Viruses of the Genus *Allium* in the Mediterranean Region. *Advances in Virus Research* 84:163-208.

Keima T., Hagiwara-Komoda Y., Hashimoto M., Neriya Y., Koinuma H., Iwabuchi N., Nishida S., Yamaji Y., Namba S. (2017) Deficiency of the eIF4E isoform nCBP limits the cell-to-cell movement of a plant virus encoding triple-gene-block proteins in *Arabidopsis thaliana*. *Scientific Reports* 6; 7:39678.

Khosa J.S., Lee R., Bräuning S., Lord J., Pither-Joyce M., McCallum J., Macknight R.C. (2016) Doubled Haploid ‘CUDH2107’ as a Reference for Bulb Onion (*Allium cepa* L.) Research: Development of a Transcriptome Catalogue and Identification of Transcripts Associated with Male Fertility. *PLOS ONE* 11(11).

Kik C. (2002) Exploitation of wild relatives for breeding of cultivated *Allium* species. In: Rabinowitch, H.D. and Currah, L. (eds) *Allium Crop Science: Recent Advances*. CAB International, Wallingford, UK, pp. 81–100.

Kim J., Kang W.H., Hwang J., Yang H.B., Dosun K., Oh C.S., Kang B.C. (2014) Transgenic *Brassica rapa* plants over-expressing eIFISO4E variants show broad-spectrum Turnip mosaic virus (TuMV) resistance. *Molecular Plant Pathology*, 15, 615–626.

Klaas M. (1998) Applications and impact of molecular markers on evolutionary and diversity studies in the genus *Allium*. *Plant Breeding* 117, 297–308.

Kopsell D.E., Randle W.M. (1997) Onion cultivars differ in pungency and bulb quality changes during storage. *Hort Science* 32(7):1260-1263.

Kritzman A., Lampel M., Raccach B., and Gera A. (2001) Distribution and transmission of *Iris yellow spot virus*. *Plant disease* 85, 338-342.

Kumar P., Dhawan P. and Mehra R. (2012) Symptoms and losses caused by Onion yellow dwarf virus and Iris yellow spot virus diseases of onion crop in Northern India. *Journal of Mycology and Plant Pathology* 42 (1), 153-160.

Kumar P., Dhawan P., Mehra R. (2011) Characterization, transmission and host range of onion yellow dwarf virus. *Plant Disease Research* 26 (2), 176.

Lagacé M., Matton D.P. (2004) Characterization of a WRKY transcription factor expressed in late torpedo-stage embryos of *Solanum chacoense*. *Planta* 219:185–189.

Laliberté J.F., Zheng H (2014) Viral manipulation of plant host membranes. *Annual Review Virology*, 1: 237–259.

Landy, A. (1989) Dynamic, Structural, and Regulatory Aspects of Lambda Site-specific Recombination. *Annual Review Biochemistry*, 58, 913-949.

Law M.D. and Moyer J.W. (1990) A tomato spotted wilt-like virus with a serologically distinct N protein. *Journal of General Virology* 71, 933-938.

Le Gall O., Aranda M.A., Caranta C. (2011). Plant resistance to viruses mediated by translation initiation factors. In: *Caranta C., Aranda M.A., Tepfer M., Lopez-Moya J., editors. Recent Advances in Plant Virology. Caister Academic Press; Wymondham, Norfolk, VA, USA: pp. 177–194.*

Lebaron C., Rosado A., Sauvage C., Gauffier C., German-Retana S., Moury B., Gallois J.L. (2016) A new eIF4E1 allele characterized by RNAseq data mining is associated with resistance to potato virus Y in tomato albeit with a low durability. *Journal General Virology*, 97(11):3063-3072.

Lellis A.D., Kasschau K.D., Whitham S.A., Carrington J.C. (2002) Loss-of-susceptibility mutants of *Arabidopsis thaliana* reveal an essential role for eIF(iso)4E during potyvirus infection. *Current Biology*, 12:1046-1051.

Levichev I.G., Krassovskaja L.S. (1981) The Pskemski onion *Allium pskemense* in the southern part of its range. *Bulletin Moskovskogo Obshchestva Ispytatelej Prirody, Otdel Biologicheskij* 86, 105–112.

Li Q.Q., Zhou S.D., He X.J., Yu Y., Zhang Y.C., Wei X.Q. (2010) Phylogeny and biogeography of *Allium* (Amaryllidaceae: Allieae) based on nuclear ribosomal internal transcribed spacer and chloroplast rps16 sequences, focusing on the inclusion of species endemic to China. *Annals of Botany* 106: 709–733.

Li W., Wang H., Yu D. (2016) The Arabidopsis WRKY transcription factors WRKY12 and WRKY13 oppositely regulate flowering under short-day conditions. *Molecular Plant*, 9:1492–1503.

Linnaeus C. Von. (1753) Species plantarum, Vol. 1. *Allium*, pp. 294–302. Laurentiis Salvii, Stockholm, Sweden. *Facsimile edition*, 1957–1959, *Ray Society*, London, UK.

Liu G. (2014) Food Losses and Food Waste in China: A First Estimate. *OECD Food, Agriculture and Fisheries Papers*, No. 66.

Livak, K.J. and Schmittgen T. (2001) Analysis of relative gene expression data using real-time quantitative PCR and the 2- $\Delta\Delta$ Ct method. *Methods* 25, 402-408.

Locatelli A. (2009) La cipolla Bianca, un ortaggio da rivalutare nei piccoli orti famigliari. *Vita in Campagna*, 7-8/2009, 17-19.

Loebenstein G., Katis N. (2014) “Control of plant virus diseases seed-propagated crops,” in *Advance Virus Reserch*, eds Gad L., Nikolaos K. (Cambridge, MA: Academic Press;), 11.

Lohse M, Nagel A, Herter T, May P, Schroda M, Zrenner R, Tohge T, Fernie AR, Stitt M, Usadel B (2014) Mercator: sequence functional annotation server. *Plant Cell Environ*, 37:1250-1258.

Luria S.E., Darnell Jr J.E. (1970) *Virologia generale*. Zanichelli.

Mabberley D.J. (2008) *Mabberley's Plant-Book: A Portable Dictionary of Plants, Their Classification and Uses*. 3rd Ed. *Cambridge University Press*.

Mahy B.W.J., van Regenmortel M.H.V. (2009) *Desk Encyclopedia of Plant and Fungal Virology*. *Cambridge MA: Academic Press*.

Manglli A., Mohamed H.S., El Hussein A.A., Agosteo G.E., Albanese G., and Tomassoli L. (2014) Molecular analysis of the 3' terminal region of Onion yellow dwarf virus from onion in southern Italy. *Phytopathologia Mediterranea* 53, 3, 438-450.

Manglli A., Tomassoli L., Tiberini A., Agosteo G.E., Fontana A., Pappu H.R., Albanese G. (2020) A survey on the infection of Onion yellow dwarf virus and Iris yellow spot tospovirus in seed and bulb productions systems of onion in Calabria, Italy. *European Journal of Plant Pathology* 156, 767–778.

Manglli A., Zicca S., Tiberini A., Albanese G., and Tomassoli L. (2012) Iris yellow spot virus on onion crops in Calabria. *Journal of Plant Pathology*, 94 (4,Suplement), S4.85-S4.105.

Marani F., e Bertaccini A. (1983) Virosi delle liliaceae ortive: cipolla, aglio, porro. In: *Le virosi delle piante ortive*. Reda Editore per l'Agricoltura (Ed), Roma Italy, 104-111.

Matsubara S., Kimura I. (1991) Changes of ABA content during bulbing and dormancy and in vitro bulbing in onion plant. *Journal of the Japanese Society for Horticultural Science*. 59 (4), 757–762.

Maule A.J., Caranta C., Boulton M.I. (2007). Sources of natural resistance to plant viruses: Status and prospects. *Molecular Plant Pathology*, 8:223–231.

Mazier M., Flamain F., Nicolai M., Sarnette V., Caranta C. (2011) Knock-down of both eIF4E1 and eIF4E2 genes confers broad-spectrum resistance against potyviruses in tomato. *PLoS ONE*, 6. (12).

McCallum J., Thomson S., Pither-Joyce M., Kenel F., Clarke A., Havey M.J. (2008) Genetic Diversity Analysis and Single-nucleotide Polymorphism Marker Development in Cultivated Bulb Onion Based on Expressed Sequence Tag–Simple Sequence Repeat Markers. *Journal of the American Society for Horticultural Science*.

MCPP Cipolla-Manuale di corretta prassi per la produzione integrata della cipolla
<http://www.parco3a.org/MC-API/Risorse/>

Mehta I. (2017) “Origin and History of Onions”. *IOSR Journal Of Humanities And Social Science*. Volume 22, Issue 9, Ver. 13 PP 07-10.

Melan M.A., Enriquez A.L.D., Peterman T.K. (1994) The LOX1 Gene of Arabidopsis Is Temporally and Spatially Regulated in Germinating Seedlings. *Plant Physiology* 105:385-393

Melhus, I. E., Reddy C., Shenderson W.J., and Vestal E. (1929) A new virus disease epidemic on onions. *Phytopathology* 19, 73-77.

Moury B., Charron C., Janzac B., Simon V., Gallois J.L., Palloix A., Caranta C. (2014) Evolution of plant eukaryotic initiation factor 4E (eIF4E) and potyvirus genome-linked protein (VPg): A game of mirrors impacting resistance spectrum and durability. *Infect. Genet. Evol.* 27, 472–480.

Moury B., Morel C., Johansen E., Guilbaud L., Souche S., Ayme V., Caranta C., Palloix A., Jacquemond M. (2004) Mutations in potato virus Y genome-linked protein determine virulence toward recessive resistances in *Capsicum annuum* and *Lycopersicon hirsutum*. *Molecular Plant Microbe Interaction*, 17, 322–329.

Movahed N., Garcia Cabanillas D., Wan J., Vali H., Laliberté J.F., Zheng H. (2019) Turnip Mosaic Virus Components Are Released into the Extracellular Space by Vesicles in Infected Leaves. *Plant Physiology*, 180(3):1375-1388.

Movahed N., Patarroyo C., Sun J., Vali H., Laliberté J.F., Zhenga H. (2017) Cylindrical Inclusion Protein of Turnip Mosaic Virus Serves as a Docking Point for the Intercellular Movement of Viral Replication Vesicles. *Plant Physiology*, 175, 1732–1744.

Mullis S.W., Langston D.B., Jr., Gitaitis R.D., Shervood J.L., and Csinos A.C. (2004) First report of onion (*Allium cepa*) naturally infected with *Tomato spotted wilt virus* and *Iris yellow spot virus* (family *Bunyaviridae*, genus *Topovirus*) in Georgia. *Plant disease* 88, 1285.

Mumford R.A., Barker I., and Wood K.R. (1996) The biology of the tospoviruses. *Annals of Applied Biology* 128, 159-183.

Murray R.R., Emblow M.S.M., Hetherington A.M., Foster G.D. (2016) Plant virus infections control stomatal development. *Scientific Reports* 6: 34507.

Nagata T., Almeida A.C.L., Resende R. de O., and de Avila A.C. (1999) The identification of the vector species of *Iris yellow spot* tospovirus occurring on onion in Brazil. *Plant Disease*. 83, 399.

Nagy P.D., Pogany J. (2012) The dependence of viral RNA replication on co-opted host factors. *Nature Reviews Microbiology*, 10:137–149.

Nakashima K., Fujita Y., Kanamori N., Katagiri T., Umezawa T., Kidokoro S., Maruyama K., Yoshida T., Ishiyama K., Kobayashi M., Shinozaki K., Yamaguchi-Shinozaki K. (2009) Three Arabidopsis SnRK2 Protein Kinases, SRK2D/SnRK2.2, SRK2E/SnRK2.6/OST1 and SRK2I/SnRK2.3, Involved in ABA Signaling are Essential for the Control of Seed Development and Dormancy. *Plant and Cell Physiology* 50(7):1345–1363.

National Onion Association, 2020. <http://www.onions-usa.org/>

Nicaise V., Gallois J.L., Chafiai F., Allen L.M., Schurdi-Levraud V., Browning K.S., Candresse T., Caranta C., Le Gall O., German-Retana S. (2007) Coordinated and selective recruitment of eIF4E and eIF4G factors for potyvirus infection in Arabidopsis thaliana. *FEBS Lett.* 581, 1041–1046.

Nieto C., Rodriguez-Moreno L., Rodriguez-Hernandez A.M., Aranda M.A., Truniger V. (2011) *Nicotiana benthamiana* resistance to non-adapted *Melon necrotic spot virus* results from an incompatible interaction between virus RNA and translation initiation factor 4E. *The Plant Journal*, 66:492–501.

NOA “History of onions”, (2011) *US National Onion Association*, Greeley, CO. Retrieved 23 January 2017. <https://www.onions-usa.org/all-about-onions/history-of-onions/>

Oracz K. and Stawska M. (2016) Cellular Recycling of Proteins in Seed Dormancy Alleviation and Germination. *Frontiers. Plant Science*, 7:1128.

Paez Valencia J., Goodman K., Otegui M. S. (2016) Endocytosis and endosomal trafficking in plants. *Annual Reviews Plant Biology*, 67 309–335.

Pak C., Van der Plas L.H.W., de Boer A.D. (1995) Importance of dormancy and sink strength in sprouting of onions (*Allium cepa*) during storage. *Physiology Plant.* 94 (2), 277–283.

Panavas T, Serviene E, Brasher J, Nagy PD (2005) Yeast genome-wide screen reveals dissimilar sets of host genes affecting replication of RNA viruses. *Proc Natl Acad Sci U S A* 102: 7326–7331.

Parrella G., De Stradis A., Volvas C., Agosteo G.E. (2005) Outbreaks of Onion yellow dwarf virus (OYDV) on onion crops in Calabria (Southern Italy). *Journal of Plant Pathology* 87 (4), 302.

Patro, R., Duggal, G., Love, M. I., Irizarry, R. A., & Kingsford, C. (2017). Salmon provides fast and bias-aware quantification of transcript expression. *Nature Methods* 14, pages417–419.

Pavan S., Jacobsen E., Visser R.G.F., Bai Y. (2010). Loss of susceptibility as a novel breeding strategy for durable and broad-spectrum resistance. *Molecular Breeding*, 25:1–12.

Petropoulos S.A, Ntatsi G. and Ferreira I.C.F.R. (2017) Long-term storage of onion and the factors that affect its quality: A critical review. *Food Reviews International* 33:1, 62-83

Pich U., Fritsch R. and Schubert I. (1996) Closely related *Allium* species (Alliaceae) share a very similar satellite sequence. *Plant Systematics and Evolution* 202, 255–264.

Pitzalis N., Heinlein M. (2018) The roles of membranes and associated cytoskeleton in plant virus replication and cell-to-cell movement. *Journal of Experimental Botany*, 69 (1) 117–132.

Platt E.S. (2003) Garlic Onion & other. Alliums, Mechanicsburg, PA: *Stackpole Books*.

Potschin M., Schlienger S., Bieker S., Zentgraf U. (2013) Senescence Networking: WRKY18 is an Upstream Regulator, a Downstream Target Gene, and a Protein Interaction Partner of WRKY53. *Journal of Plant Growth Regulation*. 33: 106-118.

Raiborg, C. and Stenmark, H. (2009) The ESCRT machinery in endosomal sorting of ubiquitylated membrane proteins. *Nature* 458, 445–452.

Regel E. (1875) Alliorum adhuc cognitorum monographia. *Trudy Imper. S.-Peterburgsk. Bot. Sada* 3: 1–266

Reveal J.L., Chase M.W. (2011) APG III: bibliographical information and synonymy of Magnoliidae. *Phytotaxa* 19:71-134.

Reyes F. C., Buono R., Otegui M. S. (2011) Plant endosomal trafficking pathways. *Curr. Opin. Plant Biol.* 14 666–673.

Robaglia C., Caranta C. (2006). Translation initiation factors: a weak link in plant RNA virus infection. *Trends Plant Science*, 11:40–45.

Rod Peakall, and Peter E. Smouse (2012) GenAlEx 6.5: genetic analysis in Excel. Population genetic software for teaching and research—an update. *Bioinformatics* 1; 28(19): 2537–2539.

Rodriguez-Hernandez A.M., Gosalvez B., Sempere R.N., Burgos L., Aranda M.A., Truniger V. (2012) Melon RNA interference (RNAi) lines silenced for Cm-eIF4E show broad virus resistance. *Molecular Plant Pathology*, 3, 755–763.

Romero-Brey I., Bartenschlager R. (2014) Membranous replication factories induced by plus-strand RNA viruses. *Viruses* 6: 2826–2857.

Ruffel S., Dussault M.H., Palloix A., Moury B., Bendahmane A., Robaglia C., Caranta C. (2002) A natural recessive resistance gene against potato virus Y in pepper corresponds to the eukaryotic initiation factor 4E (eIF4E). *Plant Journal*, 32:1067-1075.

Rutter B.D., Innes R.W. (2017) Extracellular vesicles isolated from the leaf apoplast carry stress-response proteins. *Plant Physiology*, 173: 728–741.

Sachs A. (2000) Physical and functional interactions between the mRNA cap structure and the poly(A) tail, p. 447-465. In N. Sonenberg, J. W. B. Hershey, and M. Mathew (ed.), Translational control of gene expression. *Cold Spring Harbor Laboratory Press, Cold Spring Harbor, N.Y.*

Samuel G., Bald J.G., and Pitman H.A. (1930) Investigations on “spotted wilt” of tomatoes in Australia. *Commonwealth Council Scientific and Industrial Research Bulletin* 44, 8-11.

Sanfaçon H. (2015) Plant Translation Factors and Virus Resistance. *Viruses* 7, 3392-3419.

Sanfaçon H., Jovel J. (2007) Interactions Between plant and Virus Proteomes in Susceptible Hosts: Identification of New Targets for Antiviral Strategies. In: *Punja Z.K., De Boer S.H., Sanfaçon H., editors. Biotechnology and Plant Disease Management. CAB International; Wallingford, UK: pp. 87–108.*

Sastry K. S. (2013) Seed-borne plant virus diseases. *Springer*.

Sato M., Nakahara K., Yoshii M., Ishikawa M., Uyeda I. (2005) Selective involvement of members of the eukaryotic initiation factor 4E family in the infection of *Arabidopsis thaliana* by potyviruses. *FEBS Lett.* 579, 1167–1171.

Schaad M.C., Anderberg R.J., Carrington J.C. (2000) Strain-specific interaction of the tobacco etch virus NIa protein with the translation initiation factor eIF4E in the yeast two-hybrid system. *Virology* 273, 300–306.

Schiavi M. (2012) La cipolla salvavita. *Karpos Magazine* 1: 4 68-73.

Schoelz, J.E., Harries, P.A. and Nelson, R.S. (2011) Intracellular transport of plant viruses: finding the door out of the cell. *Molecular Plant* 4, 813–31.

Scholten O.E, van Kaauwen, M.P.W., Shahin, A., Hendrickx P.M., Keizer L.C.P., Burger K., van Heusden, A.W., van der Linden C.G., Vosman B. (2016) SNP-markers in *Allium* species to facilitate introgression breeding in onion. *BMC Plant Biology* 16:187

Schwartz H.F., and Mohan S. K. (2008) Compendium of Onion and Garlic Diseases and Pests. 2nd ed., *APS Press*.

Shannon P, Markiel A, Ozier O, Baliga NS, Wang JT, Ramage D, Amin N, Schwikowski B, Ideker T. (2003) Cytoscape: a software environment for integrated models of biomolecular interaction networks. *Genome Research* 13(11):2498-504

Sharma K, Lee Y.R., Park S.W., Nile S.H. (2016) Importance of growth hormones and temperature for physiological regulation of dormancy and sprouting in onions. *Food Reviews International*, 32:3, 233-255.

Shulla A, Randall G (2016) (+) RNA virus replication compartments: A safe home for (most) viral replication. *Current Opinion Microbiology*. 32: 82–88.

Simon A.E., Miller W.A. (2013) 3' cap-independent translation enhancers of plant viruses. *Annual Reviews. Microbiology*, 67:21–42.

Smith T.N., Wylie S.J., Coutts B.A., and Jones R.A.C. (2006) Localized distribution of *Iris yellow spot virus* within leeks and its reliable large-scale detection. *Plant Disease* 90, 729–733.

Sorel, M., Garcia, J.A. and German-Retana, S. (2014) The Potyviridae cylindrical inclusion helicase: a key multipartner and multifunctional protein. *Molecular Plant Microbe Interaction*, 27, 215–26.

Stagljar I., Korostensky C., Johnsson N., te Heesen S. (1998) A genetic system based on split-ubiquitin for the analysis of interactions between membrane proteins in vivo. *Proc. Natl. Acad. Sci. U. S. A.* 95, 5187–92.

Stearn W.T. (1992) How many species of *Allium* are known? *Kew Magazine* 9, 180–182.

Storsberg J., Schulz H. and Keller E.R.J., (2003) Chemotaxonomic classification of some *Allium* wild species on the basis of their volatile sulphur compounds. *J. Appl. Bot.* 77:160-162.

Suleria H.A.R., But M.S., Anjum F.M., Saeed F., and Khalid N., 2013. Onion: Nature Protection Against Physiological Threats. *Critical Reviews in Food Scienze and Nutrition*, 00, 1-17.

Taglienti A., Tiberini A., Ciampa A., Piscopo A., Zappia A., Tomassoli L., Poiana M., Dell'Abate M.T. (2020)a Metabolites response to onion yellow dwarf virus (OYDV) infection in 'Rossa di Tropea' onion during storage: a 1 H HR-MAS NMR study. *Journal of the Science of Food and Agriculture* 100 (8)

Taglienti A., Dell'Abate M.T., Ciampa A., Tomassoli L., Albanese G., Sironi L., Tiberini A. (2020)b Study on ultra-structural effects caused by Onion yellow dwarf virus infection in 'Rossa di Tropea' onion bulb by means of magnetic resonance imaging. *Scientia Horticultura* 271

Tao Z., Liu H.B., Qiu D.Y., Zhou Y., Li X.H., Xu C.G., Wang S.P. (2009) A Pair of Allelic WRKY Genes Play Opposite Roles in Rice-Bacteria Interactions. *Plant Physiology*, 151(2):936–948.

Tiberini A, Mangano R, Micali G, Leo G, Manglli A, Tomassoli L, Albanese G (2019) Onion yellow dwarf virus $\Delta\Delta$ Ct-based relative quantification obtained by using real-time polymerase chain reaction in ‘Rossa di Tropea’ onion. *European Journal of Plant Pathology* 153: 251-264

Tilsner, J., and Oparka, K. J. (2012) Missing links? The connection between replication and movement of plant RNA viruses. *Current Opinion Virology*, 2:705-711.

Tomassoli L., Tiberini A., Masenga, V., Vicchi V., e Turina M. (2009) Characterization of *Iris yellow spot virus* isolates from onion crops in northern Italy. *Journal of Plant Pathology*, 91 (3) 733-739.

Tomassoli L., Turina M. (2012) Escursus conoscitivo sulla malattia causata da *Iris yellow spot virus* su cipolla da seme. In: Workshop Ancona 2012 “Difesa ortive da seme”. *Petria* 22 (2), 85-89.

Toribio R., Muñoz A., Castro-Sanz A.B., Merchante C., and M. Mar Castellano M.M. (2019) A novel eIF4E interacting protein that forms non-canonical translation initiation complexes. *Nature Plants* 5(12): 1283–1296.

Traub H.P., (1968) “The subgenera, sections and subsections of *Allium* L.”. *Plant Life*. 24: 147–163.

Truniger V., Aranda M.A. (2009) Recessive resistance to plant viruses. *Adv. Vir. Res.* 75, 119–159.

Tsujimoto Y., Numaga T., Ohshima K., Yano M., Ohsawa R., Goto D.B., Naito S., Ishikawa M. (2003) Arabidopsis TOBAMOVIRUS MULTIPLICATION (TOM) 2 locus encodes a transmembrane protein that interacts with TOM1. *EMBO J.* 22:335-343.

Tzfadia O, Diels T., De Meyer, S., Vandepoele, K., Aharoni, A., & Van de Peer, Y. (2015) CoExpNetViz: Comparative Co-Expression Networks Construction and Visualization Tool. *Frontiers in Plant Science*, 6, 1194

Van Dijk P. (1993) Survey and characterization of potyviruses and their strains of *Allium* species. *Netherlands Journal of Plant Pathology* 99(2), 1-48.

van Raamsdonk L.W.D., de Vries T., (1992a) Biosystematic studies in *Allium* L. section Ceba. *Botanical Journal of the Linnean Society* 109, 131–143.

van Raamsdonk L.W.D., de Vries T., (1992b) Systematics and phylogeny of *Allium cepa* L. and allies. In: Hanelt, P., Hammer, K. and Knüpffer, H. (eds) *The Genus Allium – Taxonomic Problems and Genetic Resources. Proceedings of an International Symposium, Gatersleben, 11–13 June 1991. IPK, Gatersleben, Germany*, pp. 257–263.

van Schie C.C., Takken F.L. (2014) Susceptibility genes 101: how to be a good host. *Annual Reviews Phytopathology*, 52:551–581.

Van Verk M.C., Pappaioannou D., Neeleman L., Bol J.F., Linthorst H.J. (2008) A novel WRKY transcription factor is required for induction of PR-1a gene expression by salicylic acid and bacterial elicitors. *Plant Physiology*, 146: 1983–1995.

Viana V.E., Busanello C., da Maia L.C., Pegoraro C., de Oliveira A.C. (2018) Activation of rice WRKY transcription factors: an army of stress fighting soldiers?, *Current Opinion in Plant Biology* 45:268-275.

Vijayapalani, P., Maeshima, M., Nagasaki-Takekuchi, N. and Miller, W.A. (2012) Interaction of the trans-frame potyvirus protein P3N-PIPO with host protein PCaP1 facilitates potyvirus movement. *PLoS Pathog.* 8(4).

Voinnet O, Rivas S, Mestre P, Baulcombe D. (2003) An enhanced transient expression system in plants based on suppression of gene silencing by the p19 protein of tomato bushy stunt virus. *Plant Journal*, 33:949–956.

Walkey D.G.A. (1985) Applied plant virology. *John Wiley & Sons Canada, Limited.*

Wan J, Laliberté JF (2015) Membrane-associated virus replication complexes locate to plant conducting tubes. *Plant Signal Behav.* 10 (8).

Wang A. (2015) Dissecting the Molecular Network of Virus-Plant Interactions: The Complex Roles of Host Factors. *Annual Reviews Phytopathology*, 53.

Wang A., Krishnaswamy S. (2012) Eukaryotic translation initiation factor 4E-mediated recessive resistance to plant viruses and its utility in crop improvement. *Molecular Plant Pathology*, 13:795–803.

Wang M., Vannozzi A., Wang G., Liang Y.H., Tornielli G.B., Zenoni S., Cavallini E., Pezzotti M., Cheng Z.M. (2014) Genome and transcriptome analysis of the grapevine (*Vitis vinifera* L.) WRKY gene family. *Horticulture Research* 1:16.

Wang P., Yue C., Chen D., Zheng Y., Zhang Q., Yang J., Ye N. (2019) Genome-wide identification of WRKY family genes and their response to abiotic stresses in tea plant (*Camellia sinensis*). *Genes & Genomics* 41:17–33.

Wang S., Browning K.S., Miller W.A. (1997) A viral sequence in the 3'-untranslated region mimics a 5'cap in facilitating translation of uncapped mRNA. *EMBO Journal*, 16:4107-4116.

Wang X., Kohalmi S.E., Svircev A., Wang A., Sanfacon H., Tian L. (2013) Silencing of the host factor eIFISO4E gene confers plum pox virus resistance in plum. *PLoS ONE*, 8.

Wang Y., Chu Y.J., Xue H.W. (2012) Inositol polyphosphate 5-phosphatase-controlled Ins(1,4,5)P₃/Ca²⁺ is crucial for maintaining pollen dormancy and regulating early germination of pollen. *Development* 139, 2221-2233

Wei T., Zhang C., Hong J., Xiong R., Kasschau K.D., Zhou X., Carrington J.C., Wang A. (2010) Formation of Complexes at Plasmodesmata for Potyvirus Intercellular Movement Is Mediated by the Viral Protein P3N-PIPO. *PLoS Pathog.* 6(6).

Wells S.E., Hillner P.E, Vale R.D., Sachs A.B. (1998) Circularization of mRNA by eukaryotic translation initiation factors. *Molecular Cell*, 2:135-140.

Whitham S. A., Hajimorad M. R. (2016) "Plant genetic resistance to viruses," in *Current Research Topics in Plant Virology*, eds Wang A., Zhou X. (Cham: Springer International Publishing), 87–111.

Xie Z., Zhang Z.L., Hanzlik S., Cook E., Shen Q.J. (2007) Salicylic acid inhibits gibberellin-induced alpha-amylase expression and seed germination via a pathway involving an abscisic-acid-inducible WRKY gene. *Plant Molecular Biology*, 64:293–303.

Xu J.M., Yang L., He X.J., (1998) A study on karyotype differentiation of *Allium fasciculatum* (Liliaceae) *Acta Phytotaxonomica Sinica*. 36:346–352.

Yamanaka T., Ohta T., Takahashi M., Meshi T., Schmidt R., Dean C., Naito S., Ishikawa M. (2000) TOM1, an Arabidopsis gene required for efficient multiplication of a tobamovirus, encodes a putative transmembrane protein. *Proc. Natl. Acad. Sci. USA* 97:10107-10112.

Yang Y., Zhou Y., Chi Y., Fan B., Chen Z. (2017) Characterization of soybean WRKY gene family and identification of soybean WRKY genes that promote resistance to soybean cyst nematode. *Sci. Rep.* 7:17804.

Yoshii M, Nishikiori M, Tomita K, Yoshioka N., Kozuka R., Naito S., Ishikawa M. (2004) The Arabidopsis cucumovirus multiplication 1 and 2 loci encode translation initiation factors 4E and 4G. *Journal of Virology* 78 (12): 6102-6111.

Zhang C., Zhang H., Zhan, Z., Liu B., Chen Z., Liang Y. (2016) Transcriptome Analysis of Sucrose Metabolism during Bulb Swelling and Development in Onion (*Allium cepa* L.). *Front Plant Science*, 7: 1425.

Zhang J., Roberts R., Rakotondrafara A.M. (2015) The role of the 5' untranslated regions of Potyviridae in translation. *Virus Research*.

Zhang Y.J., Wang L.J. (2005) The WRKY transcription factor superfamily: its origin in eukaryotes and expansion in plants. *BMC Evolutionary Biology* 5, 1.

Zheng C., Acheampong A.K., Shi Z., Halaly T., Kamiya Y., Ophir R., Galbraith D.W., Or E. (2018) Distinct gibberellin functions during and after grapevine bud dormancy release. *Journal of Experimental Botany* 69(7):1635–1648.

Zhou S.D., He X.J., Yu Y., Xu J.M., (2007) Karyotype studies on twenty-one populations of eight species in *Allium* section Rhiziridium. *Acta Phytotaxonomica Sinica*. 45:207–216.

List of figures

Figure 1. Evolutionary line of *Allium* Genus (Friesen *et al.*, 2006). Pag. 14

Figure 2. Third evolutionary line of *Allium* genus (Friesen *et al.*, 2006). Pag. 15

Figure 3. Onion morphology. a-leaves, b-outer tunics, c-bulb; d-disc, e-fasciculated roots, f-fleshy tunics, g-vegetative apex, h-seeds (Locatelli, 2009). Pag. 22

Figure 4. Onion world production (t) (FAOSTAT, 2018). Pag. 25

Figure 5. Top 5 Onion producers (FAOSTAT, 2018). Pag. 25

Figure 6. Genomic map of a member of the genus *Potyvirus*, using a strain of Tobacco etch virus as an example (Virus Taxonomy 9, ICTV). Pag. 32

Figure 7. Symptoms caused by OYDV
(<https://www.plantevernleksikonet.no/1/oppslag/1521/>). Pag. 34

Figure 8. Greenhouse used for the experimental trials. Pag.49

Figure 9. Seedbed used for the germination phase. Pag.50

Figure 10. Ten cm tall seedlings transplanted in pots after foliar and root tips cut.
Pag. 50

Figure 11. Preparation of the inoculum from OYDV infected leaves with phosphate buffer. Pag.51

Figure 12. Mechanical inoculation of two leaves /plant. Pag 52

Figure 13. Symptoms caused by OYDV: A, B yellowing; C, D twirling; E, F dwarfing. pag. 54

Figure 14. Measurement of the morphological parameters: height of the longest leaf and number of leaves. Pag. 55

Figure 15. Bulbs uprooted and covered until the green part is dry to simulate the agronomic conditions of the open field. Pag. 56

Figure 16. One gram of fresh bulb tissue placed at 60 °C until complete dehydration. Pag. 57

Figure 17. Percentage of plant infection index (% PII) during the first trial. Pag. 62

Figure 18. Percentage of plant infection index (% PII) in second trial. Pag. 63

Figure 19. Results of the statistical analysis in the first year, plant height panel A) T1, B) T2; number of leaves panel C) T1, D) T2. Pag 64

Figure 20. Results of the statistical analysis in the second year, plant height panel A) T1, B) T2; number of leaves panel C) T1, D) T2. Pag 65

Figure 21. Genetic relationships among onion varieties. Pag. 73

Figure 22. Principal Coordinates analysis. Pag. 74

Figure 23. Onion annual life cycle (modify by Sharma *et al.* 2016). The phase between endo-dormancy (T_{ED}), eco-dormancy (T_{EC}), and internal sprouting (T_{IS}) (the three time points investigated) was highlighted. Pag. 79

Figure 24. **A)** Sequences of forty-one (41) peptide sequences from *Arabidopsis*, tomato and onion, selected from public databases and traceable as *eIF4* genes were aligned using Clustal W and the phylogenetic tree constructed using the Neighbor-Joining method. **B)** To discover the conserved motifs MEME online tool v5.0.5 was utilized with four *eIF4G* isoforms from onion, three sequences from *Arabidopsis* (AT3G60240) and two from tomato (*Solyc01g088700.2.1* and *Solyc08g077700.2.1*). The two *eIF4E* isoforms from onion clustered with *eIF4E* from *Arabidopsis* and tomato, *AT4G18040.1* and *Solyc03g005870.2.1*. Pag. 84-85

Figure 25. Gene expression analysis of EIF4E e EIF4G isoforms in the leaves (expressed as $2^{\Delta\Delta Ct}$) compared to the Actin as reference gene). Pag. 86

Figure 26. Gene expression analysis of EIF4E e EIF4G isoforms in the onion bulbs (expressed as $2^{\Delta\Delta Ct}$) compared to the Actin as reference gene). Pag. 87

Figure 27. Transcriptome relationships among 3 time points during onion bulb dormancy of uninfected and OYDV-infected plants. VENN diagrams of transcriptome profiles at TED (A), TEC (B), and TIS (C). PCA (D) developed using five hundred most variable genes. Pag. 90

Figure 28. Overview expression level changes of genes associated to primary and secondary metabolism pathways in uninfected bulbs during dormancy, following the Mercator annotation. **A)** T_{EC}/T_{ED} , **B)** T_{IS}/T_{ED} , and **C)** T_{IS}/T_{EC} comparisons. Transcription levels with a value $\log_2 FC > 1$ for pairwise comparisons are displayed in coloured squares. The blue and red indicate up- and down-regulated genes, respectively. The scale showing the expression level is displayed in the pictures that have been exported from MapMan and their quality was further improved accordingly. Pag. 92-93

Figure 29. GO terms enrichment analysis carried out for upregulated genes at different sampling times (T_{ED} , T_{EC} , and T_{IS}) in uninfected bulbs. Pag. 95

Figure 30. Heatmap developed using DEGs isolated in uninfected bulbs in the three comparisons T_{EC}/T_{ED} , T_{IS}/T_{ED} , and T_{IS}/T_{EC} . Log₂ FC for uninfected (U) and OYDV-infected (I) conditions were displayed. Pag. 96

Figure 31. Overview expression level changes of genes associated to hormone signaling, and some key metabolism pathways involved in dormancy process between uninfected and OYDV infected, following the Mercator annotation. **A)** T_{EC}/T_{ED} , **B)** T_{IS}/T_{ED} , and **C)** T_{IS}/T_{EC} comparisons. Transcription levels with a value $\log_2 FC \geq 1$ for pairwise comparisons are displayed in coloured squares. The blue and red indicate up- and down-regulated genes, respectively. The scale showing the expression level, is displayed in the pictures that have been exported from MapMan and their quality was further improved accordingly. Pag. 97

Figure 32. Expression levels of *AcWRKY* genes isolated during dormancy phases (endo-dormancy, eco-dormancy and internal sprouting). **A)** Heatmap developed using log₂ Fold-Change (by Deseq2) values of *AcWRKYs* for T_{EC}/T_{ED} , T_{IS}/T_{ED} , and T_{IS}/T_{EC} comparisons. Genes differentially expressed between uninfected (U) and OYDV-infected (I) bulbs at each time (T_{ED} , T_{EC} , and T_{IS}) was also visualized; *AcWRKYs* showing significant differences ($p < 0.05$) by RNASeq and qPCR between the two conditions during dormancy release (T_{IS}) were underlined. **B)** RNA-Seq counts normalized of *AcWRKY2*, 30, 32, and 52 at each sampling time, detected from uninfected (red) and OYDV-infected (gray) samples. **C)** qPCR analysis of *AcWRKY2*, 30, 32, and 52 during internal-sprouting phase (T_{IS}) for uninfected (red) and OYDV-infected (gray) bulbs. Pag. 102

Figure 33. Correlation analysis between RNA-Seq and qPCR data for *AcWRKYs* differentially expressed in each comparison. The same RNAs from NGS experiment were utilized for validation. The Pearson Correlation Coefficient ($R = 0.88$) and the p-value ($p = 1e-09$) were reported. Pag. 103

Figure 34. Co-expression network analyses of four *AcWRKY* up regulated at T_{1S} in the uninfected/OYDV infected bulbs comparison (*AcWRKY2*, 30, 32, and 52). The network was obtained with Comparative Co-Expression Network Construction and Visualization tool and visualized by Cytoscape. Green and red lines denote positive correlation and negative correlation, respectively. Pag. 105

Figure 35. Schematic representation of the SUY2H system (Ivanusic *et al.*, 2015). Pag. 109

Figure 36. Schematic representation of Gateway[®] technology. Once a gene is cloned into an Entry clone it can then be moved into different Destination vectors through in vitro recombination reactions (ThermoFisher). Pag. 107

Figure 37. pENTR[™]/SD/D-TOPO[®] (Invitrogen). Pag. 111

Figure 38. Schematic view of the LR recombination: The gene of interest in the entry clone is flanked by the two attL sites that recombine with the attR sites of the destination vector in presence of LR clonase mix, leading to an expression clone. (Gateway technology manual). Pag. 113

Figure 39. Gateway binary vectors used in this study.

The pGW705 and pGW754 vectors allow the expression of C-terminal fusion with GFP- and RFP-at the C-ter of the protein of interest. The Psite vectors are used for BiFC experiments: the protein of interest is fused either at its N-ter (serie “N1”) or at its C-ter (serie C1) to the N-ter part (nEYFP) or C-ter part (cEYFP) of the YFP. SPC: spectinomycin resistance gene. P35S and T35S: transcription promoter and transcription termination derived from CaMV. Tnos: poly-adenylation signal of the nopaline synthase gene. Pag. 115

Figure 40. **A)** Schematic representation of recombinant TuMV expressing 6K2-mCherry. **B)** During TuMV-6K2-mcherry replication, the virus induces the formation of viral replication complexes (VRC) that are labelled by the 6K2-mcherry and indicated by yellow arrows. Pag. 116

Figure 41. Principle of the BiFC assay. Proteins A and B are fused to N- and C-terminal fragments of YFP, respectively. In the absence of an interaction between A and B, the fluorophore remains non-functional. With interaction between A and B, a functional fluorophore is reconstituted which exhibits emission of fluorescence upon excitation with an appropriate wavelength (Bhat *et al.*, 2006). Pag. 118

Figure 42. Analysis of interactions between WMV-6K2 and CmXX proteins by SuY2H assay. Six independent yeast colonies co-transformed with CmXX (prey) and WMV-6K2 (bait) were grown on SD-LTHA medium. Colonies boxed in green, yellow and red correspond to strong, medium and lack of interaction respectively. AtCER1 (boxed in blue) is the negative control used as a bait (no colonies grew). AtHVA22a / TuMV-6K2 interaction (boxed in green) is the internal positive control of the experiment (6/6 colonies grew). This figure is representative of the three independent experiments that were performed. Pag. 120

Figure 43. AtXX4 and TuMV-6K2 interact in *N. benthamiana*. BiFC assay was performed to check the interaction between AtXX4 and TuMV-6K2. Confocal imaging was performed at 72 h post agroinoculation (hpi). TuMV-6K2 and AtXX4 were fused to the N (nY-6K2) and C-terminal (cY-AtXX4) fragments of yellow fluorescent protein (YFP) respectively. **A)** “Trans”: image obtained in transmitted light **B)** reconstitution of a YFP fluorescence signal **C)** “Chloroplast”: fluorescence emitted by chlorophyll **D)** “merged”: superimposition of images acquired in panels B and C. Arrows indicate the YFP dots observed associated with chloroplasts. Arrowheads indicate which dots were chosen in panel B and F to perform the spectral analysis shown in S1 and S2. The peaks at 530nm are typical of the YFP maximum emission signal confirming that the YFP observed in B and F is a real

signal due to the interaction between AtXX4 and TuMV-6K2. Scale bar 10 μ m. Pag. 123

Figure 44. Negative and positive controls of the BiFC experiment. AtDIR fused to the N terminal fragment of YFP (nY-AtDIR) was used as either a negative control for AtXX4 (A-D, S1) or a positive control for TuMV-6K2 (E-H, S2). Confocal imaging was performed at 72 h post agroinoculation (hpi). Arrowheads indicate which dots were chosen in panel B and F to perform the spectral analysis. Peaks at 530nm are obtained for TuMV-6K2/AtDIR confirming the interaction (S2) and aspecific peaks for AtXX4/AtDIR (S1) confirming a lack of interaction. **A/E)** “Trans”: image obtained in transmitted light **B/F)** reconstitution of YFP fluorescence **C/G)** “Chloroplast”: fluorescence emitted by chlorophyll **D/H)** “merged”: superimposition of images acquired in panels B and C. Scale bars: 100 μ m (A-D, S1); 10 μ m (E-H, S2). Pag. 125

Figure 45. AtXX4 and TuMV-6K2 interact at the level of the Viral replication complexes (VRCs) during TuMV infection. cY-AtXX4 and nY-6K2 were co-expressed with the viral construct TuMV-6K2mcherry using agroinoculation. Confocal imaging was performed 72 hpi. **A)** “Trans”: image obtained in transmitted light **B)** YFP fluorescence **C)** “Chloroplast”: fluorescence emitted by chlorophyll **D)** mcherry fluorescence emitted by the 6K2-mcherry fusion protein expressed during TuMV-6K2-mcherry infection **E)** “merged”: superimposition of images acquired in panels B, C and D. Arrows in panels D and E indicate the VRC (viral replication complexes). The arrowheads in B indicate which dots were chosen for the spectral analysis shown in panel S: the maximum peaks at 530nm are typical of YFP emission confirming the interaction between AtXX4 and TuMV-6K2. Scale bar: 10 μ m. Pag. 126

Figure 46. The fluorophore RFP doesn't interfere with the interaction observed between AtXX4 and TuMV-6K2 in BiFC. TuMV-6K2 and AtXX4 were fused to the N (nY-6K2) and C-terminal (cY-AtXX4) fragments of yellow fluorescent protein (YFP) respectively. Confocal imaging was performed 72 hpi **A)** “Trans”:

image obtained in transmitted light **B)** “YFP fluorescence **C)** “Chloroplast”: fluorescence emitted by chlorophyll **D)**: fluorescence emitted by the RFP **E)** “merged”: superimposition of images acquired in panels B, C and D. Arrows in panel D indicate the nucleocytoplasmic localization of RFP signal. Scale bar: 10µm. Pag. 127

Figure 47. AtXX4 self-interacts in healthy condition. BiFC assay was performed to check the self-interaction of AtXX4. Confocal imaging was performed at 72 h post agroinoculation (hpi). AtXX4 was fused to the N (nY-AtXX4) and C-terminal (cY-AtXX4) fragments of yellow fluorescent protein (YFP). **A)** “Trans”: image obtained in transmitted light **B)** YFP fluorescence reconstituted **C)** “Chloroplast”: fluorescence emitted by chlorophyll **D)** “merged”: superimposition of images acquired in panels B and C. Arrows indicate the self-interaction of AtXX4. Arrowheads indicate which dots were chosen in panel B to perform the spectral analysis shown in S. The peaks at 530nm are typical of the YFP maximum emission signal confirming that the YFP observed in B is not an artefact signal. Scale bar 2µm. Pag. 128

Figure 48. Self-interacting AtXX4 shows a partial relocation during TuMV infection to the VRCs. BiFC assay was performed to check the self-interaction of AtXX4 during TuMV infection. Confocal imaging was performed at 72 h post agroinoculation (hpi). AtXX4 was fused to the N (nY-AtXX4) and C-terminal (cY-AtXX4) fragments of yellow fluorescent protein (YFP). **A)** “Trans”: image obtained in transmitted light **B)** YFP fluorescence **C)** “Chloroplast”: fluorescence emitted by chlorophyll **D)**: fluorescence emitted by the 6K2-mcherry expressed during TuMV-6K2-mcherry infection **E)** “merged”: superimposition of images acquired in panels B, C and D. The yellow arrows in F indicate a colocalization of AtXX4 with the VRC. Arrowheads in B indicate which dots were chosen to perform the spectral analysis shown in S. The peaks at 530nm are typical of the YFP maximum emission signal confirming that the YFP observed in B is a real signal. Scale bar 10µm. Pag. 129

Figure 49. Subcellular localization of AtXX4-GFP and ATXX4-RFP fusion proteins in healthy plants. (A-D) and RFP (E-H) fusion proteins. Confocal imaging was performed at 72 h post agroinfiltration of AtXX4-GFP (A-D) or AtXX4-RFP (E-H) fusion proteins. **A/E)** “Trans”: image obtained in transmitted light **B/F)** GFP and RFP fluorescence signals respectively **C/G)** “Chloroplast”: fluorescence emitted by chlorophyll **D/H)** “merged”: superimposition of images acquired in panels B and C or F and H. Red arrows in panels B and F indicate the nucleus surrounded by chloroplasts indicated by yellow arrows in panels D and H. Scale bar 10µm. Pag. 130

Figure 50. Subcellular localization of AtXX4-GFP fusion protein during TuMV infection. Confocal imaging was performed at 72 h post agroinfiltration of AtXX4-GFP fusion protein together with the viral construct TuMV-6K2mcherry. **A)** “Trans”: image obtained in transmitted light **B)** GFP fluorescence emitted by the AtXX4-GFP fusion protein **C)** “Chloroplast”: fluorescence emitted by chlorophyll **D)** fluorescence emitted by the 6K2-mcherry expressed during TuMV-6K2mcherry infection **E)** “merged”: superimposition of images acquired in panels B, C and D. Scale bar 10µm. Pag. 131

List of tables

Table 1. Twenty-six onion cultivars/ecotypes tested Pag.48

Table 2. SSR markers used in onion populations phylogenetic analysis. Pag. 58

Table 3. PCR reaction steps for DNA amplification. Pag. 59

Table 4. PCR reaction mix used DNA amplification. Pag. 59

Table 5. Results of first trial symptom observations and DAS-ELISA analysis accomplished in susceptibility/resistance evaluation trial 30 days post OYDV-inoculation (T2). Pag. 61

Table 6. Results of second trial symptom observations and DAS-ELISA analysis accomplished in susceptibility/resistance evaluation trial 30 days post OYDV-inoculation (T2). Pag. 62

Table 7. Analysis of Variance (ANOVA) for the first and second-year experiments. Pag. 66

Table 8. Percentage (%) of bulbs affected by secondary pathogens observed (from infected and healthy plants) for each cultivar during the storage phase in the first and second year. Pag. 67

Table 9. Average reduction values of infected and healthy bulbs of the first year analysed after the storage phase, including the percentage of water reduction comparing infected to healthy bulbs. Pag. 69

Table 10. Average reduction values of infected and healthy bulbs of the second year analysed after the storage, including the percentage of water reduction comparing infected to healthy bulbs. Pag. 70

Table 11. Length of fragments obtained from the analysis on Genemapper v.5. Pag. 71

Table 12. Genetic diversity parameters among Onion genotypes based on 12 SSR markers. Pag. 72

Table 13. Primers of EIF and of housekeeping genes used in gene expression analysis. Pag. 76

Table 14. Reagent used for the dsDNase step. Pag. 76

Table 15. Reagent used for the cDNA synthesis. Pag. 77

Table 16. Overview of sequencing output and assembly of *A. cepa* bulb transcriptome. Pag. 89

Table 17. Summary of DEGs ($P_{adj} < 0.05$) extracted between uninfected and OYDV infected samples at TEC/TED, TIS/TED, and TIS/TEC comparisons. Pag. 90

Table 18. List of *A. cepa* WRKY genes (*AcWRKYs*) extracted, showing a complete WRKY domain. Pag. 99-100

Table 19. Summary of *AcWRKYs* detected in both uninfected and OYDV-infected bulbs in each comparison. Pag. 101

Table 20. List of the sixteen candidate interactors of WMV-6K2. For confidentiality the exact names are not given. Pag. 108

Table 21. Composition of the reaction mix used for AtXX4 PCR amplification. Pag. 110

Table 22. PCR reaction steps for AtXX4 PCR amplification. Pag. 110

Table 23. Reaction mix used for pENTR™/ D-TOPO® cloning. Pag. 111

Table 24. PCR reaction mix used for colonies screening. Pag. 112

Table 25. PCR reaction steps for colonies screening. Pag. 112

Table 26. Reaction mix used for LR recombination in a destination vector. Pag. 113

Table 27. Synthesis of the results of three independent experiments performed for each combination. Pag. 121

Table 28. Summary of the combinations used to check AtXX4/TuMV-6K2 interaction in healthy plants using BiFC. Positive and negative control combinations are also indicated. Pag. 122